# UNIVERSIDAD DE CHILE

## FACULTAD DE CIENCIAS QUÍMICAS Y FARMACÉUTICAS

# *AN ENANTIOMERIC STUDY OF SALSOLINOL INVOLVEMENT IN ETHANOL BRAIN REINFORCING EFFECT, VIA THE ACTIVATION OF THE GI PATHWAY OF μ-OPIOID RECEPTORS*

**Tesis presentada a la Universidad de Chile para optar al grado de Doctor en Farmacología por:**


## *PABLO ANDRÉS BERRÍOS CÁRCAMO*

**Director de Tesis: Dr. Mario Herrera-Marschitz**

**Co-director de Tesis: Dr. Mario Rivera Meza**


**Santiago-CHILE**

**Enero 2018**

# UNIVERSIDAD DE CHILE
## FACULTAD DE CIENCIAS QUÍMICAS Y FARMACÉUTICAS

### INFORME DE APROBACIÓN DE TESIS DE DOCTORADO

**Se informa a la Dirección de la Escuela de Graduados de la Facultad de Ciencias Químicas y Farmacéuticas que la Tesis de Doctorado presentada por el candidato**

# PABLO ANDRÉS BERRÍOS CÁRCAMO

**Ha sido aprobada por la Comisión de Evaluadora de Tesis como requisito para optar al grado de Doctor en Farmacología, en el examen público rendido el día** _____

**Director de Tesis:**
**Dr. Mario Herrera-Marschitz** _____

**Co-director de Tesis:**
**Dr. Mario Rivera Meza** _____

**Comisión Evaluadora de Tesis:**

**Dr. Claudio Olea (Preside)** _____

**M.S.c María Elena Quintanilla** _____

**Dr. Gonzalo Bustos** _____

**Dr. Juan Segura** _____

***AGRADECIMIENTOS***

El desarrollo de esta tesis consistió principalmente en una etapa de crecimiento profesional y de colaboración; en la que participaron profesores, colegas, familia y amigos que me ayudaron a entender el sacrificio y las gratificaciones que significan ser científico.

Agradezco primero a mis directores de tesis, Dr. Mario Herrera-Marschitz y Dr. Mario Rivera, quienes me guiaron y aconsejaron con especial atención y profundidad para lograr mis objetivos y anhelos en este periodo de cuatro años.

Agradezco la compañía permanente de los laboratorios de la prof. María Elena Quintanilla y el Dr. Mario Herrera-Marschitz. El apoyo de Catalina Salinas, Cristian Silva, Jonathan Urra, Erik Jerez, Alex Bravo, Patrich Gallardo, Andrea Tapia y Carolyne Lespay, además de Juan Santibáñez, Carmen Almeyda y los profesores Diego Bustamante y Dra. Paola Morales.

Agradezco especialmente al Dr. Yedy Israel. Su consejo y enseñanzas quedarán siempre para mi desarrollo como profesional y como persona.

Agradezco también al Dr. Gerald Zapata, quien me abrió las puertas e inspiró a desarrollar el modelamiento computacional de esta tesis.

Agradezco especialmente al Dr. Vasilis Vasiliou, quien me recibió en su laboratorio y compartió su forma de trabajar conmigo. También agradezco la amistad de Ying Chen, Stephanie Marshall, Jay Golla, Nick Apostolopoulos, Ming Han, Georgia Charkoftaki y Yewei Wang.

Agradezco el apoyo y las discusiones que se suscitaron junto a la comisión de esta tesis, Dr. Claudio Olea, Dr. Gonzalo Bustos, Dr. Juan Segura y prof. Maria Elena Quintanilla. Me ayudaron a observar más allá y entender de mejor manera el contexto de este trabajo científico.

Finalmente agradezco a mi familia, primero a mis padres, Reinaldo Berríos y Ana María Cárcamo, por inculcarme los valores que me guían mi camino y a mis hermanas Camila y Javiera por su cariño permanente. También agradezco el afecto de mi nueva familia, Kristin, Carla y Cristian. Y la comprensión de mi esposa, Sarah, y nuestro juego casi permanente de viajes, estadías y lejanía, que hacen el tiempo juntos aún más significativo.

**FUNDING**

This thesis was funded by **CONICYT (beca para estudios de doctorado nacional 2013-2016, 21130865)**, and was conducted in the following laboratories:

- Program of Molecular & Clinical Pharmacology, Faculty of Medicine, Universidad de Chile. (**Proyecto FONDECYT 1120079** y **Millennium Institute BNI P09-015-F, Mario Herrera-Marschitz; Proyecto FONDECYT de Iniciación 11130241, Mario Rivera Meza; Proyecto FONDECYT 1130012, Maria Elena Quintanilla; Proyecto FONDECYT 1110263, Paola Morales**).
- Unidad de Gráfica Molecular, Facultad de Ciencias Químicas y Farmacéuticas, Universidad de Chile, Santiago, Chile. (**Proyecto FONDECYT 1120280** y **1171484, Gerald Zapata**).
- Department of Environmental Health Sciences, Yale School of Public Health, New Haven, CT, USA. (**National Institute of Health (NIH) AA022057** y **AA021724, Vasilis Vasiliou**).

**PRODUCTIVITY**

Two scientific publications:

**Quintanilla ME, Rivera-Meza M, Berríos-Cárcamo P, Cassels BK, Herrera-Marschitz M, Israel Y** (2015) (R)-salsolinol, a product of ethanol metabolism, stereospecifically induces behavioral sensitization and leads to excessive alcohol intake. Addiction Biology, 21 1063-1071. doi: 10.1111/adb.12268.

**Berríos-Cárcamo P, Quintanilla ME, Herrera-Marschitz M, Vasiliou V, Zapata-Torres G, Rivera-Meza M** (2016) Racemic salsolinol and its enantiomers act as agonists of the μ-opioid receptor by activating the gi protein-adenylate cyclase pathway. Frontiers in behavioral neuroscience, 10. doi: 10.3389/fnbeh.2016.00253.

Six scientific congress presentations:

**Berríos-Cárcamo P, Rivera-Meza M, Herrera-Marschitz M, Vasiliou V** (2017) Racemic salsolinol activity and enantiomeric specificity on the human dopamine transporter. En: VIII LASBRA INTERNATIONAL MEETING: "Neurobiological basis of alcoholism: from molecules to behavior" (Puerto Varas, Chile).

**Berríos-Cárcamo P, Herrera-Marschitz M, Rivera-Meza M, Zapata-Torres G** (2017) Enantiomeric specificity of salsolinol in the mu-opioid receptor: a molecular modelling study. En: Chilean society of Pharmacology XXXIX Annual Meeting (Puerto Varas, Chile).

**Berríos-Cárcamo P, Quintanilla ME, Herrera-Marschitz M, Vasiliou V, Zapata-Torres G, Rivera-Meza M** (2016) In vitro and in silico pharmacological characterization of the interaction between salsolinol and the μ-opioid receptor. En: ISBRA ESBRA World Congress on Alcohol an Alcoholism (Berlín, Alemania).

**Berríos-Cárcamo P, Quintanilla ME, Rivera-Meza M, Herrera-Marschitz M, Israel Y** (2015) Salsolinol: product of condensation of acetaldehyde and dopamine is reinforcing and promotes alcohol consumption. En: Satellite symposium on Alcoholism, ASH, NASH and Pancreatitis (Santiago, Chile).

**Berríos-Cárcamo P, Rivera-Meza M, Quiroz G, Iturriaga-Vásquez P, Reyes-Parada M, Zapata-Torres G, Herrera-Marschitz M, Israel Y, Quintanilla ME** (2015) Is salsolinol the final effector of ethanol reinforcement? En: Chilean society of Pharmacology XXXVII Annual Meeting (La Serena, Chile).

**Berríos-Cárcamo P, Quintanilla ME, Rivera-Meza M, Buscaglia M, Zapata-Torres G, Herrera-Marschitz M, Israel Y** (2012) Salsolinol and isosalsolinol: products of dopamine and acetaldehyde condensation as putative effectors of the reinforcing effect of ethanol. En: II International Workshop. Motivated behavior, stress and addiction: from molecules to behavior (Valparaíso, Chile).

## TABLE OF CONTENTS


***AGRADECIMIENTOS*** ..... iii

**FUNDING** ..... iv

**PRODUCTIVITY** ..... v

**TABLE OF CONTENTS** ..... vi

**TABLE OF FIGURES** ..... ix

**TABLE OF TABLES** ..... x

***1. RESUMEN*** ..... 11

**2. ABSTRACT** ..... 12

**2. INTRODUCTION** ..... 13

**2.1. Ethanol and alcohol use disorder** ..... 13

**2.2. Ethanol reinforcing effect** ..... 13

**2.3. Salsolinol as final effector of ethanol reinforcement** ..... 14

**2.4. Salsolinol mechanism of action** ..... 15

**2.5. Investigation proposal** ..... 15

*2.5.1. Salsolinol activation of μ-opioid receptors* ..... 15

*2.5.2. Salsolinol activation of the brain reward system* ..... 16

*2.5.3. Salsolinol levels determination in the brain reward system* ..... 16

**3. HYPOTHESIS** ..... 17

**4. GENERAL AIM** ..... 17

**5. SPECIFIC AIMS** ..... 17

**6. MATERIALS** ..... 18

**6.1. Animals.** ..... 18

**6.2. Chemicals.** ..... 18

**6.3. Antibodies.** ..... 18

**6.4. Cell lines.** ..... 18

**6.5. Plasmids.** ..... 18

**6.6. Commercial kits.** ..... 18

**6.7. Instruments.** ..... 18

**6.8. Equipment.** ..... 19

**6.9. Computer software** ..... 19

**7. METHODS** ..... 20

**7.1. Separation and purification of (*R*) and (*S*)-salsolinol** ..... 20

**7.2. Determination of the intrinsic activity of (*R*), (*S*) and (*R*/*S*)-salsolinol on μ-opioid receptors** 20

*7.2.1. Determination of agonistic activity through the Gi protein signaling pathway.* ..... 20

*7.2.2. Determination of agonistic activity through the β-arrestin recruitment pathway* ..... 21

**7.3. Molecular modeling of the binding of (*R*), (*S*) and (*R*/*S*)-salsolinol on μ-opioid receptors.** 21

*7.3.1. Molecular mechanics system preparation* ..... 21

*7.3.2. Molecular docking* ..... 22

*7.3.3. Molecular dynamics simulations* ..... 22

**7.4. Conditioned place preference of (*R*) and (*S*)-salsolinol** ..... 22

**7.5. Determination of (*R*), (*S*) and (*R*/*S*)-salsolinol activity on the human dopamine transporter.** ..... 23

**7.6. Determination of salsolinol levels in rat brain homogenates.** ..... 23

*7.6.1. Animal treatment to study the influence of a catechol-O-methyl transferase inhibitor* 23

*7.6.2. Animal treatment to study the appearance of salsolinol after an ethanol administration* 24

*7.6.3. Brain dissection* ..... 24

*7.6.4. Salsolinol determination* ..... 24

**8. RESULTS** ..... 25

**8.1. Separation and purification of (*R*) and (*S*)-salsolinol** ..... 25

**8.2. Determination of the intrinsic activity of (*R*), (*S*) and (*R*/*S*)-salsolinol on μ-opioid receptors** 26

**8.3. Molecular modeling of the binding of (*R*) and (*S*)-salsolinol on μ-opioid receptors** ..... 28

*8.3.1. Ligand placement and correlation of the salsolinol structure with morphinan ligands*. 28

*8.3.2. Conformation and orientation of salsolinol in the simulations* ..... 29

*8.3.3. Comparison of (R) and (S)-SAL interactions with the μ-opioid receptor binding site* ..... 32

*8.3.4. Activation of the μ-opioid receptor by (S)-salsolinol* ..... 32

**8.4. Conditioned place preference of (*R*) and (*S*)-salsolinol** ..... 36

**8.5. Examining possible mechanisms of salsolinol elimination** ..... 37

*8.5.1. Salsolinol activity in the dopamine transporter* ..... 37

*8.5.2. Effect of a catechol-O-methyl transferase inhibitor on the levels of salsolinol administered into the brain reward system* ..... 39

**8.6. Determination of rat brain SAL levels after an acute ethanol administration** ..... 41

**9. DISCUSSION** ..... 42

**9.1. The mechanism of SAL reinforcing activity** ..... 42

*9.1.1. Racemic SAL intrinsic activity* ..... 42

*9.1.2. Racemic SAL functional selectivity* ..... 42

*9.1.3. SAL μ-opioid receptor activation mechanism: enantiomeric selectivity and binding site coupling* 43

*9.1.4. Enantiomeric specificity of SAL activation of the brain reward system* ..... 43

**9.2. The presence of SAL in the brain reward system after an ethanol exposure** ..... 45

*9.2.1. Determination of the SAL brain elimination pathways* ..... 45

*9.2.2. Determination of brain SAL after an acute ethanol administration*..... 46

**9.3. Other hypotheses for the mechanism of the ethanol reinforcing effect.** ..... 46

**10. CONCLUSIONS**..... 48

**11. REFERENCES**..... 49

**12. ADDENDUM Effect of Aldh1b1 knockout on brain gene expression of mice under ethanol treatment**..... 56

## TABLE OF FIGURES

**Figure 1. The rat mesolimbic system.** ..... 13

**Figure 2. Salsolinol synthesis**..... 14

**Figure 3. Separation of (*R*) and (*S*)-salsolinol**.. ..... 25

**Figure 4. Intrinsic activity and functional selectivity of racemic salsolinol on μ-opioid receptors.** ... 26

**Figure 5. Enantiomeric specificity of salsolinol on μ-opioid receptors.**..... 27

**Figure 6. Comparison of (*R*/*S*)-salsolinol and β-funaltrexamine structures.**..... 28

**Figure 7. Stability of salsolinol molecules in the μ-opioid receptor binding site.**..... 30

**Figure 8. Salsolinol starting coordinates for molecular dynamics simulations within the μ-opioid receptor binding site, after equilibration.** ..... 31

**Figure 9. Salsolinol final coordinates within the μ-opioid receptor binding site, after 300 ns of simulation.** ..... 31

**Figure 10. Interactions and correlations of the salsolinol methyl group.** ..... 33

**Figure 11. Average interactions of (*S*)-salsolinol in its most stable simulations.**..... 33

**Figure 12. Salsolinol and μ-opioid receptor active and inactive structures distinction.**..... 34

**Figure 13. Interaction of (*S*)-salsolinol with the μ-opioid receptor and propagation of transduction signal.** ..... 35

**Figure 14. Conditioned place preference of the infusion of (*R*) or (*S*)-salsolinol intra-ventral tegmental area.** ..... 36

**Figure 15. Determination of the dopamine transporter protein on HEK293 cells transfected with the human dopamine transporter by Western blot.**..... 37

**Figure 16. Analysis of the inhibition of the uptake of the fluorescent dopamine analog by the dopamine transporter**. ..... 38

**Figure 17. HPLC chromatogram of rat ventral striatum supernatant spiked with salsolinol.** ..... 39

**Figure 18. HPLC chromatograms of rat left ventral tegmental area supernatants.**..... 40

**Figure 19. HPLC chromatograms of homogenate supernatants of nucleus accumbens and VTA.**..... 41

**Figure 20. Suggested model of salsolinol mechanism of action and enantiomeric specificity.**..... 44

## TABLE OF TABLES

**Table 1. Concentrations for producing half-maximal effect ($EC_{50}$) and coefficient of determination ($R^2$) of ligands tested on CHO-K1 cells transfected with the human μ-opioid receptor.** ..... 27

**Table 2. Molecular docking poses of (*R*) and (*S*)-salsolinol in the μ-opioid receptor dimer empty binding pockets.** ..... 29

**Table 3. Salsolinol simulation stability parameters obtained from root-mean-square deviation analyses.** ..... 30

**Table 4. (*R*) and (*S*)-salsolinol probability of interaction (less than 4 Å) with the residues of the binding site of the μ-opioid receptor**..... 32

**Table 5. Half-maximal inhibitory concentration ($IC_{50}$; when the dopamine analog was 0.5 μM) and the inhibition constant ($K_i$) of the ligands tested for the blockage of the uptake of the fluorescent dopamine analog in the human dopamine transporter**. ..... 37

## *1. RESUMEN*

El efecto reforzante del etanol contribuye a la generación de dependencia. Para que el etanol sea reforzante se requiere que este se metabolice a acetaldehído en el cerebro, el cual activa neuronas dopaminérgicas en el área del tegmento ventral (VTA). No se conoce si el acetaldehído se une a un receptor para ser reforzante, pero se puede condensar con dopamina para formar salsolinol racémico [(*R*) y (*S*)-SAL]. Se ha propuesto que SAL ejerce el efecto reforzante del etanol, ya que es un reforzante potente si se administra intracerebralmente. Además, los niveles cerebrales de SAL aumentan luego de una administración de etanol crónica a ratas. Si la administración de etanol es aguda no se observa SAL cerebral a menos que el metabolismo de acetaldehído esté inhibido. El mecanismo de acción de SAL podría ser a través de receptores de opioides μ (μOR) ya que SAL desplaza ligandos de estos receptores, aunque no existe evidencia de una acción directa de SAL sobre μORs. Este trabajo apuntó a determinar si **SAL producido luego de una dosis aguda de etanol activa el sistema de recompensa de ratas naïve a través del efecto de uno de sus enantiómeros (*R* o *S*) sobre μORs.** Experimentos basados en células transfectadas mostraron que SAL activa μORs vía proteína $G_i$ sin reclutamiento de β-arrestina, y que (*S*)-SAL purificado es 50 veces más potente que (*R*)-SAL. Para apoyar estos resultados realizamos simulaciones computacionales de (*R*) y (*S*)-SAL dentro del sitio de unión del μOR mediante dinámica molecular. Estas simulaciones nos permitieron explicar que la especificidad enantiomérica observada experimentalmente se debe a la interacción del metilo quiral de (*S*)-SAL con la Y148 del μOR, interacción que no fue estable para (*R*)-SAL. Las simulaciones mostraron que (*S*)-SAL, una molécula pequeña en comparación con todos los otros agonistas opioides, no puede interaccionar con todos los residuos calificados como importantes para la activación de μORs, mostrando que el (*S*)-SAL es un agonista muy particular de este receptor. A continuación, determinamos si la administración de (*R*) o (*S*)-SAL en el VTA de ratas activa su sistema de recompensa cerebral. La infusión de (*R*) y no de (*S*)-SAL en el VTA indujo una preferencia de lugar condicionada en ratas. El mecanismo para este efecto de (*R*)-SAL podría ser distinto a un agonismo de μORs, ya que (*S*)-SAL no indujo este efecto a pesar de ser el enantiómero más potente para agonismo en μORs. El siguiente objetivo fue determinar mecanismos de eliminación que explicaran la gran dificultad en la detección de SAL en el cerebro, a pesar de que se forma *in vitro* a pH 7,4. La actividad de SAL sobre el transportador de dopamina se estudió mediante ensayos basados en células transfectadas y encontramos que concentraciones milimolares de SAL eran necesarias para que fuera un ligando de este transportador, indicando que una recaptación por el transportador de dopamina no es un mecanismo relevante de eliminación de SAL. Para determinar el efecto de una actividad catecol-*O*-metil transferasa (COMT) en la eliminación de SAL, se inyectó esta molécula en el VTA de ratas junto o no al inhibidor de COMT entacapona, luego los niveles de SAL se midieron en el sobrenandante de homogeneizados de VTA o la vecina sustancia nigra. No se encontraron diferencias entre los niveles de SAL medidos de animales tratados o no con entacapona. El objetivo final fue detectar y cuantificar SAL en el cerebro de ratas naïve administradas con etanol sistémico. No se observó SAL en el núcleo accumbens o en el VTA de estas ratas. Tampoco se observó SAL, cuando se administró entacapona en el VTA paralelamente a la administración de etanol. En conclusión, se encontró que SAL es un agonista de μORs, que actúa *in vitro* a través de (*S*)-SAL y activa la vía de señalización de proteína $G_i$. Sin embargo, (*S*)-SAL no promovió una preferencia de lugar condicionada luego de ser infundido en el VTA, mientras que (*R*)-SAL si lo hizo. Estos resultados sugieren que hay blancos farmacológicos distintos de μORs para que (*R*)-SAL sea recompensante. No observamos SAL en el cerebro de animales administrados con etanol, incluso cuando un inhibidor de COMT se infundió en el VTA. SAL podría ser eliminado rápidamente del cerebro, sin embargo, los resultados muestran que SAL no se une al transportador de dopamina en concentraciones relevantes y el experimento de metabolización de SAL por COMT no fue concluyente. Para ser reforzante, SAL debería alcanzar concentraciones cerebrales activas en un microambiente, necesitando una metodología más precisa para monitorear su aparición local.

## 2. ABSTRACT

The reinforcing effect of ethanol is a major contributor to ethanol dependence. The formation of acetaldehyde, the first ethanol metabolite, is required for ethanol to be reinforcing, by activating dopaminergic neurons in the ventral tegmental area (VTA). Whether acetaldehyde can bind to a receptor to be reinforcing is unknown, but it can condense with dopamine to form racemic salsolinol [(*R*) and (*S*)-SAL]. It has been proposed that SAL is the substance that exerts the reinforcing effect of ethanol consumption because SAL is a potent brain reinforcer when intracerebrally administered. Further, the levels of racemic SAL rise in the brain of rats after chronic ethanol administration. After an acute dose of ethanol, the levels of SAL in the brain reward system rise only if the metabolism of acetaldehyde is inhibited. The mechanism of SAL activity could be via μ-opioid receptors (μOR) since SAL displaces ligands from these receptors, but there is no evidence that SAL can directly activate μORs. This work aimed to determine whether **SAL produced after an acute dose of ethanol activates the brain reward system of naïve rats via one of its enantiomers (either *R* or *S*) activation of μORs.** Cell-based experiments showed that SAL activated μORs via $G_i$ protein with no β-arrestin recruitment, and purified (*S*)-SAL was 50 times more potent than (*R*)-SAL. To support the experimental results we employed molecular dynamics simulations of (*R*) and (*S*)-SAL inside the binding pocket of the μOR. These simulations allowed us to explain that the enantiomeric specificity was caused by the interaction of the (*S*)-SAL chiral methyl group with the Y148 of the μOR, interaction that was not stable for (*R*)-SAL. The simulations showed that (*S*)-SAL, a small molecule compared to other opioid agonists, cannot interact with all the residues regarded as important for μOR activation, showing that (*S*)-SAL is a unique agonist of the receptor. Following, we determined whether (*R*) or (*S*)-SAL administration into the VTA of rats activate the brain reward system. The intra-VTA infusion of (*R*) and not of (*S*)-SAL induced a conditioned place preference in rats. The mechanism for this result may be different to μOR agonism since (*S*)-SAL did not induce an effect despite being a more potent agonist. Next, we intended to identify the reasons for the difficulty to detect SAL in the rat brain, despite being readily formed *in vitro* from acetaldehyde and dopamine at pH 7.4. The SAL activity at the dopamine transporter was explored using a cell-based assay, and we found that a millimolar SAL concentration was needed to be a ligand of the transporter, challenging the relevance of this uptake mechanism. To determine the effect of catechol-*O*-methyl transferase (COMT) in SAL elimination, SAL was injected intra-VTA of rats with or without the COMT inhibitor entacapone; then SAL levels were measured in VTA and substantia nigra homogenate supernatants. No differences were observed between the SAL levels measured from animals treated with, or without, entacapone. Finally, we aimed to detect and measure SAL in the brain of naïve rats administered with systemic ethanol. Rats were administered with ethanol, and brain homogenates assayed for SAL. No SAL was observed in either nucleus accumbens or VTA. When intra-VTA entacapone was administered concurrently with the ethanol administration, no SAL was observed either. In conclusion, SAL was found to be a μOR agonist, acting *in vitro* via (*S*)-SAL, activating $G_i$ protein signaling. However, (*S*)-SAL was not active to induce a rat conditioned place preference after infused intra-VTA while (*R*)-SAL was able to. These results suggest that there is another target for (*R*)-SAL to be rewarding. We did not observe SAL in the brain of animals administered ethanol, even when a COMT inhibitor was infused intra-VTA. SAL may be rapidly eliminated, yet the results show that SAL is not a relevant ligand of the dopamine transporter and SAL metabolization by COMT experiment was inconclusive. To be reinforcing, SAL could reach proper levels in its receptor microenvironment, needing an accurate methodological approach to locally monitor its occurrence.

## 2. INTRODUCTION

### 2.1. Ethanol and alcohol use disorder

The ethylic alcohol, or ethanol, is one of the most consumed drugs in the world. Its consumption can derive into an impulsive (binge drinking) or compulsive (withdrawal and relapse) behavior (Koob and Le Moal 1997) and develop into an alcohol use disorder (AUD) (American Psychiatric Association 2013). This disorder is characterized by the loss in self-control when consuming ethanol (Koob and Le Moal 1997) and can be classified as mild, moderate or severe by the Diagnostic and Statistical Manual of Mental Disorders (fifth edition) (American Psychiatric Association 2013). The alcohol use disorder is an important global burden, as 13.9% of the population in the US (Grant et al. 2015) and 3.4% in Europe (Rehm et al. 2015) were affected in the last year. In Chile, 14% of the population that consumed ethanol the last year were risky drinkers and half of those were classified as having moderate or severe AUD (Donoso 2015), following the Chilean version of the AUD identification test (Santis et al. 2009). The high prevalence of AUD is an important public health problem as it can derive into liver and cardiac diseases, cancer and labor and traffic accidents (Smyth et al. 2015; Rehm et al. 2003). Consequently, 9.7% of total mortalities in Chile during 2004 were attributable to ethanol consumption (Ministerio de Salud de Chile 2007).

### 2.2. Ethanol reinforcing effect

The impulsive consumption of alcoholic drinks is promoted by the ability of ethanol to biologically stimulate its consumption, which is called the ethanol reinforcing effect (Koob and Le Moal 1997; Koob et al. 2004). Ethanol is reinforcing by the local activation of dopaminergic neurons from the ventral tegmental area (VTA) which project and release dopamine into the nucleus accumbens (**Fig. 1**), and thus activating the brain reward system (Di Chiara and Imperato 1988; Brodie, Pesold, and Appel 1999; Rodd-Henricks, McKinzie, Crile, et al. 2000). To generate its reinforcing effect ethanol is not acting by itself but as a prodrug, metabolized into acetaldehyde in the VTA to be reinforcing (Karahanian et al. 2011; Quintanilla et al. 2012; Israel et al. 2015; Karahanian et al. 2015). Acetaldehyde is a reinforcing molecule, since it activates dopaminergic neurons from VTA slices (Melis et al. 2007) and is self-administered in the VTA by rats at micromolar concentrations (Rodd et al. 2005). However, it is not known whether acetaldehyde binds to a receptor in the brain reward system to promote reinforcement.

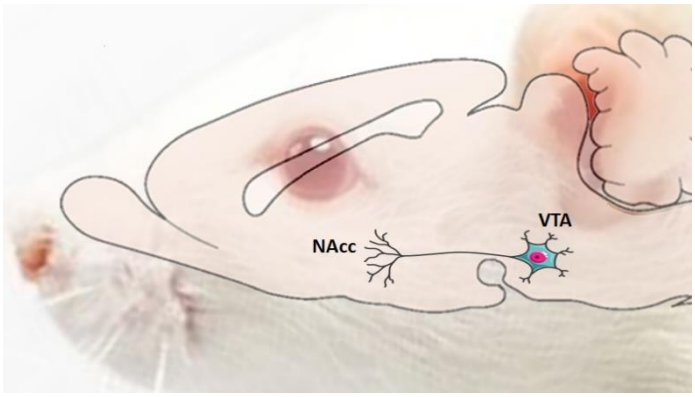


**Figure 1. The rat mesolimbic system.** Neurons from the ventral tegmental area (VTA) project to release dopamine into the nucleus accumbens (NAcc).

### 2.3. Salsolinol as final effector of ethanol reinforcement

Acetaldehyde can condense non-enzymatically with dopamine to form racemic salsolinol [(*R*/*S*)-1-methyl-5,6-dihydroxy-1,2,3,4-tetrahydroisoquinoline; SAL; **Fig. 2**], which has been proposed to exert the reinforcing effect of ethanol (Cohen and Collins 1970; Yamanaka, Walsh, and Davis 1970; Deehan, Brodie, and Rodd 2013; Melis et al. 2015). This proposal is supported by the evidence that SAL is self-administered by rats into the VTA at lower concentrations (sub-micromolar) than those required for ethanol or acetaldehyde to be reinforcing (Rodd et al. 2008), showing that SAL is a more potent reinforcer than its parent molecules. In addition, *in vitro*, SAL stimulates dopaminergic neurons from the VTA (Xie et al. 2012); *in vivo*, the infusion of SAL into the VTA of rats promotes the release of dopamine in the nucleus accumbens (Hipolito et al. 2011; Deehan et al. 2013) and induces a conditioned place preference (Hipolito et al. 2011; Quintanilla et al. 2014).

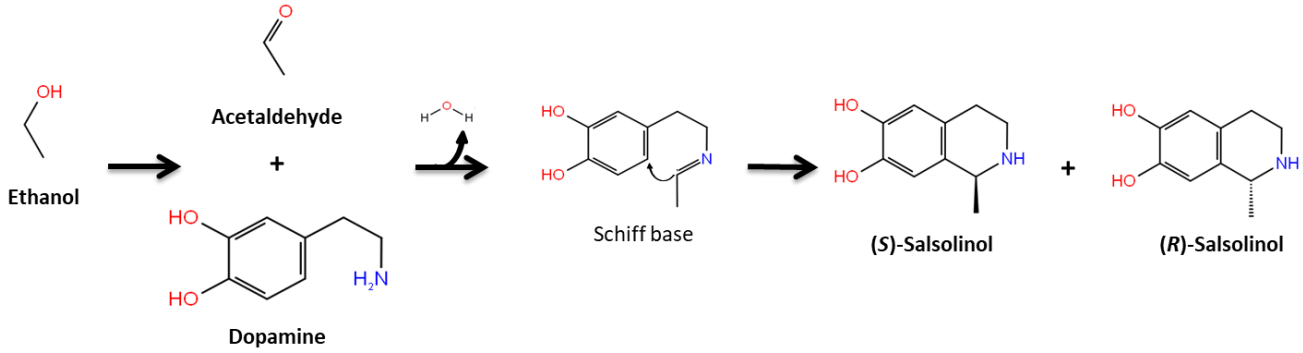


**Figure 2. Salsolinol synthesis**. Acetaldehyde derived from ethanol condenses with the dopamine in the brain to form (*R*) and (*S*)-salsolinol, through a Pictet-Spengler condensation. This reaction involves a Schiff base formation from the dopamine amine group and the acetaldehyde aldehyde group and a spontaneous orthocyclation of the Schiff base with the catechol group.

The levels of racemic SAL rise in the brain reward system of rats following chronic ethanol administration (Sjoquist, Liljequist, and Engel 1982; Myers et al. 1985; Matsubara, Fukushima, and Fukui 1987; Starkey et al. 2006; Rojkovicova et al. 2008) and higher amounts of (*R*) than (*S*)-SAL have been found (Rojkovicova et al. 2008), however, it is not known whether one or both enantiomers are pharmacologically active. An acute dose of ethanol also promotes the rise of SAL levels in the brain reward system, but the effect can only be observed when the metabolism of acetaldehyde is repressed (Jamal, Ameno, et al. 2003a; Jamal, Ameno, Kubota, et al. 2003) or a high concentration of acetaldehyde is infused directly into the nucleus accumbens (Jamal, Ameno, et al. 2003b). Because both SAL enantiomers are readily synthesized under physiological conditions (pH 7.4) (Berríos Cárcamo 2013), they are expected to be synthesized in the brain dopaminergic system in the presence of acetaldehyde. Therefore, instead of no synthesis, the difficulty in finding SAL in acute conditions could be explained by a fast SAL elimination. SAL has been shown to be a substrate for the catechol-*O*-methyl transferase (COMT), which produces *O*-methylated SAL derivatives (Hotzl and Thomas 1997) that would be harder to detect by the commonly used electrochemical detector (*O*-methylated compounds are less oxidable than the catechol group). Another possible mechanism for SAL elimination from the synaptic cleft could be the uptake by the dopamine transporter (DAT). One study found that (*R*)-SAL was taken by DAT in rat striatum synaptosomes ($K_m$ SAL = 23.64 µM) (Matsubara et al. 1998). However, two other reports suggest that there is no SAL binding to the transporter: SAL uptake by SH-SY5Y cells is not blocked by dopamine (Takahashi et al. 1994) and no increased toxicity by exposure of cultured cells transfected with the mouse DAT exposed to toxic

levels of SAL compared to non-transfected cells (Storch et al. 2002). The SAL activity on DAT was explored in this thesis.

### 2.4. Salsolinol mechanism of action

Opioid receptors are involved in the reinforcing effect of ethanol (Nutt 2014), and the opioid antagonist naltrexone is an effective drug to diminish ethanol consumption in AUD patients (Jonas et al. 2014). Interestingly, opioid receptors are also involved in the reinforcing effect of SAL. The *in vitro* activation of dopaminergic neurons of the VTA by SAL is blocked by μ-opioid receptor antagonists (Xie et al. 2012). The locomotor activation and nucleus accumbens dopamine release induced by the intra-VTA infusion of SAL is also blocked by treatment with μ-opioid receptor antagonists (Hipolito et al. 2011). Moreover, SAL displaces ligands from μ-opioid receptors with a half-maximal inhibition concentration ($IC_{50}$) of ~$10^{-5}$ M (Lucchi et al. 1982; Airaksinen et al. 1984). However, no direct activation of μ-opioid receptors by SAL has been shown. The activation of these receptors in GABAergic neurons of the VTA would hyperpolarize them, resulting in disinhibition and therefore activation of their neighbor dopaminergic neurons, resembling the action of opioid drugs (Johnson and North 1992).

### 2.5. Investigation proposal

The presented evidence shows how ethanol activates the brain to promote its consumption, but the mechanisms are not known yet. Recent results point towards the hypothesis that **the levels of an active salsolinol enantiomer rise after ethanol administration to activate μ-opioid receptors and stimulate the brain reward system**. To attest this hypothesis this work aimed to determine (i) if a salsolinol enantiomer can activate μ-opioid receptors; (ii) if the active salsolinol enantiomer also activates the brain reward system, and (iii) if salsolinol is generated at relevant concentrations in the brain reward system of the rat after ethanol administration.

#### *2.5.1.Salsolinol activation of μ-opioid receptors*

To determine if SAL activates μ-opioid receptors we chose *in vitro* and *in silico* approaches. We studied if cells that express human μ-opioid receptors trigger a transduction pathway after exposed to racemic, (*R*), or (*S*)-SAL; and supported those experiments by computational modelling of the SAL enantiomers interactions with the binding site of the receptor to determine if they were consistent with μ-opioid receptor activation, following crystallographic and computational observations (Manglik et al. 2012; Shim, Coop, and MacKerell 2013; Huang et al. 2015). Ensuing μ-opioid receptors activation two independent signaling pathways can follow: $G_i$ protein activation and/or β-arrestin protein recruitment. The transduction through the $G_i$ protein pathway leads to a decrease of cAMP levels (Raffa, Martinez, and Connelly 1994) and the opening of G-protein-gated inwardly rectifying potassium channels (Marker et al. 2005), promoting hyperpolarization, and therefore inhibition, of a hosting neuron. Transduction through the β-arrestin pathway lead to the receptor phosphorylation by a GPCR kinase and recruitment of a β-arrestin protein. This prevents the coupling of a G protein and promotes receptor internalization and a secondary signaling (Shenoy and Lefkowitz 2011). The activation of one or both transduction pathways depends on the agonist that is bound to the receptor. Opioids administration to mice that don't express β-arrestin, resembling the effect of a $G_i$ protein pathway biased agonist, generate stronger analgesia (Bohn et al. 2000; Bohn, Lefkowitz, and Caron 2002) and reinforcement (Bohn et al. 2003) while developing a diminished tolerance and secondary effects (Bohn, Lefkowitz, and Caron 2002; Bohn et al. 2000; Raehal, Walker, and Bohn

2005). Ligands can be full agonists, partial agonists or antagonists to either transduction pathway independently (Molinari et al. 2010).

*2.5.2.Salsolinol activation of the brain reward system*

To study if a SAL enantiomer could activate the brain reward system we infused (*R*) and (*S*)-SAL directly into the VTA of UChB rats, and determined if this infusion induced a conditioned place preference. We chose to infuse the VTA because the acetaldehyde synthesis, and possibly SAL synthesis, is necessary to occur in this area for ethanol to be reinforcing (Karahanian et al. 2011; Quintanilla et al. 2012; Israel et al. 2015). SAL most sensitive area is also the VTA, where rats self-administer this substance as low as $3 \cdot 10^{-7}$ M (Rodd et al. 2008), while higher concentrations were needed for nucleus accumbens SAL self-administration (Engleman et al. 2009).

*2.5.3.Salsolinol levels determination in the brain reward system*

The SAL formation significance in the pathogenesis of alcoholism occurs when the reinforcing effect is the main trigger for ethanol consumption, before developing a compulsive state commanded by negative reinforcement (Israel et al. 2015; Koob et al. 2004). Therefore, is important to study the occurrence of SAL in animals that are naïve to ethanol and have not developed the conditions for the change to a compulsive response to ethanol. Regarding the location of SAL synthesis, it could be formed in any area where dopamine accumulates and acetaldehyde diffuses from its synthesis in peroxisomes. SAL could be synthesized in the VTA inside dopaminergic somas or extracellularly in the somatodendritic synaptic cleft, or in the dopaminergic terminals in the nucleus accumbens. The work by Jamal in 2003 (Jamal, Ameno, et al. 2003a, 2003b; Jamal, Ameno, Kubota, et al. 2003) and Wang in 2007 (Wang et al. 2007) shows that SAL synthesis needs to be stimulated to be detected by brain microdialysis in the nucleus accumbens, increasing the acetaldehyde availability in the brain. They also showed that there is a delay between the administration of acetaldehyde in the nucleus accumbens and the occurrence of SAL (Wang et al. 2007). We propose here that a fast elimination is the explanation for the difficulty of SAL detection, which is consistent with the mentioned delay in the detection of SAL that would account for the elimination saturation. For this reason, we studied whether SAL is removed from the synaptic cleft by the dopamine transporter, determining if SAL is a ligand of the transporter using a cell-based assay. We also assessed brain SAL after inhibiting the catechol-o-methyl transferase (COMT) of which SAL is a known substrate (Hotzl and Thomas 1997). The preparation of rat brain homogenate supernatants allowed us to study the VTA, substantia nigra and nucleus accumbens as possible locations of SAL synthesis after acute ethanol administration.

## 3. HYPOTHESIS

**Salsolinol generated after an acute dose of ethanol activates the brain reward system of naïve rats via μ-opioid receptors via one of its enantiomers (either *R* or *S*).**

## 4. GENERAL AIM

**To demonstrate whether ethanol-derived (*R*) or (*S*)-salsolinol activates the brain reward system of naïve rats via μ-opioid receptors.**

## 5. SPECIFIC AIMS

1. To purify (*R*) and (*S*)-salsolinol from commercial racemates by HPLC.
2. To determine the intrinsic activity of racemic, (*S*)-salsolinol and (*R*)-salsolinol on μ-opioid receptors, using a cell-based assay and a computational molecular dynamics model.
3. To determine whether the administration of (*R*) or (*S*)-salsolinol into the ventral tegmental area of naïve rats activate the brain reward system, assessed by conditioned place preference.
4. To identify the reasons for the difficulty to detect SAL in the rat brain, with special attention on:
   - 4.1 The activity of salsolinol at the dopamine transporter.
   - 4.2 The brain levels of salsolinol following inhibition of the enzyme catechol-*O*-methyl transferase.
5. To detect and measure the levels of racemic salsolinol, (*S*)-salsolinol and (*R*)-salsolinol in the brain reward system of naïve rats following an acute systemic ethanol administration.

## 6. MATERIALS

### 6.1. Animals.

**Mice:** C57BL/6 mice. Housed in the animal facility at The Anlyan Center, Yale University, New Haven, CT, USA.

**Rats:** Wistar rats from the University of Chile Bibulous line (UChB). Selectively bred for over 80 generations for its voluntary ethanol consumption (Quintanilla et al. 2006). They are housed in the animal house from the Clinical and Molecular Pharmacology Program, Biomedical Sciences Institute, Faculty of Medicine, University of Chile. The procedures performed in this thesis were approved by the Bioethics Committee of the Faculty of Medicine, University of Chile (Responsible investigator: Pablo Berríos Cárcamo. CBA # 0718 FMUCH).

### 6.2. Chemicals.

**Alfa Aesar** (WardHill, MA, USA): Naltrexone.

**Baxter Chile** (Santiago, Chile): Isoflurane.

**DiscoveRx** (Fremont, CA, USA): DADLE ([D-Ala2, D-Leu5]-Enkephalin), met-enkephalin.

**Gibco** (Grand Island, NY, USA): Hank's balanced salt solution.

**Merck** (Darmstadt, Germany): Acetic acid, ammonium acetate, calcium chloride, ethylenediaminetetraacetic acid (EDTA), hydrochloric acid, methanol (HPLC grade), potassium chloride, potassium dihydrogen phosphate, sodium bicarbonate, sodium chloride.

**Santa Cruz** (Santa Cruz, CA, USA): (±)-Salsolinol hydrochloride (98% purity).

**Sigma** (St.Louis, MO, EE.UU.): L-ascorbic acid, D-glucose, magnesium sulfate, perchloric acid (67-72% TraceSELECT), sodium octanesulfonate monohydrate, triethylamine.

**Tocris** (Bioscience, Bristol, UK): β-Funaltrexamine.

### 6.3. Antibodies.

**Santa Cruz** (Santa Cruz, CA, USA): anti-dopamine transporter, 6-5G10 (monoclonal).

### 6.4. Cell lines.

**HEK293:** (a kind gift from Dr. Gary Rudnick at Department of Pharmacology, Yale University)**.**

### 6.5. Plasmids.

**phDAT:** (a kind gift from Dr. Gary Rudnick at Department of Pharmacology, Yale University)**.**

### 6.6. Commercial kits.

**DiscoveRx** (Fremont, CA, USA): cAMPHunter eXpress OPRM1 CHO-K1 GPCR assay; PathHunter® eXpress OPRM1 CHO-K1 β-Arrestin GPCR Assay.

**Molecular Devices** (Sunnyvale, CA, USA): Neurotransmitter Transporter Uptake Assay Kit.

**Promega** (Madison, WI, USA): FuGENE HD Transfection Reagent.

### 6.7. Instruments.

**Animal surgery:**

**Plastics One:** 22-gauge guide cannula.

**Analytic chemistry:**

**Macherey-Nagel** (Düren, Alemania): NUCLEODEX β-OH, 200 mm × 4 mm i.d., filled with particles of 5 µm of silica gel modified with β-cyclodextrin.

**Sigma-Aldrich** (St. Louis, MO, USA): SUPELCOSIL LC-18 column, 250 mm × 4.6 mm, filled with particles of 5 µm of silica gel-C18.

### 6.8. Equipment.

**Animal surgery:**

- **Anesthesia unit:** Univentor 410.
- **Microinjection pump:** CMA 100.
- **Temperature controller:** CMA 150.

**Behavioral study:**

- **Conditioning place preference chamber:** Custom made, with two connected compartments with different wall colors (black and white) and floor textures.

**High pressure liquid chromatography (HPLC):**

- **Bombs: Shimadzu** (Kyoto, Japan), LC-AD; **YL Instrument** (Seoul, Korea), YL-9111.
- **Column oven: Shimadzu**, CTO-10A.
- **Detector: BAS** (West Lafayette, IN, USA), LC-4C.

**Microplate reader:**

- **Molecular devices** (Sunnyvale, CA, USA), Spectramax M3.
- **Biotek** (Winooski, VT, USA), Synergy HT.

**Sample preparation:**

- **Ultrasonic homogenizer: OMNI International** (Kennesaw, GA, USA), Omni-Ruptor 250.

### 6.9. Computer software

GraphPad Prism 6 (San Diego, CA, USA); VMD: Visual Molecular Dynamics (1.9.3).

## 7. METHODS

### 7.1. Separation and purification of (*R*) and (*S*)-salsolinol

(*R*) and (*S*)-SAL were separated from a commercial racemic salsolinol by high-pressure liquid chromatography (HPLC) as described previously with modifications (Juricic et al. 2012). A solution of (*R*/*S*)-SAL ($2\times10^{-2}$ M) was prepared in distilled and deionized water. Then, 50 µL of this solution was injected into a NUCLEODEX β-cyclodextrin-modified column 200×4 mm i.d. packed with silica gel covalently bound to β-cyclodextrin (Macherey-Nagel, Düren, Germany) kept at 20°C using a column oven (Shimadzu, Kyoto, Japan). The chromatographic column was coupled to an LC-4C BAS amperometric detector (ED) set to a potential of 0.7 V. The mobile phase, composed of 100 mM ammonium acetate and 10 mM triethylamine (pH 4.0), was passed through at a flow rate of 0.40 mL/minute using an isocratic pump (Shimadzu, LC-10AD). Using a similar chiral HPLC system, it was reported that (*S*)-SAL was the first enantiomer to elute (Baum and Rommelspacher 1994; Deng et al. 1995; Toth et al. 2001; Cai and Liu 2008; Rojkovicova et al. 2008; Lee et al. 2010). This elution pattern is also supported by a computational modeling study that evaluated the total energy for stabilization; they showed that the inclusion complex formed by (*R*)-SAL and β-cyclodextrin is stronger than the complex of (*S*)-SAL and β-cyclodextrin (Huang, Quan, and Liu 2009). Once an (*R*/*S*)-SAL sample was injected into the HPLC, the enantiomers were separated and collected according to their corresponding elution time (with the electrochemical detector disconnected). The procedure was repeated ten times to obtain sufficient amounts of the corresponding enantiomers. The fractions were lyophilized at −54°C for 9 hours to eliminate the mobile phase from each collected sample, then dissolved in a correspondent solvent depending on the experiment, and injected into the HPLC system to check their purity. The quantification of purified enantiomers was performed using (*R*/*S*)-SAL as standard.

### 7.2. Determination of the intrinsic activity of (*R*), (*S*) and (*R*/*S*)-salsolinol on µ-opioid receptors

#### *7.2.1. Determination of agonistic activity through the Gi protein signaling pathway.*

The activation of the µ-opioid receptor Gi protein pathway by ligands was studied using a cell-based assay kit (cAMPHunter eXpress OPRM1 CHO-K1 GPCR assay, DiscoveRx, Fremont, CA, USA). For this assay, we used recombinant cells that stably express the human µ-opioid receptor, and measured the levels of cAMP which correlates with the activation of the $G_i$ protein pathway by these receptors. This system uses enzyme fragment complementation between two fragments of β-galactosidase to measure the levels of cAMP. The cAMP generated from the cells and cAMP coupled with a truncated β-galactosidase fragment compete for binding to an anti-cAMP antibody. Only the unbound cAMP-β-galactosidase fragment binds to a complementary β-galactosidase fragment to form the active enzyme. The activity of this enzyme can be measured following addition of a chemiluminescent substrate, which reflects the levels of cellular cAMP proportionally. The µ-opioid receptor ligands (morphine, met-enkephalin, (*R*)-SAL, (*S*)-SAL and (*R*/*S*)-SAL, dissolved in HCl $10^{-5}$ M), including the adenylate cyclase activator forskolin (20 µM), were incubated at 11 different concentrations with the recombinant cells for 30 minutes. Control cells were incubated with forskolin only. The resulting luminescence was measured with a microplate reader Synergy HT (Biotek, Winooski, VT, USA) or a microplate reader SpectraMax M3 (Molecular Devices, Sunnyvale, CA, USA). The $EC_{50}$ for each ligand was determined by correlating the data to a curve of ligand concentration (log M) vs. response using GraphPad Prism (San Diego, CA, USA). The experiment was repeated three times in duplicate for (*R*)-SAL, (*S*)-SAL and (*R*/*S*)-SAL and two times in duplicate for morphine and met-enkephalin. In a subsequent experiment, the activation of the µ-opioid receptor by racemic SAL (150 µM) was studied

after the addition of the antagonist naltrexone to the recombinant cells ($3\times10^{-10}$ M to $10^{-5}$ M), dissolved in the assay buffer, 30 minutes before the addition of (*R*/*S*)-SAL. All measurements were expressed as relative luminescence to the controls with no ligands added. Each concentration of naltrexone was assayed once in duplicate. The antagonistic action of naltrexone was specific for the μ-opioid receptor since the recombinant cells used in the experiment only overexpressed this type of opioid receptor.

*7.2.2. Determination of agonistic activity through the β-arrestin recruitment pathway*

To study the recruitment of the β-arrestin after the activation of the μ-opioid receptor, we used the PathHunter eXpress β-Arrestin GPCR chemiluminescent assay (DiscoverX) following the manufacturer instructions. In this system, the human μ-opioid receptor is tagged with a small fragment of β-galactosidase (Prolink, PK) and co-expressed with a fusion protein of β-arrestin-2 and the complementary fragment of β-galactosidase (Enzyme acceptor, EA) in CHO-K1 cells. Activation of the μ-opioid receptor stimulates the binding of β-arrestin to the PK-tagged receptor allowing the complementation of the two enzyme fragments of β-galactosidase. This process leads to the activation of the enzyme that metabolizes a substrate to generate chemiluminescence, which is proportional to the recruitment of β-arrestin. DADLE ([D-Ala2, D-Leu5]-Enkephalin), (*R*/*S*)-SAL and morphine ($10^{-8}$ M to $10^{-3}$ M, dissolved in HCl $10^{-5}$ M, pH 5.0) were incubated with the cells for 30 min. In a parallel experiment, we determined the ability of ligands to block the recruitment of β-arrestin. Naltrexone, β-funaltrexamine, or (*R*/*S*)-SAL ($3\times10^{-9}$ M to $10^{-4}$ M) were added 30 min before $3\times10^{-6}$ M DADLE. Each experiment was performed once in duplicate for each concentration of ligand. The resulting luminescence was determined with a microplate reader (Synergy HT, Biotek) and the $EC_{50}$ values were determined using GraphPad.

**7.3. Molecular modeling of the binding of (*R*), (*S*) and (*R*/*S*)-salsolinol on μ-opioid receptors.**

*7.3.1. Molecular mechanics system preparation*

The receptor systems were prepared using the crystal structure of the mouse μ-opioid receptor bound to the covalent antagonist β-funaltrexamine (bound to K233), obtained from the protein data bank (ID: 4DKL) (Manglik et al. 2012). This structure was modified for the simulations. A region corresponding to the T4 lysozyme was replaced with the six original residues that were missing from the crystallized μ-opioid receptor, from M264 to K269 (Manglik et al. 2012), using the loop module of Modeller (Fiser, Do, and Sali 2000). A dimer system with an extensive contact between TM5 and TM6 was prepared following the observed dimerization in the crystal structure (Manglik et al. 2012). The coordinates of water molecules, a chloride ion and a cholesterol that came along the crystal structure were kept for the full system which was assembled adding a rectangular membrane of palmitoyl-oleoyl-glycerophosphocholine (POPC) with 10% cholesterol and 0.15 NaCl in TIP3P water. This structure was built using the online platform CHARMM-GUI (Jo et al. 2008) and was minimized for 3000 steps using the conjugate gradient method. The minimization was harmonically restrained with forces that preserved the coordinates of the protein backbone and sidechain (10 and 5 kcal/mol/Å$^2$ respectively), the ions (10 kcal/mol/Å$^2$), the β-funaltrexamine ligand (10 kcal/mol/Å$^2$), the tail and heads of the lipids (2.5 kcal/mol/Å$^2$) and their double bonds and chirality (500 kcal/mol/rad$^2$), and prevented the water molecules to enter the membrane (2.5 kcal/mol/Å$^2$). These forces were gradually diminished during a subsequent equilibration using NAMD (2 fs per step) (Phillips et al. 2005). The temperature of the system during equilibration started at 303.15 K and was reassigned every 500 steps. Lennard-Jones interactions were calculated with a cutoff from 10 to 12 Å using a switching function. After 10 ns, the β-funaltrexamine ligand was removed from both monomers, and

the complete side chain of the K233's were restored, leaving two empty binding sites. This equilibration and the rest of the molecular dynamics simulations used the CHARMM36 force field and were performed with periodic boundary conditions, where the infinite electrostatic interactions were calculated by the Particle mesh Ewald summation method (Darden, York, and Pedersen 1993).

### *7.3.2. Molecular docking*

Four dimer systems were used for the molecular simulations, which meant eight empty binding sites in where the SAL enantiomers were positioned. Autodock Vina (Trott 2010) was used to calculate 9 possible poses of (*R*) and (*S*)-SAL on each monomer of the dimer, with a searching exhaustiveness of 800 (default 8). The search space was 24 $Å^3$ around a side-chain oxygen of D147. Only systems with the same enantiomer in both monomers were prepared. For each receptor monomer, two poses for each enantiomer were chosen using the following criteria: SAL:N-O:D147 distance of <4 Å, prioritizing minimum docking score. The docking poses were also defined as orthosteric if they had similar coordinates compared to the morphinan scaffold of β-funaltrexamine. None of the poses obtained for (*R*)-SAL on monomer B fulfilled the three criteria, so the poses chosen for simulation were similar to the ones chosen for (*S*)-SAL in the same monomer.

### *7.3.3. Molecular dynamics simulations*

The molecular dynamics parameters for the salsolinol molecule were prepared using the CHARMM General Force Field (Vanommeslaeghe et al. 2010), and the high penalty parameters were optimized using the ForceField Toolkit (Mayne et al. 2013). First, 100 ns equilibrations were completed for each system, reassigning the temperature every 500 steps as above. For the production simulations (300 ns for each system), the temperature (303.15 K) and pressure (1 atm) were kept constant using Langevin dynamics and Langevin Piston dynamics, respectively. Coordinates were saved every 25.000 steps, completing 6.000 frames for each simulation. Analyses were performed using VMD software (Humphrey, Dalke, and Schulten 1996).

## 7.4. Conditioned place preference of (*R*) and (*S*)-salsolinol

To determine whether (*R*) or (*S*)-salsolinol can induce a conditioned place preference, 12 female rats selectively bred for their ethanol consumption (UChB line) were used. Under isoflurane anesthesia, the rats were stereotaxically implanted with a 22-gauge guide cannula (Plastics One, Virginia, USA) into the left VTA (anteroposterior, -5.6 mm; lateral,-0.5 mm, dorsoventral,-7.4 mm; from Bregma, (Paxinos and Watson 1998)). One week after surgery the rats were habituated to a chamber with two different connected compartments, black walls/flat floor and white walls/perforated floor. The animals least preferred compartment was determined, allowing them to roam between compartments for 20 minutes in three consecutive days. The conditioning phase was performed in the following sessions. The rats were distributed into three groups and were injected with 1 µL of: i) (*R*)-SAL $10^{-5}$ M diluted in artificial cerebrospinal fluid (aCSF: 120.0 mM NaCl, 4.8 mM KCl, 1.2 mM $KH_2PO_4$, 1.2 mM $MgSO_4$, 25.0 $NaHCO_3$, 1.2 mM $CaCl_2$, 10 mM D-glucose, and 0.2 mM ascorbate, pH 6.5), ii) (*S*)-SAL $10^{-5}$ M diluted in aCSF or iii) vehicle solution (aCSF) into the VTA and placed in their least preferred compartment for 30 minutes (described by (Quintanilla et al. 2014)). This was performed on days 1, 3 and 5. On days 2, 4 and 6, aCSF (1 µL) was injected into the VTA of rats, then placed in the opposite compartment from their previous injection. On day 7, the rats were placed in the chamber for 20 minutes allowing them to move between compartments to determine their post-conditioning compartment preference. In all cases, rats in the chamber were recorded on video to establish the time spent in each compartment.

### 7.5. Determination of (*R*), (*S*) and (*R*/*S*)-salsolinol activity on the human dopamine transporter.

To determine the inhibitory activity of ligands on the dopamine transporter, a fluorescent dopamine analog was used (proprietary name, Neurotransmitter Transporter Assay Kit, Molecular Devices) to be taken by the dopamine transporter in a cell-based assay. This fluorescent analog is mixed in a solution with a fluorescence quencher that extinguishes any signal of the analog in the assay media. The combination of the fluorescent analog and the quencher allows measuring the analog only when it is separated from the quencher by entering to tightly adhered cells. For this study HEK293 cells were transfected with a plasmid encoding the human dopamine transporter (phDAT, a kind gift from Dr. Gary Rudnick, Department of Pharmacology, Yale University), using FuGENE HD (Promega, Madison, WI, USA) following the manufacturer instructions. The expression of the transfected protein was determined by Western blots. As a positive control for the presence of the dopamine transporter, mouse synaptosomes were used. To obtain the synaptosomes, whole brains extracted from 2 mice (C57BL/6 strain) were homogenized together in 20 volumes of 320 mM sucrose, 5 mM HEPES, pH = 4; using a Teflon-glass homogenizer. The homogenate was centrifuged at 1000 g for 20 minutes at 4°C. The supernatant was centrifuged at 12000 g for 20 minutes at 4°C. The pellet, enriched for the synaptosomal fraction, was stored at -80°C until further analysis. For analysis, proteins from the synaptosomes or HEK293 cells, transfected or non-transfected, were extracted using RIPA buffer.

The presence of a ligand of the human dopamine transporter delays the entrance of the fluorescent dopamine analog into the cell, allowing for the determination of the ligand inhibitory concentration. The assay buffer was Hank's balanced salt solution (Gibco, Grand Island, NY, USA), 1 mM ascorbic acid, 20 mM HEPES, pH 7.3. The (*R*) and (*S*) enantiomers and racemic salsolinol were dissolved in HCl $10^{-5}$ M and assayed at nine different concentrations. Dopamine was also assayed as a control. The transfected HEK293 cells were incubated with the ligands in assay buffer for 30 min at 37°C. Then, 0.5 µM of a the fluorescent dopamine analog (final concentration) was added to the cells, measuring the emitted fluorescence every 22 seconds for 30 minutes at 37°C (excitation 440 nm, emission 520 nm) using a microplate reader (SpectraMax M3, Molecular Devices). The total fluorescence area under the curve was plotted v/s the ligand concentration (log, M) using GraphPad. The $IC_{50}$ was determined for each ligand from a non-linear log. inhibitor vs. response (three parameters) graph. To determine the inhibition constant ($K_i$) of the ligands the Cheng-Prusoff equation was employed:

$$K_i = \frac{IC_{50}}{1 + \frac{[AG]}{K_m}}$$

In this case, the agonist (AG) was the fluorescent dopamine analog at 0.5 µM. The $K_m$ was determined by a Michaelis-Menten plot of the velocity (slope) of uptake v/s concentration. The plot was prepared from the fluorescence emitted by the transfected cells, incubated with the analog alone for 10 min, 37°C, at six different concentrations (0.1 to 4 µM). The slope of the fluorescence readings was fitted to determine the analog $K_m$, calculating the $K_i$ for each ligand.

### 7.6. Determination of salsolinol levels in rat brain homogenates.

#### *7.6.1. Animal treatment to study the influence of a catechol-O-methyl transferase inhibitor*

To study the effect of COMT inhibition on the levels of salsolinol, we used male UChB rats naïve to ethanol consumption. Animals were anesthetized with chloral hydrate and set in a stereotaxic apparatus. Under isoflurane anesthesia a rat was administered 3 µL of 100 µM SAL + 500 µM entacapone in artificial cerebrospinal fluid (aCSF: 145 mM NaCl, 2.7 mM KCl, 1.2 mM $CaCl_2$, 1.2 mM

$MgCl_2$, 2 mM $Na_2HPO_4$) with 1.5% DMSO into the left VTA (coordinates from bregma: -5.6 mm AP, -0.6 mm L, -7.4 mm DV from the surface of the dura mater) in 30 min at 0.1 µL/min. Another animal was administered 3 µL of 100 µM SAL alone in the same vehicle (1 rat per group).

*7.6.2. Animal treatment to study the appearance of salsolinol after an ethanol administration*

To determine the brain levels of SAL after ethanol administration, we used male UChB rats naïve to ethanol consumption. Animals were anesthetized with chloral hydrate and set in a stereotaxic apparatus. Under isoflurane anesthesia rats were administered with ethanol 4 g/kg in saline i.p. and, at the same time, 3 µL of aCSF with 1.5% of DMSO in the left VTA for 30 min at 0.1 µL/min (n = 2). Other animal was administered with ethanol 4 g/kg i.p. and 3 µL of a COMT inhibitor (entacapone 500 µM in aCSF with 1.5% of DMSO) into the left VTA in parallel to the ethanol i.p. administration in 30 min at 0.1 µL/min (n = 1).

*7.6.3. Brain dissection*

Two minutes after the brain infusion was done, the brain was extracted and placed on its dorsal side in a metallic matrix cast prepared for slicing the brain. A 4 mm thick slice from the anterior end of the mammillary bodies to the olfactory bulb was collected to dissect out the striatum, and from a 3 mm thick slice from the end of the pons to the first third of the mammillary bodies was dissected out to obtain the midbrain. The left and right nucleus accumbens were obtained from the striatum slice using a 2-mm diameter punch to puncture a piece on the ventral area of the slice. The left and right VTA and substantia nigra were obtained from the midbrain slice, puncturing pieces of the ventromedial area using a 1 mm punch (VTA) or ventrolateral area using a 2 mm punch (substantia nigra). The samples were weighed using pre-weighed Eppendorf tubes and immediately placed in liquid nitrogen. The tubes were stored at -80°C until homogenization.

*7.6.4. Salsolinol determination*

Depending on the tissue weight, 100-150 µL of PCA 0.1 M, EDTA 0.1 mM was added to the frozen tissue. The tissue was homogenized using an ultrasonic homogenizer (OMNI International, Kennesaw, GA, USA) and centrifuged at 18000 g for 30 min at 2°C. For HPLC analysis, 50 µL of the supernatant was injected onto a silica gel-C18 SUPELCOSIL LC-18 column, 250 mm × 4.6 mm, 5 mm particle size (Sigma-Aldrich, St. Louis, MO) kept at 25°C. The mobile phase was flowed at 0.5 mL/min using an isocratic pump (Shimadzu). It consisted of methanol 1:4 aqueous 100 mM dihydrogen sodium phosphate, $10^{-5}$ M EDTA, 1 mM sodium octanesulfonate adjusted to pH 4.0 with hydrochloric acid. The detector was an amperometric LC-4C BAS set to 0.7 V. Standard samples of dopamine, SAL, 3,4-dihydroxyphenylacetic acid (DOPAC), homovallinic acid (HVA), 5-hydroxyindolacetic acid and serotonin, prepared in distilled deionized water were injected onto the HPLC system, to determine their corresponding retention times. The same standards were used for SAL, dopamine, DOPAC and HVA calibration curves.

## 8. RESULTS

### 8.1. Separation and purification of (*R*) and (*S*)-salsolinol

The β-cyclodextrin-modified column separated the two SAL enantiomers after the injection of commercial racemic SAL. The retention time of the enantiomers was ~6.7 minutes for (*S*)-SAL and ~8.3 minutes for (*R*)-SAL with a flow rate of 0.8 ml/min, in chromatographs that show equal areas for (*R*) and (*S*)-SAL in samples from racemic salsolinol (**Fig. 3A**). The quantification of the chromatographic areas for (*R*) and (*S*)-SAL show that both purified solutions contained >99 percent of enantiomerically pure (*R*) or (*S*)-SAL (**Fig. 3B and C**) when compared to a calibration curve prepared with racemic SAL.

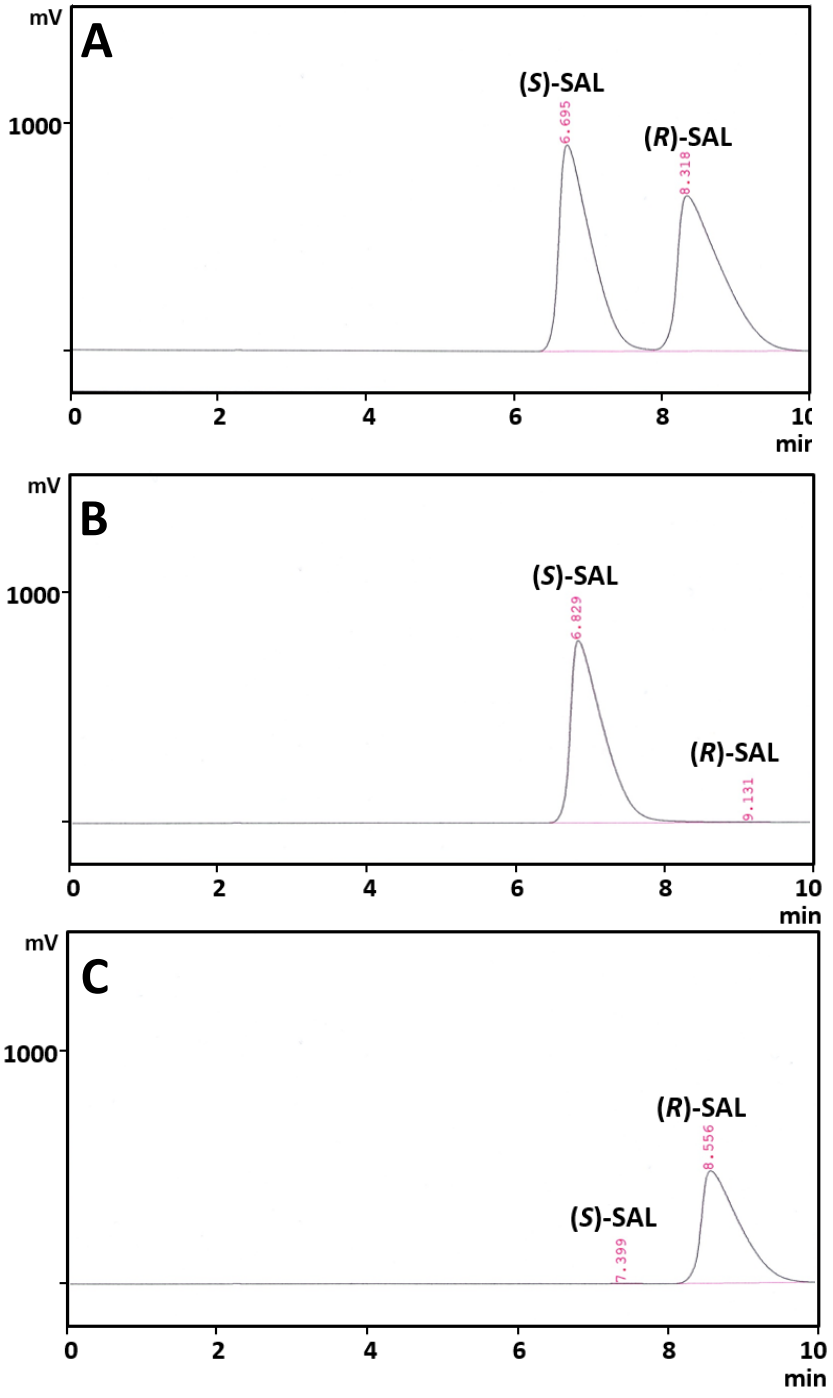


**Figure 3. Separation of (*R*) and (*S*)-salsolinol**. HPLC chromatographs of (**A**) racemic salsolinol $10^{-2}$ M ($5 \cdot 10^{-3}$ M of each enantiomer), (**B**) purified (S)-salsolinol $4.4 \cdot 10^{-3}$ M (non-detectable levels of (R)-salsolinol) and (**C**) purified (R)-salsolinol $3 \cdot 10^{-3}$ M ((S)-salsolinol $2.7 \cdot 10^{-5}$ M). Each sample was injected in 50 µL at a flow rate of 0.8 ml/min. The concentrations of the enantiomers in the purified solutions were determined using racemic salsolinol as standard.

### 8.2. Determination of the intrinsic activity of (*R*), (*S*) and (*R*/*S*)-salsolinol on μ-opioid receptors

The activation of μ-opioid receptors was studied using recombinant CHO-K1 cells that express the human μ-opioid receptor. We assayed this activation through two possible transduction pathways, $G_i$ protein activation and β-arrestin recruitment. Racemic SAL activated the receptor $G_i$ protein pathway, shown as a decrease in cAMP levels (previously raised by forskolin treatment) (**Fig. 4A**). The results show a decrease in cAMP down to similar levels when comparing SAL agonistic effect with the full agonists, met-enkephalin and morphine, showing a full agonist effect. On the other hand, SAL had a lower potency than the other assayed ligands (**Table 1**). Racemic SAL did not promote the recruitment of β-arrestin in CHO-K1 cells (**Fig. 4B**).

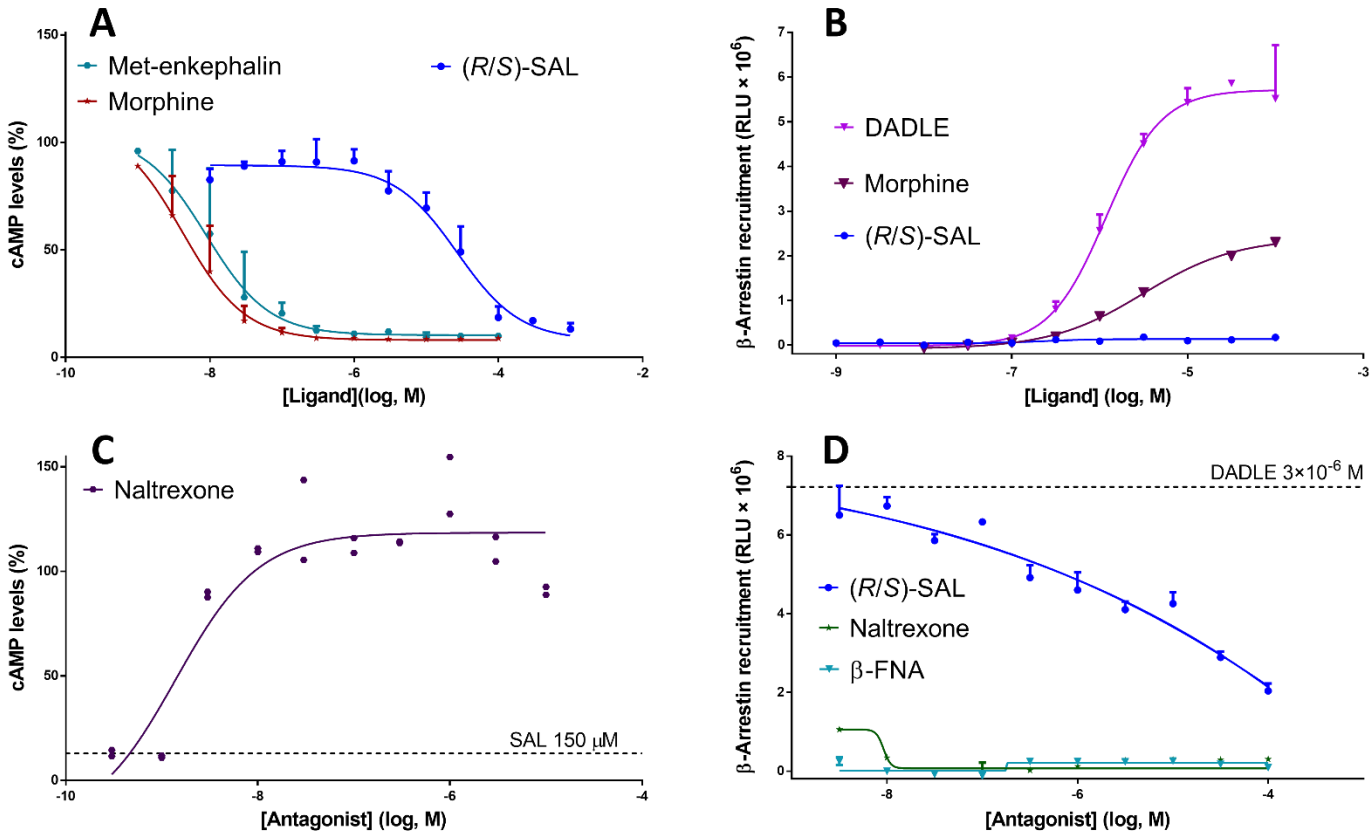


**Figure 4. Intrinsic activity and functional selectivity of racemic salsolinol on μ-opioid receptors.** Functional analysis of dose-response activation of the μ-opioid receptor. (**A**) cAMP levels after the exposure of recombinant CHO-K1 expressing the human μ-opioid receptor to morphine (n = 2), met-enkephalin (n = 2) or (R/S)-salsolinol (n = 3) (forskolin was added before the ligands to raise cAMP levels; % of cAMP levels are relative to control with no ligand added). (**B**) Degree of β-Arrestin recruitment after the treatment with DADLE, morphine or (R/S)-SAL, in recombinant CHO-K1 cells expressing the human μ-opioid receptor (n = 1). (**C**) cAMP levels in cells pre-treated with different concentrations of naltrexone for 30 min and then exposed to SAL 150 μM (n = 1). (**D**) Degree of β-arrestin recruitment in cells pre-treated with naltrexone, β-funaltrexamine or (R/S)-SAL and then exposed with DADLE 3 μM (n = 1). All the experiments were performed in duplicate (Berrios-Carcamo et al. 2016).

When studying the ability of a pre-exposure to an antagonist to block SAL activation of the $G_i$ protein pathway, we observed that naltrexone dose-dependently blocked that effect (**Fig. 4C**). Similarly, a pre-exposure with SAL blocked the β-arrestin recruitment induced by DADLE in CHO-K1 cells (**Fig. 4D**). In the experiments studying the effect of SAL on the $G_i$ protein pathway (as an agonist) or β-arrestin recruitment (as an antagonist) there was a similar dose-response potency (**Fig 4A, D**), suggesting that the two effects produced by SAL depend upon binding to the same site. When analyzing enantiomeric specificity, purified (*S*)-SAL was 50 times more potent than purified (*R*)-SAL on the activation of the μ-opioid receptor $G_i$ protein pathway (**Fig. 5**), showing a similar potency that the observed for racemic SAL (**Table 1**).

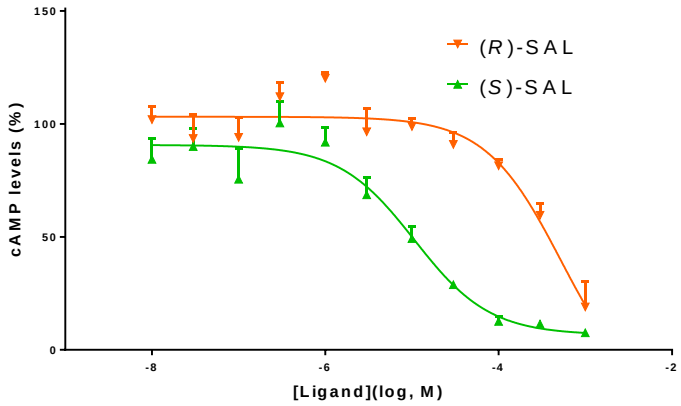


**Figure 5. Enantiomeric specificity of salsolinol on μ-opioid receptors.** Analysis of enantiomeric selectivity in the activation of the μ-opioid receptor. cAMP levels after the exposure of recombinant CHO-K1 that expressed the human μ-opioid receptor with (*R*) or (*S*)-salsolinol (n = 3) (forskolin was added before the ligands to raise cAMP levels; % of cAMP levels relative to control with no ligand added).

**Table 1. Concentrations for producing half-maximal effect ($EC_{50}$) and coefficient of determination ($R^2$) of ligands tested on CHO-K1 cells transfected with the human μ-opioid receptor.**

| Ligand | $EC_{50}$ (M) | $R^2$ |
|---|---|---|
| **Met-enkephalin** | $8.9 \cdot 10^{-9}$ | 0.884 |
| **Morphine** | $4.2 \cdot 10^{-9}$ | 0.928 |
| **(*R*/*S*)-Salsolinol** | $2.7 \cdot 10^{-5}$ | 0.881 |
| **(*R*)-Salsolinol** | $5.2 \cdot 10^{-4}$ | 0.827 |
| **(*S*)-Salsolinol** | $1.1 \cdot 10^{-5}$ | 0.907 |

### 8.3. Molecular modeling of the binding of (*R*) and (*S*)-salsolinol on μ-opioid receptors

To support our experimental results showing the agonistic effect of SAL on μ-opioid receptors, we performed computational molecular dynamics simulations of (*R*) and (*S*)-SAL docked into the mouse μ-opioid receptor binding pocket. The prepared receptor used the protein coordinates of the crystallized receptor bound to the opioid antagonist β-funaltrexamine (Manglik et al. 2012). Following the crystal remarks, we prepared a protein dimer located in a lipid bilayer surrounded by explicit water. We expected these simulations to show differences that favor the enantiomer with higher agonistic potency, regarding stability of the ligand coordinates with respect to the protein and in terms of prevalent interactions with residues of the binding site.

#### *8.3.1. Ligand placement and correlation of the salsolinol structure with morphinan ligands*

To our knowledge, this is the first time that a salsolinol molecule is modeled in the binding site of the μ-opioid receptor. For this reason, the first challenge to perform the simulation was to locate the SAL molecules in the binding site, choosing the direction they will face. An important consideration was the similarity of the structures of salsolinol and the morphinan scaffold of opioid ligands (**Fig. 6**), this allowed us to compare the coordinates of the crystallographic β-funaltrexamine and establish a theoretical orthosteric position for SAL. Then, we used molecular docking to screen for positions with favored interactions. From the nine positions screened, we choose two poses for (*R*) and (*S*)-SAL on each monomer of the μ-opioid receptor dimer, prioritizing the mentioned opioid orthosteric position, higher docking score, and interaction with D147 (<4 Å from the SAL basic nitrogen), critical for the binding of almost every μ-opioid receptor ligand (Mansour et al. 1997; Harding et al. 2005). We termed the eight simulations: S1A-B, S2A-B, R1A-B and R2A-B (**Table 2**).

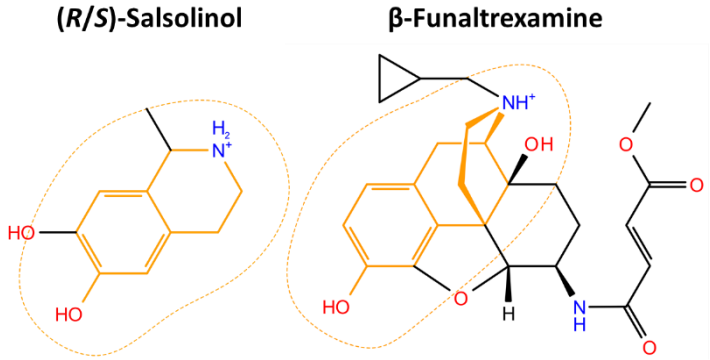


**Figure 6. Comparison of (*R*/*S*)-salsolinol and β-funaltrexamine structures.** The parts of the molecule that were correlated for the determination of the orthosteric coordinates are highlighted in yellow.

**Table 2. Molecular docking poses of (*R*) and (*S*)-salsolinol in the μ-opioid receptor dimer empty binding pockets.** Each dimer was prepared four times, totaling eight sites for salsolinol simulation. The used poses are highlighted in gray. ‡ Refers to the minimum distance between the secondary amine nitrogen of salsolinol and a side chain oxygen of D147. * Orthosteric location but facing the opposite direction.

| **(*R*)-Salsolinol** | | | | | | | |
|---|---|---|---|---|---|---|---|
| **Monomer A** | | | | **Monomer B** | | | |
| **Score** | **N-O (Å) ‡** | **Orthosteric?** | **Simulation** | **Score** | **N-O (Å) ‡** | **Orthosteric?** | **Simulation** |
| **-6.5** | 5.5 | No | | -6.6 | 5.72 | No | |
| **-6.3** | 3.13 | Yes | R1A | -6.6 | 6.32 | No | |
| **-6.2** | 3.17 | Yes* | R2A | -6.6 | 4.2 | No | R1B |
| **-6.2** | 5.8 | No | | -6.5 | 3.22 | No | |
| **-6.2** | 5.96 | No | | -6.4 | 5.45 | No | |
| **-6.1** | 7.07 | No | | -6.4 | 7.37 | No | |
| **-6.0** | 4.92 | Yes | | -6.2 | 5.91 | No | R2B |
| **-6.0** | 4.53 | Yes | | -6.2 | 6.96 | No | |
| **-5.9** | 7.67 | Yes* | | -6.1 | 6.41 | No | |
| **(*S*)-Salsolinol** | | | | | | | |
| **Monomer A** | | | | **Monomer B** | | | |
| **Score** | **N-O (Å) ‡** | **Orthosteric?** | **Simulation** | **Score** | **N-O (Å) ‡** | **Orthosteric?** | **Simulation** |
| **-6.4** | 3.15 | Yes | S1A | -6.7 | 5.59 | No | |
| **-6.0** | 3.39 | Yes* | S2A | -6.6 | 7 | No | |
| **-6.0** | 5.33 | No | | -6.5 | 5.26 | No | |
| **-6.0** | 6.21 | No | | -6.5 | 3.08 | No | S1B |
| **-5.9** | 6.69 | No | | -6.5 | 3.1 | Yes | S2B |
| **-5.9** | 4.74 | No | | -6.5 | 5.27 | No | |
| **-5.8** | 9 | No | | -6.4 | 6.09 | No | |
| **-5.7** | 7.58 | Yes* | | -6.4 | 4.39 | No | |
| **-5.7** | 4.42 | No | | -6.3 | 5.26 | No | |

### *8.3.2. Conformation and orientation of salsolinol in the simulations*

Simulations were first analyzed by root-mean-square deviation (RMSD) comparing the SAL position over time to their respective monomer initial coordinates after equilibration (**Fig 7**). This analysis sought to determine in which simulations SAL showed stable dynamics, which would be consistent with the behavior of a ligand with stable interactions, which are necessary for μOR agonistic activity (Shim, Coop, and MacKerell 2013). For (*S*)-SAL the simulations with lower deviation, less than 2 Å in average (**Table 3**), were the ones with starting coordinates closer to the orthosteric position (S1A and S2B, **Fig. 8**). The orthosteric position for (*S*)-SAL was anchored to D147 and H297 via the SAL basic nitrogen and a catechol oxygen, respectively. In S1B and S2A simulations (*S*)-SAL was less stable (**Table 3**) and transitioned to a different position from the starting point (**Fig. 8**). S1B transitioned to a more stable position after ~120 ns (**Fig 7**) and reached the orthosteric position at the end of the simulation (**Fig**. **9**), however, its chiral methyl group pointed to the opposite side compared to the positions of (*S*)-SAL in S1A and S2B (**Fig. 9**). Of the four (*S*)-SAL simulations, in S1A and S2B (*S*)-SAL contacted most residues of the μ-opioid receptor binding site, mainly with D147, Y148, V236 and H297 (**Table 4**). The simulations that included (*R*)-SAL also varied in their stability. In the most stable simulation R1B (**Table 3**)-(*R*)-SAL did not start in the orthosteric position, interacted mostly with D147

and W293, but missed the interaction with the rest of the binding site (**Table 4**). The simulations with (*R*)-SAL starting closer the orthosteric position (R2A and R2B, **Fig. 8**) were not stable in their starting coordinates and diverged with an RMSD that reached 8.1 Å and 3.7 Å by the end of the simulation, respectively (**Table 3**, **Fig. 7**). Regarding (*R*)-SAL interaction with the binding site, R2B simulation was closer to what is expected for μ-opioid receptor agonists. In this simulation, (*R*)-SAL contacted the key residues D147, W293 and H297 for more than half of the simulation (**Table 4**). However this was still less than the full interaction expected for agonists, especially with D147 (Shim, Coop, and MacKerell 2013).

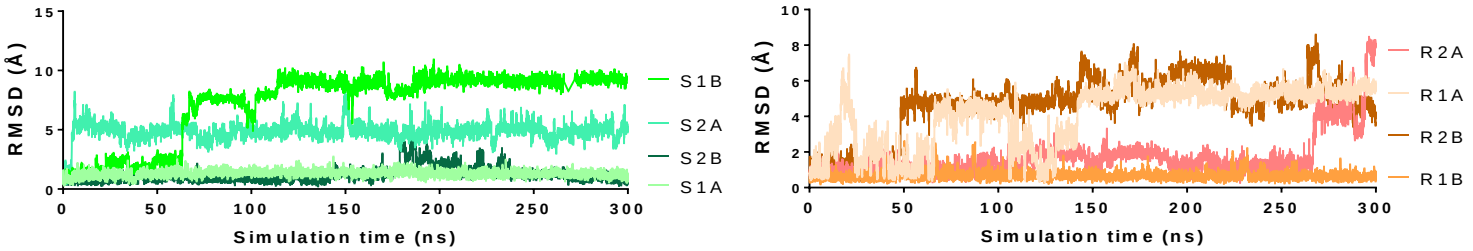


**Figure 7. Stability of salsolinol molecules in the μ-opioid receptor binding site.** Salsolinol root mean square deviation (RMSD) within the μOR binding site, after 300 ns equilibration. S1A, S1B, S2A and S2B; R1A, R1B, R2A and R2B correspond to simulations of (S)-SAL and (R)-SAL, respectively, in the monomers A or B of the receptor dimer.

**Table 3. Salsolinol simulation stability parameters obtained from root-mean-square deviation analyses.**

| | (*S*)-Salsolinol simulations | | | | (*R*)-Salsolinol simulations | | | |
|---|---|---|---|---|---|---|---|---|
| | **S1A** | **S1B** | **S2A** | **S2B** | **R1A** | **R1B** | **R2A** | **R2B** |
| **Average RMSD (Å)** | 1.313 | 7.220 | 4.871 | 1.223 | 4.088 | 0.683 | 1.695 | 4.619 |
| **Final RMSD (Å)** | 0.737 | 8.885 | 5.273 | 1.014 | 6.009 | 0.494 | 8.092 | 3.697 |

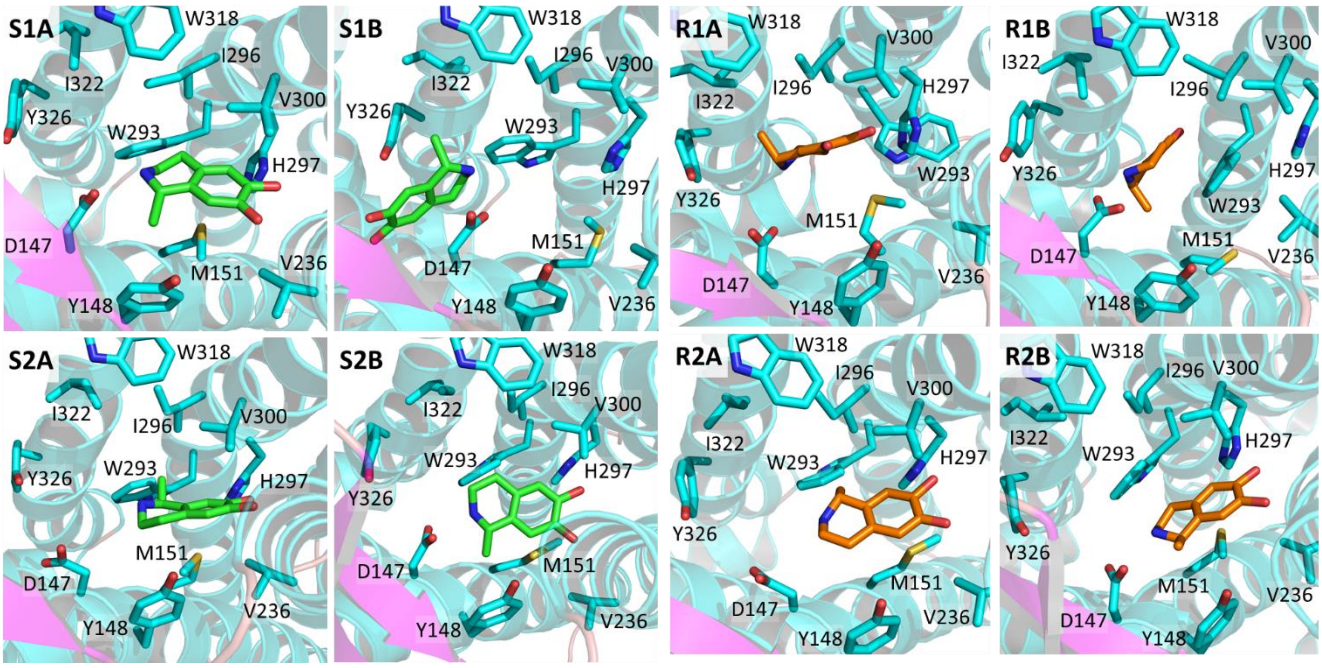


**Figure 8. Salsolinol starting coordinates for molecular dynamics simulations within the μ-opioid receptor binding site, after equilibration.** S1A, S1B, S2A and S2B; R1A, R1B, R2A and R2B correspond to simulations of (*S*)-SAL and (*R*)-SAL, respectively, in the monomers A or B of the receptor dimer.

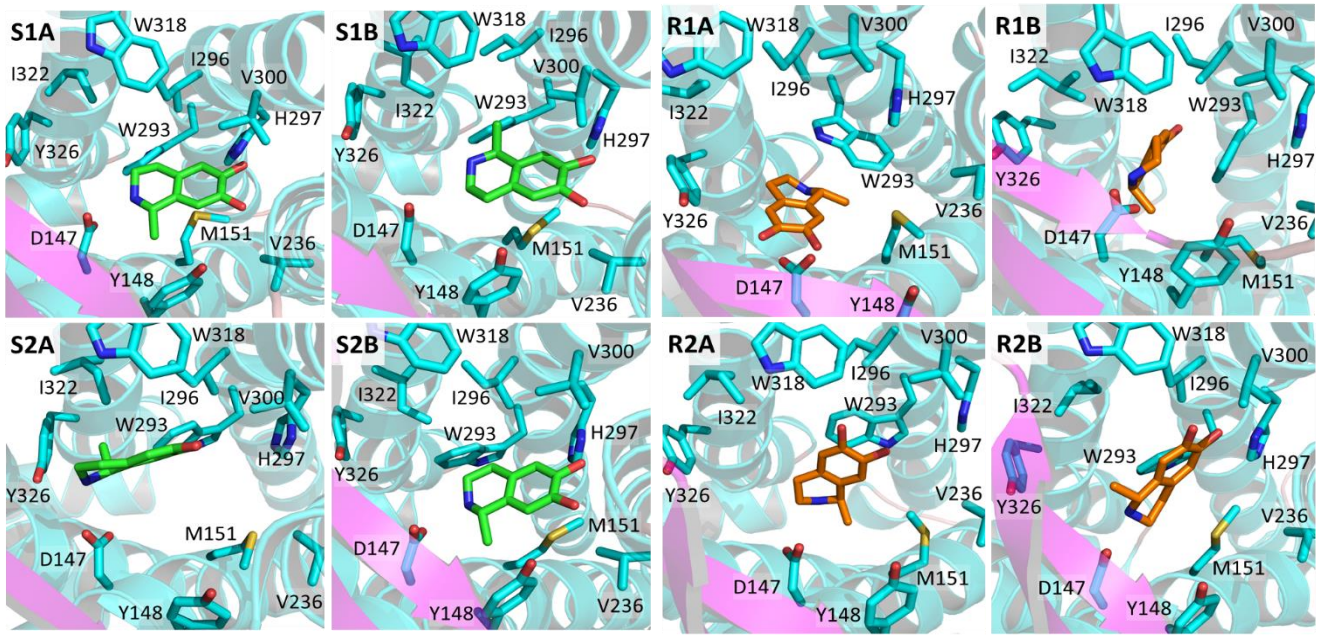


**Figure 9. Salsolinol final coordinates within the μ-opioid receptor binding site, after 300 ns of simulation.** S1A, S1B, S2A and S2B; R1A, R1B, R2A and R2B correspond to simulations of (*S*)-SAL and (*R*)-SAL, respectively, in the monomers A or B of the receptor dimer.

**Table 4. (*R*) and (*S*)-salsolinol probability of interaction (less than 4 Å) with the residues of the binding site of the μ-opioid receptor** (interactions highlighted: blue 1-0.5, green 0.5-0.1, red < 0.1; Av: average probability. *Including every residue except W318, I322 and Y326).

| Sim. | D147 | Y148 | M151 | V236 | W293 | I296 | H297 | V300 | Av.* | W318 | I322 | Y326 |
|---|---|---|---|---|---|---|---|---|---|---|---|---|
| **S1A** | 0.988 | 0.820 | 0.513 | 0.930 | 0.292 | 0.123 | 0.996 | 0.130 | **0.599** | 0.000 | 0.005 | 0.000 |
| **S1B** | 0.796 | 0.426 | 0.330 | 0.495 | 0.389 | 0.045 | 0.707 | 0.347 | **0.442** | 0.000 | 0.021 | 0.005 |
| **S2A** | 0.983 | 0.001 | 0.090 | 0.061 | 0.507 | 0.040 | 0.262 | 0.028 | **0.247** | 0.017 | 0.133 | 0.649 |
| **S2B** | 0.961 | 0.764 | 0.438 | 0.824 | 0.428 | 0.065 | 0.884 | 0.640 | **0.626** | 0.000 | 0.027 | 0.002 |
| **R1A** | 0.630 | 0.027 | 0.234 | 0.108 | 0.405 | 0.072 | 0.267 | 0.195 | **0.242** | 0.002 | 0.126 | 0.018 |
| **R1B** | 0.979 | 0.000 | 0.011 | 0.000 | 0.600 | 0.003 | 0.000 | 0.000 | **0.160** | 0.000 | 0.061 | 0.000 |
| **R2A** | 0.439 | 0.385 | 0.391 | 0.618 | 0.398 | 0.252 | 0.173 | 0.399 | **0.382** | 0.010 | 0.000 | 0.000 |
| **R2B** | 0.763 | 0.062 | 0.414 | 0.155 | 0.543 | 0.021 | 0.748 | 0.236 | **0.368** | 0.001 | 0.147 | 0.027 |
| **Av.** | **0.817** | **0.311** | **0.303** | **0.399** | **0.406** | **0.078** | **0.505** | **0.247** | **0.383** | **0.004** | **0.065** | **0.088** |

### *8.3.3. Comparison of (R) and (S)-SAL interactions with the μ-opioid receptor binding site*

The only difference between the (*S*) and (*R*)-SAL molecular structures is the orientation of the chiral methyl group in position 1 (**Fig. 2**). As shown (**Fig. 5**), this difference generated a gap of 50 times in the potency of μ-opioid receptor agonism and that should be reflected in their behavior within the receptor binding site. The simulations of (*S*)-SAL in the orthosteric position show that the methyl group interacted with Y148 for almost the whole simulation (**Fig. 8, 9**; **Table 4**). This interaction promoted (*S*)-SAL position in the site as it significantly correlated with the contact to D147 in S1A and S2B (**Fig. 10A**). The interaction of (*R*)-SAL with D147 and Y148 also correlated positively in R2A and R2B (**Fig. 10B**), however the binding to Y148 was unstable as it only happened for a minority of the simulation (**Table 4**). For example, in R2B the chiral methyl group interacted with Y148 while (*R*)-SAL was located in the orthosteric position (**Fig. 10C**, 250 ns). (*R*)-SAL, however, was not stable in that position and shifted away from D147 and the methyl group moved to contact with I322 and Y326 (**Fig. 10C,** 280 ns). We conclude that the chiral methyl group contributed to the stability of (*S*)-SAL, but hindered (*R*)-SAL permanence in the orthosteric position.

### *8.3.4. Activation of the μ-opioid receptor by (S)-salsolinol*

After analyzing enantiomeric specificity, we examined the interactions (*S*)-SAL established to activate the receptor. The simulations of (*S*)-SAL showed that it could only bind a subset of the residues of the binding site at the same time, which is expected considering that SAL is a small molecule (179 Da) compared to other μ-opioid ligands. In the simulations where (*S*)-SAL was most stable, it contacted the most residues of the receptor binding site. The probability of contact (at a distance of <4 Å) with the residues of the binding site was 0.599 in S1A and 0.626 in S2B, in average (**Table 4**). The calculated averages did not consider interaction with W318, I322, or Y326 that also belong to the receptor binding site. These residues are far from the defined orthosteric site, and SAL cannot interact with them without leaving the site. Consequently, SAL did not contact these residues in most of the simulations (contact probability < 0.1 in average considering all eight simulations, **Table 4**).

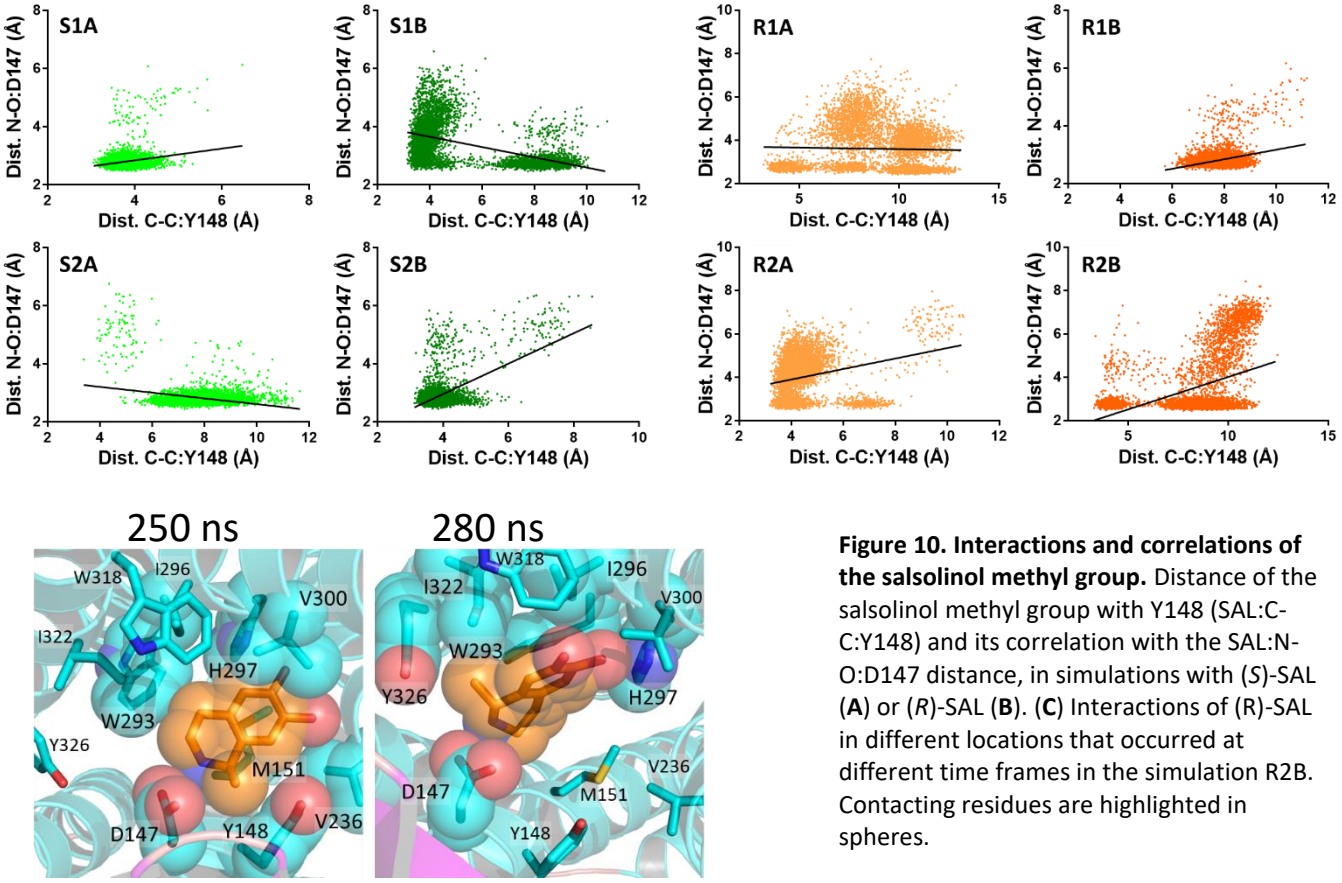


**Figure 10. Interactions and correlations of the salsolinol methyl group.** Distance of the salsolinol methyl group with Y148 (SAL:C-C:Y148) and its correlation with the SAL:N-O:D147 distance, in simulations with (*S*)-SAL (**A**) or (*R*)-SAL (**B**). (**C**) Interactions of (R)-SAL in different locations that occurred at different time frames in the simulation R2B. Contacting residues are highlighted in spheres.

(*S*)-SAL interacted mostly with D147 and H297 (**Table 4**). In S1A the average SAL:N-O:D147 and SAL:O-N:H297 distances in the simulation were 2.8 Å and 2.9 Å, respectively, which are consistent with hydrogen bonding (**Fig. 11**). (*S*)-SAL also established a polar interaction with the main chain carbonyl of K233, at 3.45 Å in average in S1A and S2B (**Fig. 11**). The hydrophobic interactions that (*S*)-SAL established ranged from the average distance of the chiral methyl to the aromatic ring of Y148 (3.79 Å), to a less prevalent interaction with I296 at 4.64 Å in average (**Fig. 11**).

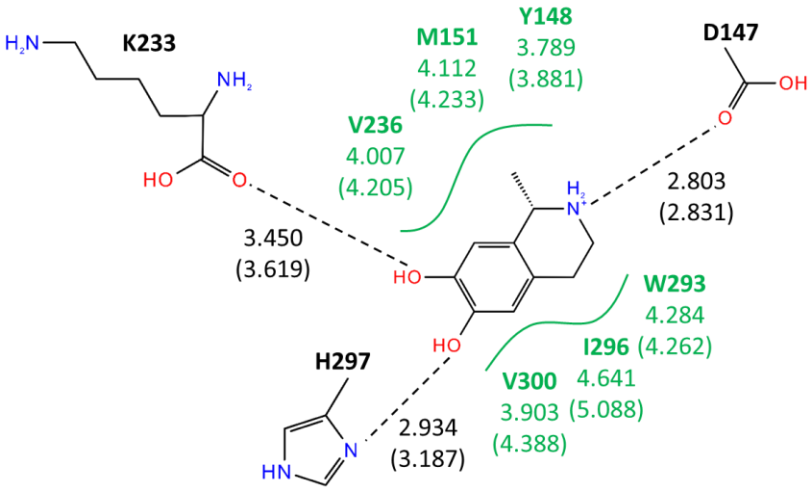


**Figure 11. Average interactions of (*S*)-salsolinol in its most stable simulations.** Hydrogen bonds are showed with dotted lines and hydrophobic interactions are showed with residues in green. Average interaction distances found in simulation S1A are shown in Å (distances found in S2B are shown in parenthesis).

To further study how (*S*)-SAL could activate μ-opioid receptors we compared the modeled protein and SAL structures to the published crystallographic inactive (Manglik et al. 2012) and active μ-opioid receptor (Huang et al. 2015). As an example, we show (*S*)-SAL S1A simulation at 210 ns compared to the positions of the crystallographic and the crystallographic agonist, and their correspondent protein coordinates. The overall simulated protein structure is similar to the aligned inactive receptor covalently bound to the antagonist β-funaltrexamine (**Fig. 12A**). However, we observed differences in two residues (W293 and N150) that are positioned closer to the receptor bound to the agonist BU72 (**Fig. 12B**). When comparing whole simulations, (*S*)-SAL promoted W293 to rotate to a position towards the W293 $\chi_2$ dihedral position in the active receptor, early in the equilibration part of the simulation (**Fig. 13A-B**). Although this is not the exact position observed in the active receptor (red dotted line in **Fig. 13A-B**), a ~700 simulation of the inactive μ-opioid receptor with the agonist β-fuoxymorphamine stabilized the W293 rotamer to the same degree (*S*)-SAL did (Huang et al. 2015). (*S*)-SAL and β-fuoxymorphamine simulations suggest that agonists need more time to complete the signal propagation. The N150 rotamer also changed position when transitioning to an active conformation. In the inactive receptor, N150 binds a sodium ion, also stabilized by D114 and S154. This ion is not found in the active crystallographic structure where N150 shifts to interact with the main chain carbonyl of I146 (**Fig. 12B**). Interestingly, a sodium ion entered the protein in the simulation S1A and got stabilized by N150, D114 and S154 in that same place (**Fig. 13D**). However, N150 shifted to a similar location to that occupied by the active receptor in S1A, despite the presence of the sodium ion (**Fig. 13C, E, F**), and in S2B (**Fig. 13D**). This shift of N150 could represent an early effect of the mechanism of μ-opioid receptor activation by (*S*)-SAL.

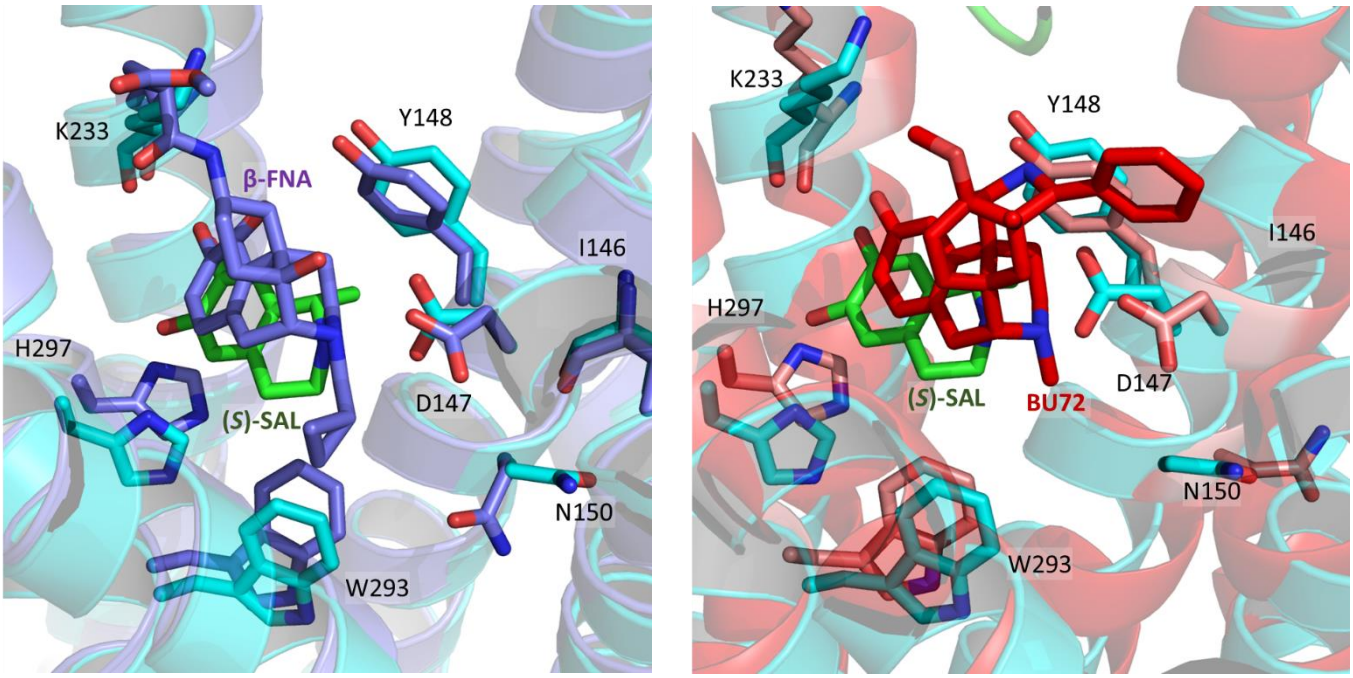


**Figure 12. Salsolinol and μ-opioid receptor active and inactive structures distinction.** Comparison of (*S*)-salsolinol and μ-opioid receptor structure in simulation S1A at 210 ns with the crystallographic coordinates of the antagonist β-funaltrexamine (β-FNA, purple) covalently attached through K233 to the μ-opioid receptor inactive structure (**A**) or with the crystallographic coordinates of the agonist BU72 (red) inside the active μ-opioid receptor structure (**B**).

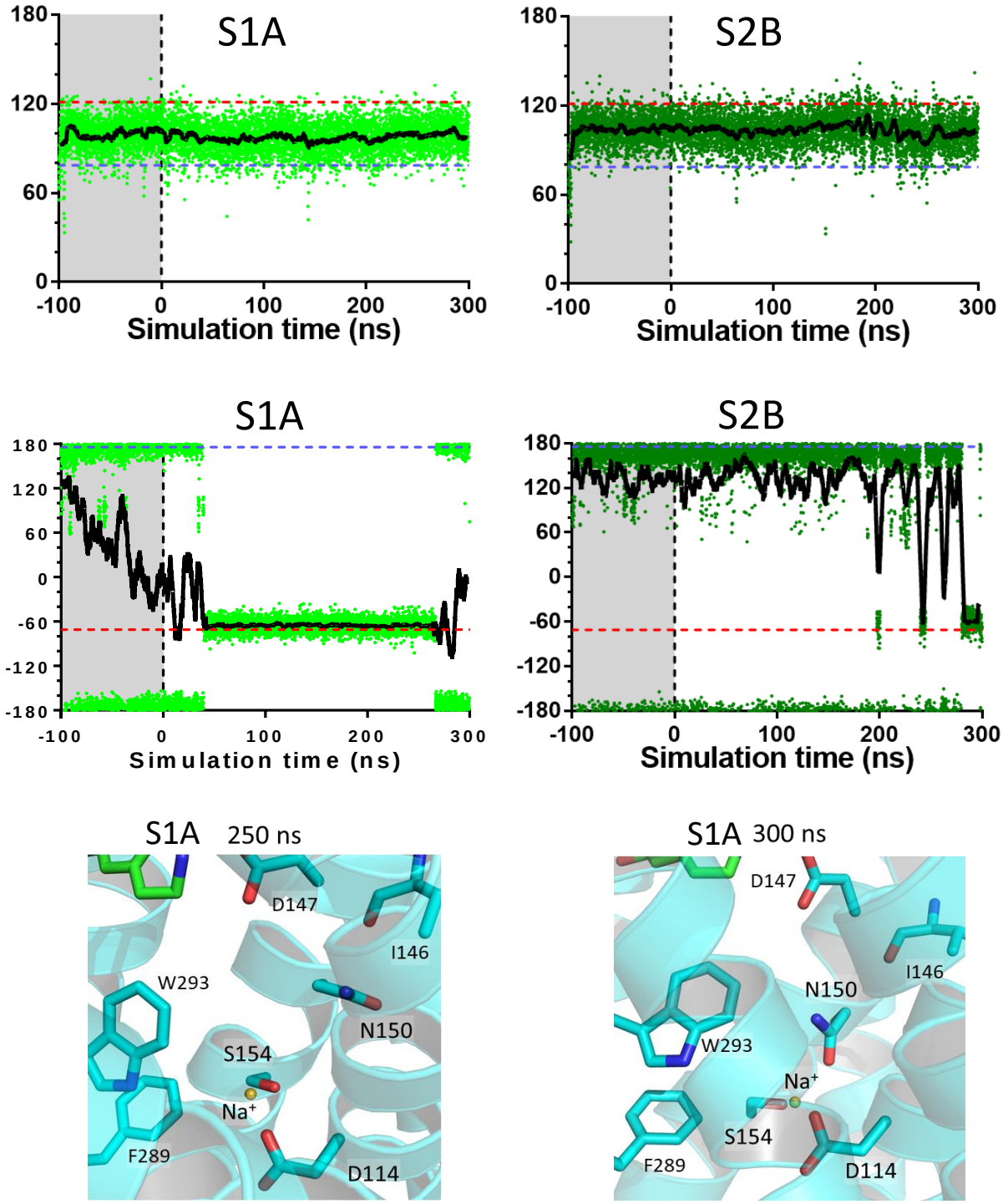


**Figure 13. Interaction of (*S*)-salsolinol with the μ-opioid receptor and propagation of transduction signal.** Dihedral $\chi_2$ angle of W293 (**A**-**B**) or $\chi_1$ angle of N150 (**C**-**D**) throughout S1A and S2B simulations, including 100 ns of equilibration time (gray area) and 300 ns of production time. The dihedral W293 $\chi_2$ angle of W293 or $\chi_1$ angle of N150 of the inactive and active μ-opioid receptors are shown as blue and red dotted lines, respectively. Coordination of the sodium ion in the μ-opioid receptor in S1A at 250 ns (**E**) and 300 ns (**F**).

### 8.4. Conditioned place preference of (*R*) and (*S*)-salsolinol

The ability of the intra-VTA infusion of (*R*) or (*S*)-SAL ($10^{-5}$ M) to induce a conditioned place preference in UChB rats was studied. The animals infused with (*R*)-SAL spent significantly more time in their initially non-preferred compartment after the conditioning phase compared with the time spent in the same compartment before the conditioning (**Fig. 14**). On the other hand, the infusion of (*S*)-SAL, or the vehicle aCSF, had no significant effect on the time spent in the compartments after or before the conditioning.

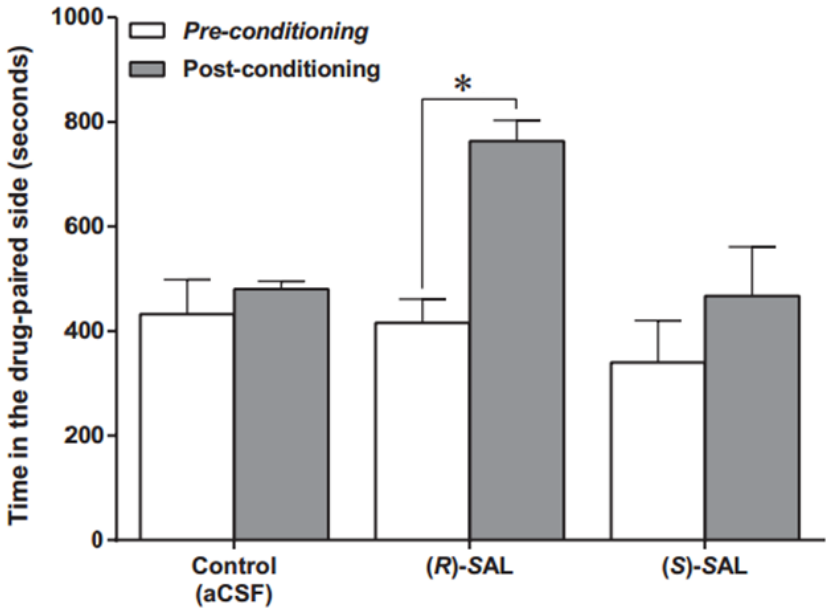


**Figure 14. Conditioned place preference of the infusion of (R) or (S)-salsolinol intra-ventral tegmental area** (n=12, 4 animals per group). Rats were infused with (R)-SAL ($10^{-5}$ M/1µl), (S)-SAL ($10^{-5}$ M/1µl) or artificial cerebrospinal fluid (aCSF) (1µl) in their non-preferred compartment. The control group received aCSF (1µl) in both compartments. Data represent means ± SEM during the pre- and post-conditioning phases. *Indicates significant difference between the time the rats spent in the drug-paired side during the post-conditioning phase versus the pre-conditioning phase ($p<0.05$; ANOVA). From (Quintanilla et al. 2016).

### 8.5. Examining possible mechanisms of salsolinol elimination

*8.5.1. Salsolinol activity in the dopamine transporter*

As a first approach to SAL activity in the dopamine transporter, we studied if SAL was a ligand of the transporter. We studied whether SAL exposure delayed the uptake of a dopamine transporter substrate. For this experiment, we transfected HEK293 cells with the human dopamine transporter (**Fig. 15**). The cells were preincubated with different concentrations of (*S*), (*R*) or (*R*/*S*)-SAL before the addition of a fluorescent dopamine analog. The inhibitory effect of dopamine on the fluorescent dopamine analog intake was also analyzed as a control. (*R*/*S*)-SAL produced a dose-dependent inhibition of the intake of 0.5 µM of the fluorescent dopamine analog (**Fig. 16A**), resulting in an $IC_{50}$ of $1.4 \cdot 10^{-3}$ M (**Table 5**). The inhibitory effect of dopamine on this system was 100 times more potent than the one by (*R*/*S*)-SAL. The effect of preincubation with (*R*) and (*S*)-SAL was difficult to see since the availability of these purified molecules was low and the points generated were not enough to fit the curve to determine an $IC_{50}$. Nonetheless, a trend of (*R*)-SAL producing the same effect as the racemic form was observed (**Fig. 16A**). The same trend was observed when preincubating both enantiomers with 1 µM of the dopamine analog, further suggesting that (*R*)-SAL was responsible for the effect observed of (*R*/*S*)-SAL (**Fig. 16B**). For (*R*/S)-SAL and dopamine, the inhibitory constants ($K_i$) were calculated using the Cheng-Prussof equation (detailed in the method section; **Table 5**).

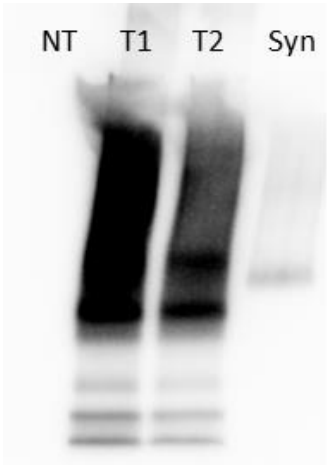


**Figure 15. Determination of the dopamine transporter protein on HEK293 cells transfected with the human dopamine transporter by Western blot.** Cells transfected in two separate occasions are showed (T1 and T2). A negative control of non-transfected cells (NT) and a positive control of whole brain mouse synaptosomes (Syn) are also shown.

**Table 5. Half-maximal inhibitory concentration ($IC_{50}$; when the dopamine analog was 0.5 µM) and the inhibition constant ($K_i$) of the ligands tested for the blockage of the uptake of the fluorescent dopamine analog in the human dopamine transporter**.

| Ligand | $IC_{50}$ (M) | $K_i$ (M) |
|---|---|---|
| **Dopamine** | $1.8 \cdot 10^{-5}$ | $1.0 \cdot 10^{-5}$ |
| **(*R*/*S*)-Salsolinol** | $1.4 \cdot 10^{-3}$ | $1.2 \cdot 10^{-3}$ |

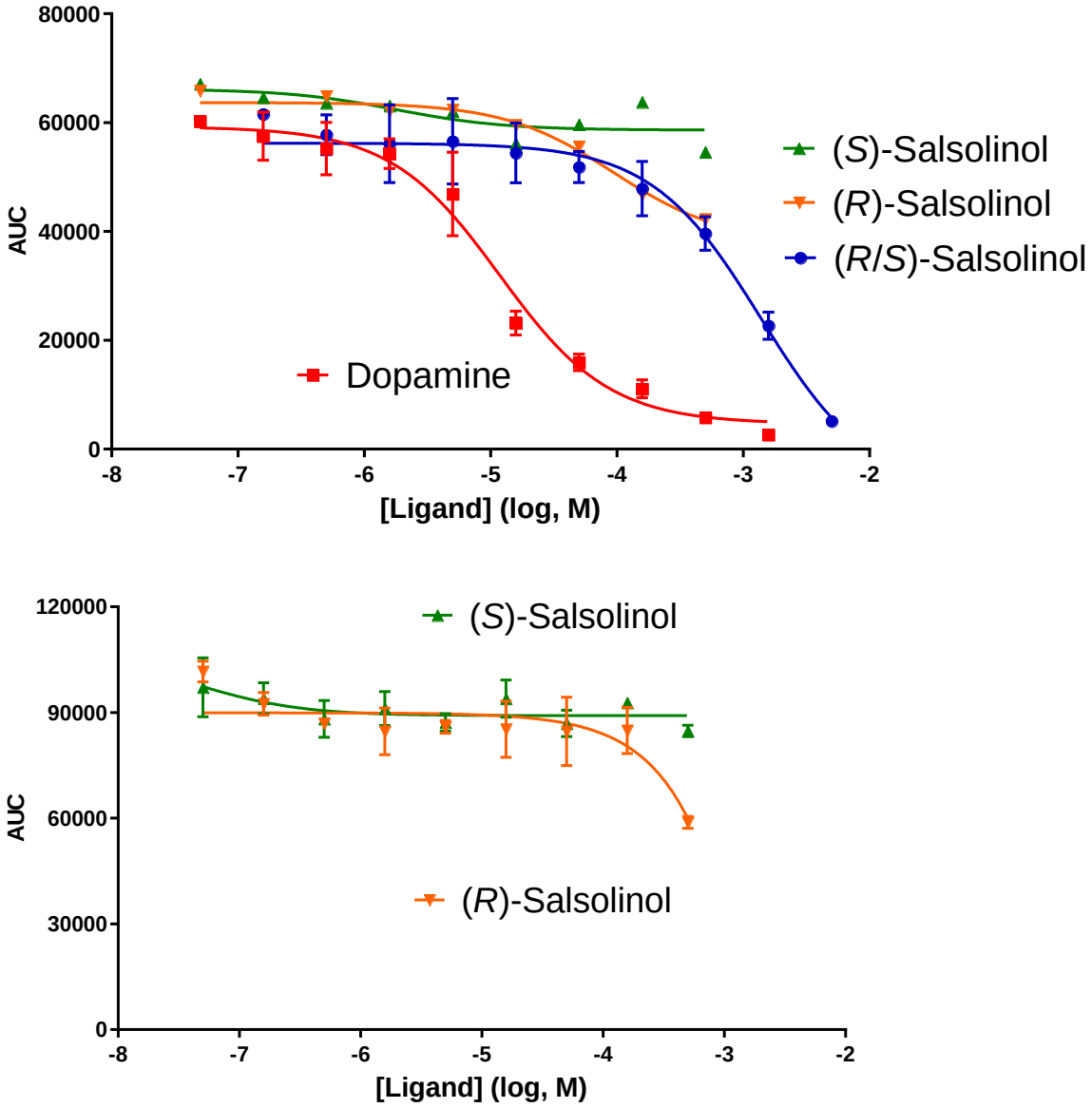


**Figure 16. Analysis of the inhibition of the uptake of the fluorescent dopamine analog by the dopamine transporter**. (**A**) HEK293 cells transfected with the human dopamine transporter were preincubated with dopamine (n=3), (R/S)-salsolinol (n=3) or the purified salsolinol enantiomers (n=1) 30 minutes before 0.5 µM dopamine analog. The analog uptake was determined by its fluorescence, only observable when it is inside the cell, as the area under the curve of a continuous measurement for 30 minutes. (**B**) In a similar experiment purified (R)-salsolinol or (S)-salsolinol (n=2 for both) were preincubated with 1 µM of the dopamine analog.

### *8.5.2. Effect of a catechol-O-methyl transferase inhibitor on the levels of salsolinol administered into the brain reward system*

The levels of dopamine, racemic SAL, and the dopamine metabolites: 3,4-dihydroxyphenylacetic acid (DOPAC), and homovanillic acid (HVA) were determined by HPLC. The analytic method was able to resolve these molecules in the matrix of a nucleus accumbens homogenate supernatant (**Fig. 17A**). DOPAC, dopamine, SAL, 5-hydroxyindoleacetic acid, homovanillic acid, and serotonin were identified using analytical standards (**Fig. 17B, C**).

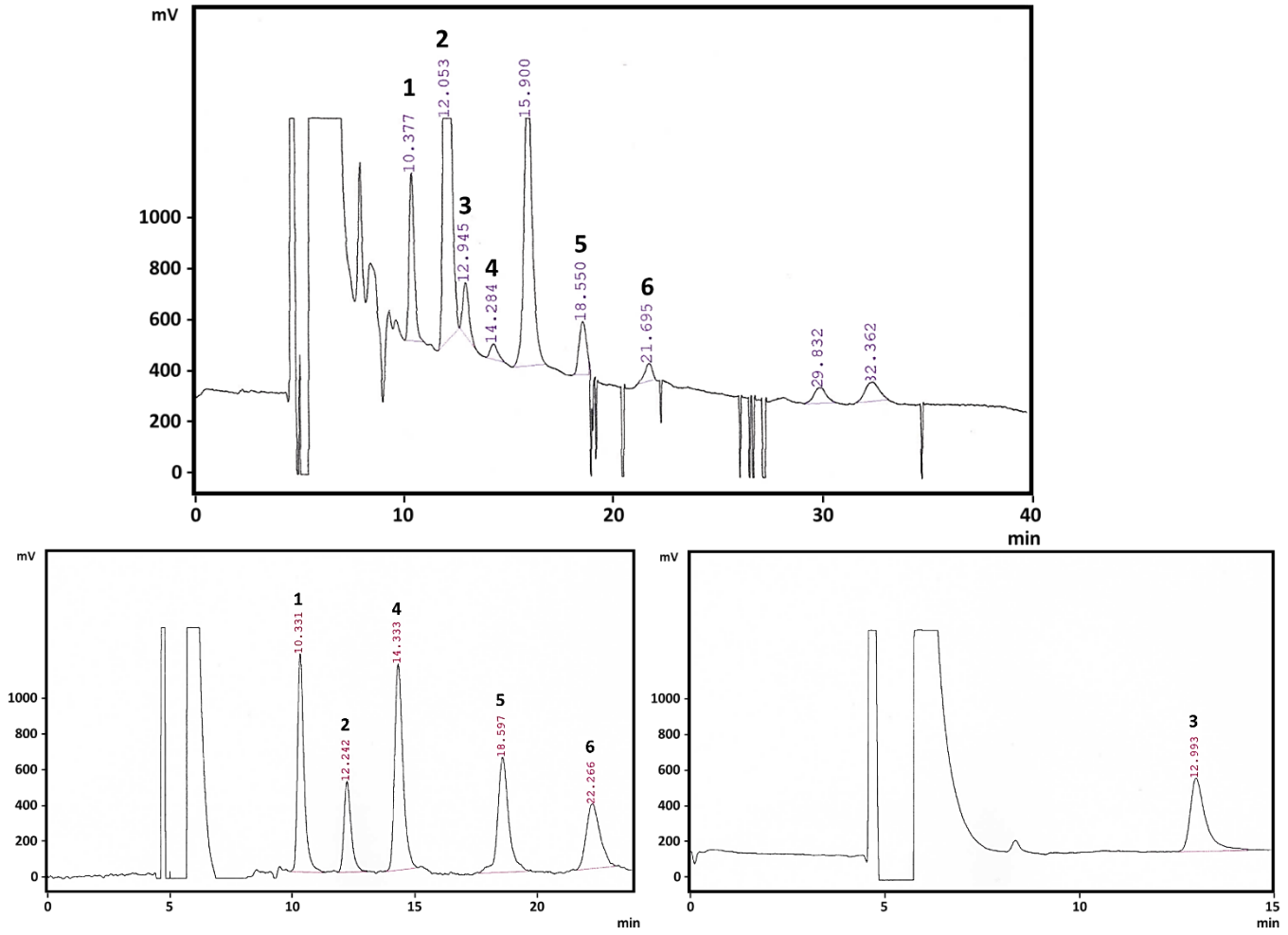


**Figure 17. HPLC chromatogram of rat ventral striatum supernatant spiked with salsolinol.** (**A**) A sample was injected in 50 µL at a flow rate of 0.5 ml/min. The retention times of the identified molecules were determined in separate injections of analytical standards (**B**, **C**). **1**, DOPAC; **2**, dopamine; **3**, salsolinol; **4**, 5-hydroxyindoleacetic acid; **5**, homovanillic acid; **6**, serotonin.

To determine whether SAL could be metabolized in the brain by a COMT, we co-injected 0.3 pmol of SAL with or without the COMT inhibitor entacapone (500 µM) into the left VTA of rats for 30 min. Then, we measured SAL levels in homogenates of the left/right VTA and left/right substantia nigra. We found SAL in homogenates from the site of injection (left VTA; **Fig. 18**; **Table 6**) and surrounded areas (right VTA and left substantia nigra; **Table 6**). No SAL was found in the right substantia nigra. When comparing the samples of animals treated or not with entacapone there were no significant differences in SAL levels when the samples were averaged. Therefore, from the experiment, it was not able to conclude if the presence of a COMT inhibitor affected the SAL levels. When analyzing whether the presence of entacapone increased the ratio of a COMT substrate (DOPAC) versus a COMT product (HVA), results were also inconclusive (**Table 6**). The inability to observe differences could be related to the high dispersion observed, which was caused by the high variability of the weight measurements of small samples that were compared as molecule mass per tissue weight.

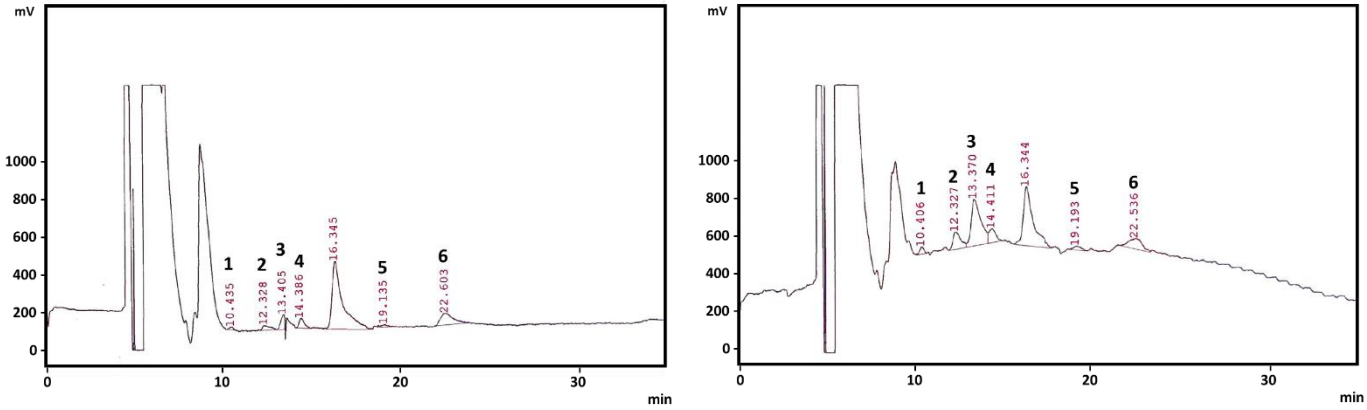


**Figure 18. HPLC chromatograms of rat left ventral tegmental area supernatants.** Analyzed tissue from an animal administered with SAL (100 µM) into the left VTA (**A**). Analyzed tissue from an animal administered SAL (100 µM) + entacapone (500 µM) into the left VTA (**B**). **1**, DOPAC; **2**, dopamine; **3**, salsolinol; **4**, 5-hydroxyindoleacetic acid; **5**, homovanillic acid; **6**, serotonin.

**Table 6**. Determination of dopamine and metabolites in supernatants from dissected brain homogenates. SAL (100 µM) or SAL (100 µM) + entacapone (500 µM) were injected into the left VTA of rats (n = 1 for each group). The levels are expressed as pmol/mg of tissue. Analyzed tissues: left substantia nigra (lSN), left VTA (lVTA), right VTA (rVTA), right substantia nigra (rSN). Averages of SAL levels don't consider the right substantia nigra (±SD).

| **Treatment** | **SAL** | | | | | **SAL + Entacapone** | | | | |
|---|---|---|---|---|---|---|---|---|---|---|
| | **lSN** | **lVTA** | **rVTA** | **rSN** | **Average** | **lSN** | **lVTA** | **rVTA** | **rSN** | **Average** |
| **Dopamine** | 7.95 | 0.63 | 2.72 | 0.95 | **3.1±3.4** | 5.79 | 1.82 | 6.04 | 3.73 | **4.3±2.0** |
| **Salsolinol** | 5.90 | 2.39 | 1.81 | - | **3.4±2.2** | 3.16 | 6.01 | 10.41 | - | **6.5±3.6** |
| **DOPAC/HVA** | 1.27 | 0.65 | 0.42 | 0.33 | **0.7±0.4** | 0.95 | 0.90 | 1.25 | 1.03 | **1.0±0.2** |

### 8.6. Determination of rat brain SAL levels after an acute ethanol administration

To determine the occurrence of brain SAL after ethanol administration rats were administered with ethanol 4 g/kg i.p. After 30 min, the brain was extracted and dissected. The method for the determination of dopamine and SAL was the same as the one discussed in section **7.5.2**. Since the homogenization method releases molecules from all cellular pools, the highest levels of dopamine in the brain reward system were observed in the nucleus accumbens, a region rich with dopaminergic terminals (24.4 pmol/mg, n = 1). In this region, concentrated dopamine in vesicles could be a substrate for SAL synthesis after ethanol exposure. However, no SAL was observed (**Fig. 19A**). When examining the VTA, that houses the dopaminergic somas, no SAL was observed either (**Fig. 19B**; dopamine reached 2.1 pmol/mg, n = 2). To account for the possibility that SAL was metabolized too fast as to be detected, the COMT inhibitor entacapone was injected for 30 min in parallel to the ethanol injection into the left VTA. No SAL was observed in either the left or the right VTA (n =1) (**Fig. 19C, D**).

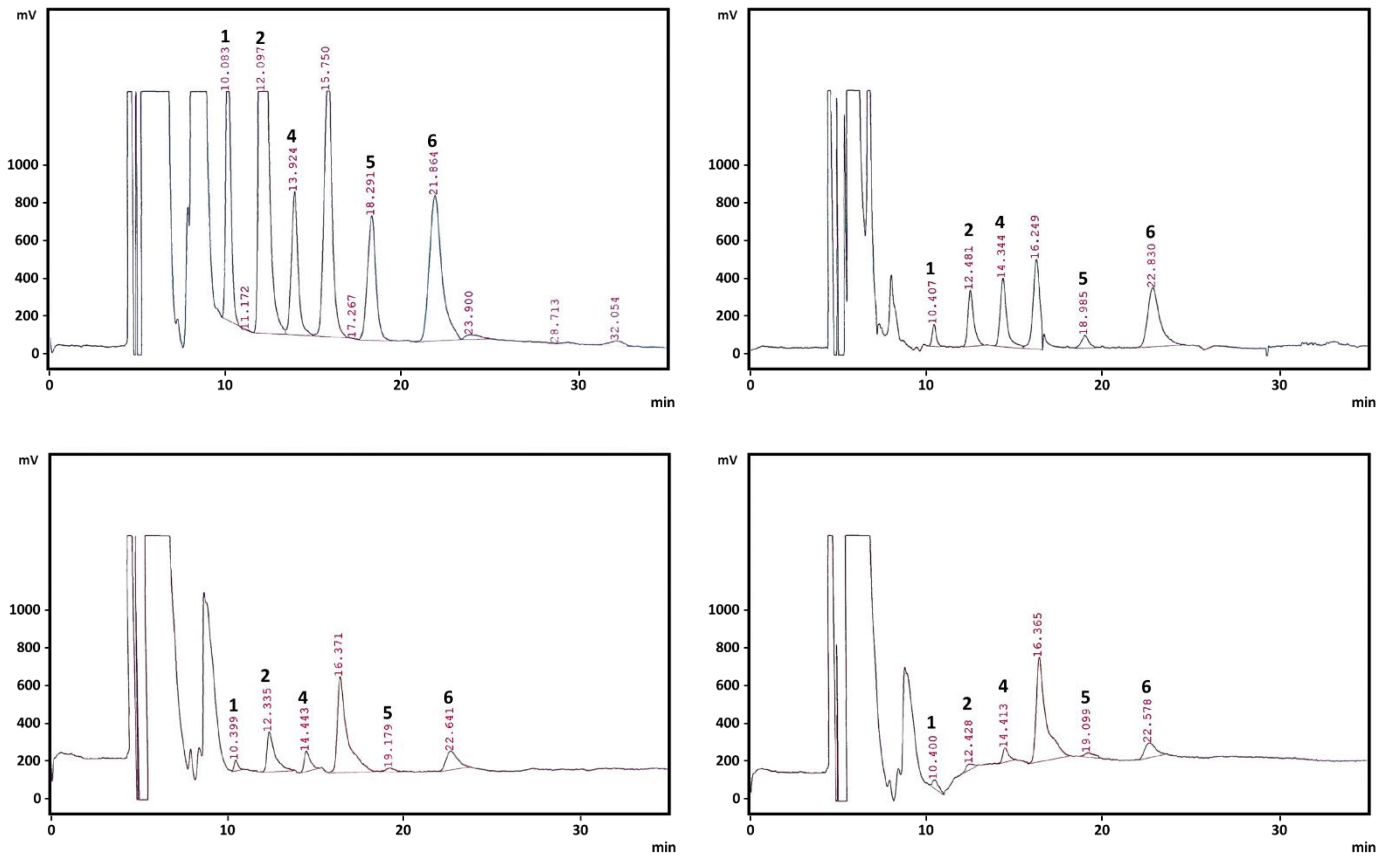


**Figure 19. HPLC chromatograms of homogenate supernatants of nucleus accumbens** (**A**) **and VTA** (**B**), from a rat administered with ethanol 4 g/kg i.p., or of homogenate supernatants of the left VTA (**C**) and the right VTA (**D**) from a rat administered with ethanol 4 g/kg i.p. in parallel to an intra left VTA administration of entacapone (500 µM) for 30 min. **1**, DOPAC; **2**, dopamine; **3**, salsolinol; **4**, 5-hydroxyindoleacetic acid; **5**, homovanillic acid; **6**, serotonin.

## 9. DISCUSSION

This thesis aimed to approach the problem of a lack of a mechanism for the ethanol reinforcing effect. The hypothesis that ethanol is biotransformed into acetaldehyde-derived SAL was proposed in the early 70' (Yamanaka, Walsh, and Davis 1970; Cohen and Collins 1970). However, it lost momentum due to the inability to detect it after ethanol exposure. In recent years the SAL hypothesis regained strength due to two major findings: SAL was found to be a very potent reinforcing molecule, that was self-administered by rats into the VTA (Rodd et al. 2008) and nucleus accumbens (Rodd et al. 2003), and it was shown that ethanol metabolism to acetaldehyde in the VTA was necessary for ethanol to be consumed voluntarily by rats (Karahanian et al. 2011). This work sought to find evidence to support the SAL hypothesis regarding: (i) the mechanism of SAL reinforcing activity and (ii) the presence of SAL in the brain reward system after ethanol exposure. In addition, the experiments focused on SAL enantiomeric specificity, expected to support a common scenario (same active enantiomer), or to discard a direct relation between the *in vitro* and *in vivo* SAL effects (different enantiomer responsible for different effects).

### 9.1. The mechanism of SAL reinforcing activity

#### *9.1.1. Racemic SAL intrinsic activity*

The first analyzed aspect was whether SAL acted directly on a receptor or needed to be further activated for exerting its effect. We found that racemic SAL is an agonist of the $G_i$ protein pathway of the μ-opioid receptor. This finding is in line with evidence showing that several SAL effects are blocked by μ-opioid receptor antagonists; i.e., conditioned place preference (Matsuzawa, Suzuki, and Misawa 2000), *in vitro* dopaminergic neurons activation (Xie et al. 2012), dopamine release in the nucleus accumbens (Hipolito et al. 2011), rats locomotor activation (Hipolito et al. 2010), and increased ethanol consumption (Quintanilla et al. 2014). Moreover, it has been found that SAL displaces μ-opioid receptor ligands (Airaksinen et al. 1984; Lucchi et al. 1982). Our experiments showed that SAL was 3000 times less potent that met-enkephalin, with an $EC_{50}$ of $2.7 \cdot 10^{-5}$ M vs. $8.9 \cdot 10^{-9}$ M, respectively (**Table 1**). These two ligands were also assayed in binding experiments by Lucchi, and they showed a similar potency difference between SAL and met-enkephalin (Lucchi et al. 1982).

#### *9.1.2. Racemic SAL functional selectivity*

The present experimental approach allowed us to further study the mechanism of SAL activation of μ-opioid receptors. We observed that, unlike most other μ-opioid receptor agonists (Molinari et al. 2010), it did not promote the recruitment of β-arrestin. This means that the SAL μ-opioid effect would not promote the internalization of the receptor and would produce less tolerance, comparing to the effects observed after μ-opioid agonists in animals lacking β-arrestin (Bohn et al. 2000; Bohn et al. 2003; Bohn, Lefkowitz, and Caron 2002; Raehal, Walker, and Bohn 2005); or SAL effects may be similar to the action of morphine, which is a weak β-arrestin recruitment promoter (**Fig. 4B**) (Molinari et al. 2010), that generates less receptor recycling that develops in receptor tolerance (Whistler and von Zastrow 1998; Finn and Whistler 2001). Nonetheless, more research needs to be carried out to confirm these assumptions. Functional selective agonists with little β-arrestin pathway activation have been recently synthesized, like herkinorin (Groer et al. 2007) and oliceridine (Chen et al. 2013). Oliceridine has finalized a phase II clinical trial, showing a similar analgesic effect to morphine while producing less secondary effects (Singla et al. 2017). These advances support the idea that the SAL mechanism of μ-opioid receptor activation is special among opioid ligands, because of its functional

selectivity and small molecular weight (179 Da), which augur a unique coupling to the μ-opioid receptor binding site.

### *9.1.3. SAL μ-opioid receptor activation mechanism: enantiomeric selectivity and binding site coupling*

We found that (*S*)-SAL was the active SAL enantiomer of the racemic form, being 50 times more potent than its (*R*) counterpart (**Table 1**). We provide computational results to explain how could (*S*)-SAL be a better ligand than (*R*)-SAL, activating the binding pocket of the μ-opioid receptor. After 2.4 μsec of molecular dynamics simulation of a SAL enantiomer in the binding pocket of the mouse μ-opioid receptor, we found that the orientation of the chiral methyl group of (*S*)-SAL (the only difference between the two enantiomers, **Fig. 2**) was important for the binding of (*S*)-SAL. This methyl group promoted an interaction with Y148 that was synergistic with the main SAL:N-O:D147 salt bridge, promoting its stability in the site (**Fig. 10A**). Our simulations showed that (*S*)-SAL was stable in the orthosteric area of the binding site (**Fig. 7**), where (*S*)-SAL bound to the residues that are critical for μ-opioid receptor agonism (Mansour et al. 1997; Shim, Coop, and MacKerell 2013; Huang et al. 2015), including D147, H297 and W293 (**Table 4**, **Fig 11**), and promoted changes in the receptor binding site that approached the receptor-activated state (**Fig. 12**), like W293 $\chi_2$ dihedral rotamer and N150 $\chi_1$ dihedral rotamer changes (**Fig. 13**). Interestingly, (*S*)-SAL did not interact with other common residues involved in μ-opioid receptor ligand binding, i.e., W318, I322 and Y326 (Shim, Coop, and MacKerell 2013; Huang et al. 2015), because of its small size (**Fig. 8, 9**; **Table 4**). Our observations, (*S*)-SAL simulations added to our experimental results of SAL functional selectivity, imply that binding to W318, I322 and Y326 is not necessary for μ-opioid receptor binding or $G_i$ protein activation, and suggest that those residues are involved in the mechanism for β-arrestin recruitment.

Another consideration provided by our results is that (*R*)-SAL may not be a μ-opioid receptor ligand after all. Our simulations of (*R*)-SAL did not show the behavior of an agonist, as (*R*)-SAL did not fully interact with D147 in any of the simulation, except in R1B (**Table 4**), where its location away from the orthosteric site is not consistent with μ-opioid receptor agonism (Shim, Coop, and MacKerell 2013). On the other hand, our experimental results show that (*R*)-SAL activated the μ-opioid receptor, with 50 times less potency than (*S*)-SAL. However, that finding can be explained by a contamination of the (*R*)-SAL solution with exactly 2% of (*S*)-SAL. We report that the (*R*)-SAL purified solution contained less than 1% of (*S*)-SAL (**Fig. 3**), but the possibility that the actual value was higher in the tested solutions cannot be ruled out.

### *9.1.4. Enantiomeric specificity of SAL activation of the brain reward system*

The agonistic action of racemic SAL on the μ-opioid receptor can explain its reinforcing properties. Agonists on μ-opioid receptors can indirectly activate dopaminergic neurons in the VTA by inhibition of local GABAergic interneurons, as a mechanism for rewarding responses (Johnson and North 1992). The opioid hypothesis for SAL activity also agrees with a prominent expression of μ-opioid receptors on non-dopaminergic neurons of the VTA (Garzon and Pickel 2001). However, comparing with the present results, the *in vivo* experiments of rat conditioned place preference are not consistent with this μ-opioid receptor hypothesis. As commented, the shown enantiomeric specificity allowed us to either determine a common mechanism or help to discard one. The finding that (*R*)-SAL was the only active enantiomer to induce a conditioned place preference after intra-VTA infusion (**Fig. 14**), suggests that the mechanism of SAL activation of the brain reward system is not related to μ-opioid receptor agonism (**Fig. 20**). To this inconsistency it can be argued the following: (i) the mechanism by

which (*R*)-SAL induces a conditioned place preference is different to that produced by direct μ-opioid receptor activation. The dose used here ($3 \cdot 10^{-5}$ M) should have been enough for (*S*)-SAL to activate μ-opioid receptors ($EC_{50}=1.1 \cdot 10^{-5}$ M), but not enough for (*R*)-SAL ($EC_{50}=5.2 \cdot 10^{-4}$ M) (**Table 1**) and, as it has already been discussed, (*R*)-SAL μ-opioid receptor agonism is not certain. Still, no alternative mechanisms are known as there is no evidence for SAL activity on other receptors. A direct activation of dopamine receptors is unlikely as racemic SAL does not displace ligands on these receptors (Antkiewicz-Michaluk et al. 2000). (ii) The concentrations used for the *in vivo* assay in the present study could have been too high for (*S*)-SAL, reaching the end of a U-shaped dose-response curve that different laboratories have reported for the action of SAL in the VTA; e.g. $3 \cdot 10^{-8}$ M to $10^{-6}$ M by (Rodd et al. 2008) and $3 \cdot 10^{-7}$ M to $3 \cdot 10^{-6}$ M by (Deehan et al. 2013). The concentration used in this experiment was ~3 times the $EC_{50}$ for the agonist effect of (*S*)-SAL on μ-opioid receptors, which could have nullified the rat conditioned place preference as was observed, by acting in an unknown secondary target with an opposite effect (i.e. agonism of κ-opioid receptor).

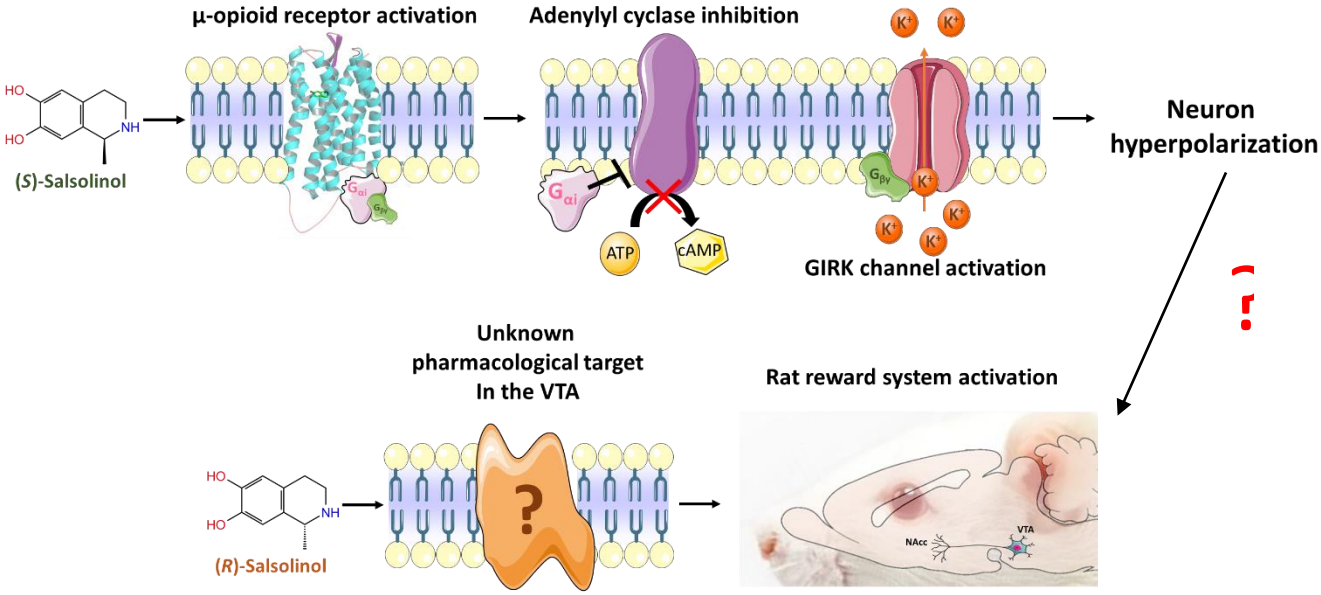


**Figure 20. Suggested model of salsolinol mechanism of action and enantiomeric specificity.** (Top) (*S*)-salsolinol stimulation of μ-opioid receptor promotes the $G_i$ protein pathway activation, where $G_{\alpha i}$ inhibits the cAMP synthesis by adenylyl cyclase and $G_{\beta\gamma}$ promotes the GIRK K+ channel activation, which leads to the hosting neuron hyperpolarization (the activation of the brain reward system upon this mechanism was not shown in this work). (Down) (R)-salsolinol activates the rat reward system by an unknown mechanism after infused into the VTA, determined by conditioned place preference.

## 9.2. The presence of SAL in the brain reward system after an ethanol exposure

To connect the findings of the pharmacology of SAL to the reinforcing mechanism of ethanol is paramount to demonstrate that SAL is generated in the brain reward system after the administration of the drug. Dopamine and acetaldehyde condensation to form SAL occurs readily *in vitro* (Berríos Cárcamo 2013). Thus, SAL may arise in areas of the brain where dopamine and acetaldehyde coexist after ethanol exposure. Acetaldehyde cannot be observed after an ethanol administration unless its elimination is prevented (Jamal et al. 2007) (older reports of brain acetaldehyde have been explained by an artefactual -not biological- generation (Eriksson, Sippel, and Forsander 1977)). However, there is general consensus that it is generated in the brain after local metabolism of ethanol (Correa et al. 2012; Deehan, Brodie, and Rodd 2013; Israel et al. 2015), which has been observed *in vitro* and up to 60% is explained by catalase activity (Zimatkin et al. 2006) and this enzyme occurs uniformly throughout the brain (Brannan, Maker, and Raes 1981). Dopamine occurs at dopaminergic somas and terminals (including somatodendritic regions) and SAL has been found in the dopaminergic brain reward system after a chronic administration of ethanol by many groups (Sjoquist, Liljequist, and Engel 1982; Myers et al. 1985; Matsubara, Fukushima, and Fukui 1987; Starkey et al. 2006; Rojkovicova et al. 2008). However, this molecule is more likely to be involved in the initial hit of the development of alcohol use disorder (Israel et al. 2015), therefore it should be observable after acute ethanol administration. Nevertheless, in the brain of naïve rats SAL was only measured when its synthesis was forced by increasing the availability of brain acetaldehyde (Jamal, Ameno, et al. 2003a, 2003b; Jamal, Ameno, Kubota, et al. 2003; Wang et al. 2007). **Here, we proposed that SAL could be measured provided: (i) the SAL elimination pathway is inhibited, and (ii) that the animals withstand a high concentration of ethanol (UChB rats).**

### *9.2.1. Determination of the SAL brain elimination pathways*

SAL could be rapidly eliminated from the area before it is measurable, especially by microdialysis experiments, where a fast uptake of salsolinol would impede its detection. Interestingly, the reason it has been possible to measure brain SAL after a chronic ethanol treatment, and not in naïve rats, could be an impaired SAL elimination. A decreased catechol-*O*-methyl transferase (COMT, discussed below) activity was observed in astrocytes from a rat model of inflammation (Hartung et al. 2015) and a high inflammatory evironment in the brain is hypothesized to be a hallmark of the effect of alcoholism (Vetreno and Crews 2014).

As first possible mechanism of SAL brain elimination, we studied the SAL activity on the dopamine transporter, which could remove SAL from the synaptic cleft and extracellular locations. Using HEK293 cells transfected with the human dopamine transporter, we found that SAL was a weak blocker of the uptake of a dopamine transporter substrate (**Fig. 16A**). With a $K_i$ of $1.2 \cdot 10^{-3}$ M (**Table 5**) a fast elimination of SAL from the synaptic cleft via the dopamine transporter seems therefore unlikely. The inhibitory effect of dopamine was used as a control. Supporting the present results another study used dopamine as an inhibitor of the human dopamine transporter transfected into HEK293 cells, finding a very similar $K_i$ for that molecule to the one used here (our $K_i$ for dopamine was $1.0 \cdot 10^{-5}$ M versus the $K_i$ of $2.84 \cdot 10^{-6}$ M (Chen, Vaughan, and Reith 2001)). It is important to note that this experiment did not establish whether SAL was a substrate or just an inhibitor of the transporter, as its effect preventing the intake of a substrate (**Fig. 16A**) would be the same regardless of SAL activity.

The second target for the metabolism of SAL studied in this thesis is the COMT, as it has already been shown to metabolize SAL (Hotzl and Thomas 1997). The approach for measuring molecules in brain homogenate supernatants to show the elimination of SAL by COMT was ineffective. The imprecision of our method, regarding the weight of the tissues and administration of the COMT inhibitor entacapone in a specific brain area, hindered our ability to observe differences (finding an animal showing higher SAL levels in the left substantia nigra, while other in the right VTA; **Table 6**). Although we know that SAL is metabolized in the brain (Melchior 1979), the question of the effect of COMT or other enzymes in the metabolism of SAL remains open.

### *9.2.2. Determination of brain SAL after an acute ethanol administration*

To approach the determination of brain SAL after ethanol exposure, it was important to define areas where SAL may be synthesized -where dopamine and acetaldehyde can interact- and areas where SAL could be reinforcing. As discussed above, SAL has shown to be reinforcing in the mesolimbic system (Rodd et al. 2003; Rodd et al. 2008), where dopaminergic neurons from the VTA release dopamine from vesicular and newly synthesized pools in the terminals in the nucleus accumbens, and also dopamine release in the VTA by somatodendritic transmission (Adell and Artigas 2004). We used supernatants of brain homogenates from different brain areas, monitoring molecules present in extracellular and intracellular compartments of rats treated with ethanol 4 g/kg i.p. No SAL was observed in the nucleus accumbens or the VTA, despite measuring high levels of dopamine in samples obtained from nucleus accumbens (**Fig. 19**). In addition to the lack of SAL activity at the dopamine transporter, the lack of SAL in samples from the nucleus accumbens suggests that SAL is not synthetized nor captured by dopaminergic terminals. In a second experiment, the COMT inhibitor entacapone was injected intra-VTA concurrently with ethanol administration, but again no SAL was observed in the same area where the COMT inhibitor was infused or in the neighboring substantia nigra.

To envision what approach could increase the chance to observe SAL after an acute ethanol administration one could propose a more sensitive analytical method. The used HPLC system coupled to electrochemical detection has a limit of detection in the low nanomolar level, which is similar to other SAL detection methods used in brain homogenate (Rojkovicova et al. 2008) and brain microdialysis experiments (Jamal, Ameno, et al. 2003b). SAL was shown to be self-administered by rats at micromolar levels (Rodd et al. 2003; Rodd et al. 2008) and its $EC_{50}$ for μ-opioid receptor activation was shown at a tenth of micromolar (**Table 1**). To be reinforcing, SAL could reach active levels in its receptor microenvironment, needing a methodological approach to measure it locally to assess its occurrence. Until more assay systems are developed, the relevance of SAL for the reinforcing effect of ethanol remains to be demonstrated.

## 9.3. Other hypotheses for the mechanism of the ethanol reinforcing effect.

Following the results of this thesis after the investigation of SAL brain levels, the hypothesis of SAL occurrence after ethanol administration could not be supported. As an alternative, there is evidence supporting that ethanol by itself can bind to receptors to promote a reinforcing effect. To account for a reinforcing effect, ethanol must act at low millimolar levels, which would resemble the concentrations reached in the blood after voluntary alcohol intake. There is evidence on the action of low millimolar levels of ethanol on excitatory glutamate N-methyl-D-aspartate (NMDA) receptors and inhibitory pentameric ligand-gated ion channels (i.e. $\alpha\beta_3\delta$ $GABA_A$ receptors, $5\text{-}HT_3$ receptors, and glycine receptors).

The NMDA receptors are antagonized by ethanol in the hippocampus at 5 to 50 mM (Lovinger, White, and Weight 1989). The use of NMDA receptors antagonists reduced ethanol intake in rats (Vengeliene et al. 2005), maybe by preventing further antagonism by ethanol. NMDA receptors are an integral part of the brain reward system, and the sole activation of glutamatergic neurons from the VTA is enough to promote reinforcement (Wang et al. 2015), therefore, NMDA receptor antagonism by ethanol cannot be considered a general reinforcing mechanism.

Ethanol, at concentrations as low as 3 mM, co-administered with GABA promotes $\alpha\beta_3\delta$ $GABA_A$ currents (Wallner, Hanchar, and Olsen 2014). The knock down of $\alpha\beta_3\delta$ $GABA_A$ receptors in the nucleus accumbens shell, using adenoviral vectors, reduced ethanol intake in rats (Nie et al. 2011); similarly the ethanol $\alpha\beta_3\delta$ $GABA_A$ antagonist Ro15-4513 (specifically blocks ethanol action) (Glowa et al. 1988) administered intra-VTA reduced ethanol intake in mice (Melon and Boehm 2011). Another candidate is the ionotropic receptor of serotonin, $5\text{-}HT_3$, as its specific antagonist, ICS 205-930, administered subcutaneously reduced ethanol consumption in Wistar (McKinzie et al. 1998) and alcohol-preferring rats (Rodd-Henricks, McKinzie, Edmundson, et al. 2000). Interestingly, this same antagonist co-administered with SAL intra-VTA blocked the SAL reinforcing effect (Rodd et al. 2008). Evidence also supports the involvement of glycine receptors in the ethanol reinforcing effect since ethanol, at concentrations as low as 10 mM, enhances glycine evoked currents via ethanol action on $G_{\beta\gamma}$ proteins (Yevenes et al. 2003). In addition, the glycine receptor strychnine administered into the nucleus accumbens blocked the local raise of dopamine levels by ethanol (Jonsson et al. 2014). However, strychnine administration into the nucleus accumbens promoted ethanol consumption in rats instead of reducing it (Molander et al. 2005). In the same line, the systemic inhibition of the glycine transporter, that raises the synaptic glycine available, inhibited ethanol intake in rats (Molander et al. 2007; Vengeliene et al. 2010). However, the same glycine transporter inhibitor failed to reduce ethanol consumption in humans (de Bejczy et al. 2014). The mechanism which inhibitory pentameric ligand-gated ion channels may be involved in ethanol reinforcement is the inhibition of neurons that are tonically inhibiting dopaminergic neurons. It has been hypothesized that ethanol could promote inhibition of GABAergic neurons in the nucleus accumbens through these receptors, triggering a nucleus accumbens (inhibition)-VTA (disinhibition)-nucleus accumbens (activation) loop; or directly inhibiting GABAergic neurons of the VTA (Soderpalm, Lido, and Ericson 2017).

Regardless of how complex the mechanisms involved in ethanol reinforcing effect are, it is important to acknowledge that the acetaldehyde participation was critical enough to completely block the initial ethanol consumption in rats, which was shown by inhibiting acetaldehyde production (Karahanian et al. 2011) or accelerating its elimination (Karahanian et al. 2015) in the VTA. Still, acetaldehyde involvement in the ethanol reinforcing effect could be different than SAL synthesis. There is evidence that micromolar levels of acetaldehyde, and not salsolinol, can promote the release of β-endorphins in hypothalamic neurons primary cultures (Reddy and Sarkar 1993; Pastorcic, Boyadjieva, and Sarkar 1994), which could account for the opioid component of the ethanol reinforcing action (Nutt 2014). Nevertheless, there is no evidence that acetaldehyde can promote the release of endorphins in the VTA or nucleus accumbens.

## 10. CONCLUSIONS

**The conclusions are grouped regarding which part of the hypothesis they are answering.**

**Salsolinol activates μ-opioid receptors via one of its enantiomers (either *R* or *S*):**

- (*R*) and (*S*)-salsolinol were successfully separated and purified from racemic salsolinol.
- Salsolinol is an agonist of the $G_i$ protein pathway of the human μ-opioid receptor.
- Salsolinol exposure does not promote the recruitment of β-arrestin in CHO-K1 cells transfected with the human μ-opioid receptor.
- Salsolinol exerts its μ-opioid receptor agonistic effect *in vitro* via its (*S*) enantiomer, which is 50 times more potent than the (*R*) enantiomer.
- (*S*)-salsolinol stably interacts with the mouse μ-opioid receptor binding site in a molecular dynamics simulation.
- (*R*)-salsolinol is less potent than (*S*)-salsolinol due to the opposite orientation of the chiral methyl group, which interacts with a hydrophobic moiety of the receptor, away from the Asp147.
- (*S*)-salsolinol binds most residues of the μ-opioid receptor binding site, including the critical D147, H297, and W293.
- (*S*)-salsolinol does not bind W318, I322, and Y326 due to its small size. Interaction with these residues seems to not be necessary for activating the μ-opioid receptor $G_i$ protein pathway.

This hypothesis is considered to be fully answered.

**Salsolinol activates the brain reward system of rats via one of its enantiomers (either *R* or *S*):**

- The direct infusion of $3 \cdot 10^{-5}$ M (*R*)-salsolinol into the ventral tegmental area induces a conditioned place preference in rats. While the same dose of (*S*)-salsolinol does not induce a place conditioning.

This hypothesis is considered to be answered. However, it cannot be ruled out that (S)-salsolinol could be reinforcing at doses different from the one tested.

**Salsolinol is generated in the brain reward system of naïve rats after an acute dose of ethanol:**

- Salsolinol is a weak inhibitor, and therefore not a ligand, of the human dopamine transporter. Effect exerted by the (*R*) enantiomer.
- Salsolinol was not observed in supernatant homogenates of the VTA or nucleus accumbens of rats administered with ethanol 4 g/kg i.p. with or without a concomitant intra-VTA administration of the COMT inhibitor entacapone.

This hypothesis is considered to not be answered. However, the results support that SAL is at least not accumulated in dopaminergic vesicles at the nucleus accumbens (as discussed above).

## 11. REFERENCES


Adell, A., and F. Artigas. 2004. 'The somatodendritic release of dopamine in the ventral tegmental area and its regulation by afferent transmitter systems', *Neurosci Biobehav Rev*, 28: 415-31.

Airaksinen, M. M., V. Saano, E. Steidel, H. Juvonen, A. Huhtikangas, and J. Gynther. 1984. 'Binding of beta-carbolines and tetrahydroisoquinolines by opiate receptors of the delta-type', *Acta Pharmacol Toxicol (Copenh)*, 55: 380-5.

American Psychiatric Association. 2013. *Diagnostic and statistical manual of mental disorders (DSM-5®)* (American Psychiatric Pub).

Antkiewicz-Michaluk, L., J. Michaluk, I. Romanska, I. Papla, and J. Vetulani. 2000. 'Antidopaminergic effects of 1,2,3,4-tetrahydroisoquinoline and salsolinol', *J Neural Transm (Vienna)*, 107: 1009-19.

Baum, S. S., and H. Rommelspacher. 1994. 'Determination of total dopamine, R- and S-salsolinol in human plasma by cyclodextrin bonded-phase liquid chromatography with electrochemical detection', *J Chromatogr B Biomed Appl*, 660: 235-41.

Berrios-Carcamo, P., M. E. Quintanilla, M. Herrera-Marschitz, V. Vasiliou, G. Zapata-Torres, and M. Rivera-Meza. 2016. 'Racemic Salsolinol and its Enantiomers Act as Agonists of the mu-Opioid Receptor by Activating the Gi Protein-Adenylate Cyclase Pathway', *Front Behav Neurosci*, 10: 253.

Berríos Cárcamo, Pablo Andrés. 2013. 'Salsolinol e isosalsolinol: productos de la condensación de dopamina y acetaldehído como efectores finales del efecto reforzante del etanol', Master's thesis, Universidad de Chile, Santiago, Chile.

Bohn, L. M., R. R. Gainetdinov, F. T. Lin, R. J. Lefkowitz, and M. G. Caron. 2000. 'Mu-opioid receptor desensitization by beta-arrestin-2 determines morphine tolerance but not dependence', *Nature*, 408: 720-3.

Bohn, L. M., R. R. Gainetdinov, T. D. Sotnikova, I. O. Medvedev, R. J. Lefkowitz, L. A. Dykstra, and M. G. Caron. 2003. 'Enhanced rewarding properties of morphine, but not cocaine, in beta(arrestin)-2 knock-out mice', *J Neurosci*, 23: 10265-73.

Bohn, L. M., R. J. Lefkowitz, and M. G. Caron. 2002. 'Differential mechanisms of morphine antinociceptive tolerance revealed in (beta)arrestin-2 knock-out mice', *J Neurosci*, 22: 10494-500.

Brannan, T. S., H. S. Maker, and I. P. Raes. 1981. 'Regional distribution of catalase in the adult rat brain', *J Neurochem*, 36: 307-9.

Brodie, M. S., C. Pesold, and S. B. Appel. 1999. 'Ethanol directly excites dopaminergic ventral tegmental area reward neurons', *Alcohol Clin Exp Res*, 23: 1848-52.

Cai, M., and Y. M. Liu. 2008. 'Quantification of salsolinol enantiomers by stable isotope dilution liquid chromatography with tandem mass spectrometric detection', *Rapid Commun Mass Spectrom*, 22: 4171-7.

Chen, N., R. A. Vaughan, and M. E. Reith. 2001. 'The role of conserved tryptophan and acidic residues in the human dopamine transporter as characterized by site-directed mutagenesis', *J Neurochem*, 77: 1116-27.

Chen, X. T., P. Pitis, G. Liu, C. Yuan, D. Gotchev, C. L. Cowan, D. H. Rominger, M. Koblish, S. M. Dewire, A. L. Crombie, J. D. Violin, and D. S. Yamashita. 2013. 'Structure-activity relationships and discovery of a G protein biased mu opioid receptor ligand, [(3-methoxythiophen-2-yl)methyl](cate)amine (TRV130), for the treatment of acute severe pain', *J Med Chem*, 56: 8019-31.

Cohen, G., and M. Collins. 1970. 'Alkaloids from catecamines in adrenal tissue: possible role in alcoholism', *Science*, 167: 1749-51.

Correa, M., J. D. Salamone, K. N. Segovia, M. Pardo, R. Longoni, L. Spina, A. T. Peana, S. Vinci, and E. Acquas. 2012. 'Piecing together the puzzle of acetaldehyde as a neuroactive agent', *Neurosci Biobehav Rev*, 36: 404-30.

Darden, Tom, Darrin York, and Lee Pedersen. 1993. 'Particle mesh Ewald: An N· log (N) method for Ewald sums in large systems', *The Journal of chemical physics*, 98: 10089-92.

de Bejczy, A., K. R. Nations, A. Szegedi, J. Schoemaker, F. Ruwe, and B. Soderpalm. 2014. 'Efficacy and safety of the glycine transporter-1 inhibitor org 25935 for the prevention of relapse in alcohol-dependent patients: a randomized, double-blind, placebo-controlled trial', *Alcohol Clin Exp Res*, 38: 2427-35.

Deehan, G. A., Jr., M. S. Brodie, and Z. A. Rodd. 2013. 'What is in that drink: the biological actions of ethanol, acetaldehyde, and salsolinol', *Curr Top Behav Neurosci*, 13: 163-84.

Deehan, G. A., Jr., E. A. Engleman, Z. M. Ding, W. J. McBride, and Z. A. Rodd. 2013. 'Microinjections of acetaldehyde or salsolinol into the posterior ventral tegmental area increase dopamine release in the nucleus accumbens shell', *Alcohol Clin Exp Res*, 37: 722-9.

Deng, Y., W. Maruyama, P. Dostert, T. Takahashi, M. Kawai, and M. Naoi. 1995. 'Determination of the (R)- and (S)-enantiomers of salsolinol and N-methylsalsolinol by use of a chiral high-performance liquid chromatographic column', *J Chromatogr B Biomed Appl*, 670: 47-54.

Di Chiara, G., and A. Imperato. 1988. 'Drugs abused by humans preferentially increase synaptic dopamine concentrations in the mesolimbic system of freely moving rats', *Proc Natl Acad Sci U S A*, 85: 5274-8.

Donoso, MP. 2015. 'Análisis de Resultados del Alcohol Use Disorders Identification Test (AUDIT) Resultados Escala', Accessed October, 10. http://www.senda.gob.cl/media/boletines/Boletin%203%20An%C3%A1lisis%20de%20Resultados%20del%20Alcohol%20Use%20Disorders%20Identification%20Test%20(AUDIT)%20Resultados%20Escala.pdf.

Engleman, E. A., Z. M. Ding, S. M. Oster, J. E. Toalston, R. L. Bell, J. M. Murphy, W. J. McBride, and Z. A. Rodd. 2009. 'Ethanol is self-administered into the nucleus accumbens shell, but not the core: evidence of genetic sensitivity', *Alcohol Clin Exp Res*, 33: 2162-71.

Eriksson, C. J., H. W. Sippel, and O. A. Forsander. 1977. 'The determination of acetaldehyde in biological samples by head-space gas chromatography', *Anal Biochem*, 80: 116-24.

Finn, A. K., and J. L. Whistler. 2001. 'Endocytosis of the mu opioid receptor reduces tolerance and a cellular hallmark of opiate withdrawal', *Neuron*, 32: 829-39.

Fiser, A., R. K. Do, and A. Sali. 2000. 'Modeling of loops in protein structures', *Protein Sci*, 9: 1753-73.

Garzon, M., and V. M. Pickel. 2001. 'Plasmalemmal mu-opioid receptor distribution mainly in nondopaminergic neurons in the rat ventral tegmental area', *Synapse*, 41: 311-28.

Glowa, J. R., J. Crawley, P. D. Suzdak, and S. M. Paul. 1988. 'Ethanol and the GABA receptor complex: studies with the partial inverse benzodiazepine receptor agonist Ro 15-4513', *Pharmacol Biochem Behav*, 31: 767-72.

Grant, B. F., R. B. Goldstein, T. D. Saha, S. P. Chou, J. Jung, H. Zhang, R. P. Pickering, W. J. Ruan, S. M. Smith, B. Huang, and D. S. Hasin. 2015. 'Epidemiology of DSM-5 Alcohol Use Disorder: Results From the National Epidemiologic Survey on Alcohol and Related Conditions III', *JAMA Psychiatry*, 72: 757-66.

Groer, C. E., K. Tidgewell, R. A. Moyer, W. W. Harding, R. B. Rothman, T. E. Prisinzano, and L. M. Bohn. 2007. 'An opioid agonist that does not induce mu-opioid receptor--arrestin interactions or receptor internalization', *Mol Pharmacol*, 71: 549-57.

Harding, W. W., K. Tidgewell, N. Byrd, H. Cobb, C. M. Dersch, E. R. Butelman, R. B. Rothman, and T. E. Prisinzano. 2005. 'Neoclerodane diterpenes as a novel scaffold for mu opioid receptor ligands', *J Med Chem*, 48: 4765-71.

Hartung, J. E., O. Eskew, T. Wong, I. E. Tchivileva, F. A. Oladosu, S. C. O'Buckley, and A. G. Nackley. 2015. 'Nuclear factor-kappa B regulates pain and COMT expression in a rodent model of inflammation', *Brain Behav Immun*, 50: 196-202.

Hipolito, L., L. Marti-Prats, M. J. Sanchez-Catalan, A. Polache, and L. Granero. 2011. 'Induction of conditioned place preference and dopamine release by salsolinol in posterior VTA of rats: involvement of mu-opioid receptors', *Neurochem Int*, 59: 559-62.

Hipolito, L., M. J. Sanchez-Catalan, T. Zornoza, A. Polache, and L. Granero. 2010. 'Locomotor stimulant effects of acute and repeated intrategmental injections of salsolinol in rats: role of mu-opioid receptors', *Psychopharmacology (Berl)*, 209: 1-11.

Hotzl, B. K., and H. Thomas. 1997. 'O-methylation of (+)-(R)- and (-)-(S)-6,7-dihydroxy-1-methyl-1,2,3,4-tetrahydroisoquinoline (salsolinol) in the presence of pig brain catechol-O-methyltransferase', *Chirality*, 9: 367-72.

Huang, M. J., Z. Quan, and Y. M. Liu. 2009. 'Computational Modeling of Inclusion Complexes of beta-Cyclodextrin with enantiomers of Salsolinol, N-Methyl-Salsolinol, and 1-Benzyl-Tetrahydroisoquinoline', *Int J Quantum Chem*, 109: 81-90.

Huang, W., A. Manglik, A. J. Venkatakrishnan, T. Laeremans, E. N. Feinberg, A. L. Sanborn, H. E. Kato, K. E. Livingston, T. S. Thorsen, R. C. Kling, S. Granier, P. Gmeiner, S. M. Husbands, J. R. Traynor, W. I. Weis, J. Steyaert, R. O. Dror, and B. K. Kobilka. 2015. 'Structural insights into micro-opioid receptor activation', *Nature*, 524: 315-21.

Humphrey, W., A. Dalke, and K. Schulten. 1996. 'VMD: visual molecular dynamics', *J Mol Graph*, 14: 33-8, 27-8.

Israel, Y., M. E. Quintanilla, E. Karahanian, M. Rivera-Meza, and M. Herrera-Marschitz. 2015. 'The "first hit" toward alcohol reinforcement: role of ethanol metabolites', *Alcohol Clin Exp Res*, 39: 776-86.

Jamal, M., K. Ameno, S. Ameno, N. Okada, and I. Ijiri. 2003a. 'Effect of different doses of cyanamide on striatal salsolinol formation after ethanol treatment', *Leg Med (Tokyo)*, 5 Suppl 1: S79-82.

———. 2003b. 'In vivo study of salsolinol produced by a high concentration of acetaldehyde in the striatum and nucleus accumbens of free-moving rats', *Alcohol Clin Exp Res*, 27: 79s-84s.

Jamal, M., K. Ameno, T. Kubota, S. Ameno, X. Zhang, M. Kumihashi, and I. Ijiri. 2003. 'In vivo formation of salsolinol induced by high acetaldehyde concentration in rat striatum employing microdialysis', *Alcohol Alcohol*, 38: 197-201.

Jamal, M., K. Ameno, I. Uekita, M. Kumihashi, W. Wang, and I. Ijiri. 2007. 'Catalase mediates acetaldehyde formation in the striatum of free-moving rats', *Neurotoxicology*, 28: 1245-8.

Jo, S., T. Kim, V. G. Iyer, and W. Im. 2008. 'CHARMM-GUI: a web-based graphical user interface for CHARMM', *J Comput Chem*, 29: 1859-65.

Johnson, S. W., and R. A. North. 1992. 'Opioids excite dopamine neurons by hyperpolarization of local interneurons', *J Neurosci*, 12: 483-8.

Jonas, D. E., H. R. Amick, C. Feltner, G. Bobashev, K. Thomas, R. Wines, M. M. Kim, E. Shanahan, C. E. Gass, C. J. Rowe, and J. C. Garbutt. 2014. 'Pharmacotherapy for adults with alcohol use disorders in outpatient settings: a systematic review and meta-analysis', *Jama*, 311: 1889-900.

Jonsson, S., L. Adermark, M. Ericson, and B. Soderpalm. 2014. 'The involvement of accumbal glycine receptors in the dopamine-elevating effects of addictive drugs', *Neuropharmacology*, 82: 69-75.

Juricic, M. A., P. A. Berrios-Carcamo, M. L. Acevedo, Y. Israel, I. Almodovar, and B. K. Cassels. 2012. 'Salsolinol and isosalsolinol: condensation products of acetaldehyde and dopamine. Separation of their enantiomers in the presence of a large excess of dopamine', *J Pharm Biomed Anal*, 63: 170-4.

Karahanian, E., M. E. Quintanilla, L. Tampier, M. Rivera-Meza, D. Bustamante, V. Gonzalez-Lira, P. Morales, M. Herrera-Marschitz, and Y. Israel. 2011. 'Ethanol as a prodrug: brain metabolism of ethanol mediates its reinforcing effects', *Alcohol Clin Exp Res*, 35: 606-12.

Karahanian, E., M. Rivera-Meza, L. Tampier, M. E. Quintanilla, M. Herrera-Marschitz, and Y. Israel. 2015. 'Long-term inhibition of ethanol intake by the administration of an aldehyde dehydrogenase-2 (ALDH2)-coding lentiviral vector into the ventral tegmental area of rats', *Addict Biol*, 20: 336-44.

Koob, G. F., S. H. Ahmed, B. Boutrel, S. A. Chen, P. J. Kenny, A. Markou, L. E. O'Dell, L. H. Parsons, and P. P. Sanna. 2004. 'Neurobiological mechanisms in the transition from drug use to drug dependence', *Neurosci Biobehav Rev*, 27: 739-49.

Koob, G. F., and M. Le Moal. 1997. 'Drug abuse: hedonic homeostatic dysregulation', *Science*, 278: 52-8.

Lee, J., V. A. Ramchandani, K. Hamazaki, E. A. Engleman, W. J. McBride, T. K. Li, and H. Y. Kim. 2010. 'A critical evaluation of influence of ethanol and diet on salsolinol enantiomers in humans and rats', *Alcohol Clin Exp Res*, 34: 242-50.

Lovinger, D. M., G. White, and F. F. Weight. 1989. 'Ethanol inhibits NMDA-activated ion current in hippocampal neurons', *Science*, 243: 1721-4.

Lucchi, L., A. Bosio, P. F. Spano, and M. Trabucchi. 1982. 'Action of ethanol and salsolinol on opiate receptor function', *Brain Res*, 232: 506-10.

Manglik, A., A. C. Kruse, T. S. Kobilka, F. S. Thian, J. M. Mathiesen, R. K. Sunahara, L. Pardo, W. I. Weis, B. K. Kobilka, and S. Granier. 2012. 'Crystal structure of the micro-opioid receptor bound to a morphinan antagonist', *Nature*, 485: 321-6.

Mansour, A., L. P. Taylor, J. L. Fine, R. C. Thompson, M. T. Hoversten, H. I. Mosberg, S. J. Watson, and H. Akil. 1997. 'Key residues defining the mu-opioid receptor binding pocket: a site-directed mutagenesis study', *J Neurochem*, 68: 344-53.

Marker, C. L., R. Lujan, H. H. Loh, and K. Wickman. 2005. 'Spinal G-protein-gated potassium channels contribute in a dose-dependent manner to the analgesic effect of mu- and delta- but not kappa-opioids', *J Neurosci*, 25: 3551-9.

Matsubara, K., S. Fukushima, and Y. Fukui. 1987. 'A systematic regional study of brain salsolinol levels during and immediately following chronic ethanol ingestion in rats', *Brain Res*, 413: 336-43.

Matsubara, K., T. Senda, T. Uezono, S. Fukushima, S. Ohta, K. Igarashi, M. Naoi, Y. Yamashita, K. Ohtaki, N. Hayase, S. Akutsu, and K. Kimura. 1998. 'Structural significance of azaheterocyclic amines related to Parkinson's disease for dopamine transporter', *Eur J Pharmacol*, 348: 77-84.

Matsuzawa, S., T. Suzuki, and M. Misawa. 2000. 'Involvement of mu-opioid receptor in the salsolinol-associated place preference in rats exposed to conditioned fear stress', *Alcohol Clin Exp Res*, 24: 366-72.

Mayne, C. G., J. Saam, K. Schulten, E. Tajkhorshid, and J. C. Gumbart. 2013. 'Rapid parameterization of small molecules using the Force Field Toolkit', *J Comput Chem*, 34: 2757-70.

McKinzie, DL, R Eha, R Cox, RB Stewart, W Dyr, JM Murphy, WJ McBride, L Lumeng, and T-K Li. 1998. 'Serotonin 3 receptor antagonism of alcohol intake: effects of drinking conditions', *Alcohol*, 15: 291-98.

Melchior, C. L. 1979. 'Interaction of salsolinol and tetrahydropapaveroline with catecholamines', *Alcohol Clin Exp Res*, 3: 364-7.

Melis, M., E. Carboni, P. Caboni, and E. Acquas. 2015. 'Key role of salsolinol in ethanol actions on dopamine neuronal activity of the posterior ventral tegmental area', *Addict Biol*, 20: 182-93.

Melis, M., P. Enrico, A. T. Peana, and M. Diana. 2007. 'Acetaldehyde mediates alcohol activation of the mesolimbic dopamine system', *Eur J Neurosci*, 26: 2824-33.

Melon, L. C., and S. L. Boehm, 2nd. 2011. 'GABAA receptors in the posterior, but not anterior, ventral tegmental area mediate Ro15-4513-induced attenuation of binge-like ethanol consumption in C57BL/6J female mice', *Behav Brain Res*, 220: 230-7.

Ministerio de Salud de Chile. 2007. 'ESTUDIO DE CARGA DE ENFERMEDAD Y CARGA ATRIBUIBLE', Accessed October 10. http://www.cienciasdelasalud-udla.cl/portales/tp76246caadc23/uploadImg/File/Informe-final-carga-Enf-2007.pdf.

Molander, A., H. H. Lido, E. Lof, M. Ericson, and B. Soderpalm. 2007. 'The glycine reuptake inhibitor Org 25935 decreases ethanol intake and preference in male wistar rats', *Alcohol Alcohol*, 42: 11-8.

Molander, A., E. Lof, R. Stomberg, M. Ericson, and B. Soderpalm. 2005. 'Involvement of accumbal glycine receptors in the regulation of voluntary ethanol intake in the rat', *Alcohol Clin Exp Res*, 29: 38-45.

Molinari, P., V. Vezzi, M. Sbraccia, C. Gro, D. Riitano, C. Ambrosio, I. Casella, and T. Costa. 2010. 'Morphine-like opiates selectively antagonize receptor-arrestin interactions', *J Biol Chem*, 285: 12522-35.

Myers, W. D., L. Mackenzie, K. T. Ng, G. Singer, G. A. Smythe, and M. W. Duncan. 1985. 'Salsolinol and dopamine in rat medial basal hypothalamus after chronic ethanol exposure', *Life Sci*, 36: 309-14.

Nie, H., M. Rewal, T. M. Gill, D. Ron, and P. H. Janak. 2011. 'Extrasynaptic delta-containing GABAA receptors in the nucleus accumbens dorsomedial shell contribute to alcohol intake', *Proc Natl Acad Sci U S A*, 108: 4459-64.

Nutt, D. J. 2014. 'The role of the opioid system in alcohol dependence', *J Psychopharmacol*, 28: 8-22.

Pastorcic, M, N Boyadjieva, and DK Sarkar. 1994. 'Comparison of the effects of alcohol and acetaldehyde on proopiomelanocortin mRNA levels and β-endorphin secretion from hypothalamic neurons in primary cultures', *Molecular and Cellular Neuroscience*, 5: 580-86.

Paxinos, G, and Ch Watson. 1998. 'A stereotaxic atlas of the rat brain', *New York: Academic*.

Phillips, J. C., R. Braun, W. Wang, J. Gumbart, E. Tajkhorshid, E. Villa, C. Chipot, R. D. Skeel, L. Kale, and K. Schulten. 2005. 'Scalable molecular dynamics with NAMD', *J Comput Chem*, 26: 1781-802.

Quintanilla, M. E., Y. Israel, A. Sapag, and L. Tampier. 2006. 'The UChA and UChB rat lines: metabolic and genetic differences influencing ethanol intake', *Addict Biol*, 11: 310-23.

Quintanilla, M. E., M. Rivera-Meza, P. A. Berrios-Carcamo, D. Bustamante, M. Buscaglia, P. Morales, E. Karahanian, M. Herrera-Marschitz, and Y. Israel. 2014. 'Salsolinol, free of isosalsolinol, exerts ethanol-like motivational/sensitization effects leading to increases in ethanol intake', *Alcohol*, 48: 551-9.

Quintanilla, M. E., M. Rivera-Meza, P. Berrios-Carcamo, B. K. Cassels, M. Herrera-Marschitz, and Y. Israel. 2016. '(R)-Salsolinol, a product of ethanol metabolism, stereospecifically induces behavioral sensitization and leads to excessive alcohol intake', *Addict Biol*, 21: 1063-71.

Quintanilla, M. E., L. Tampier, E. Karahanian, M. Rivera-Meza, M. Herrera-Marschitz, and Y. Israel. 2012. 'Reward and relapse: complete gene-induced dissociation in an animal model of alcohol dependence', *Alcohol Clin Exp Res*, 36: 517-22.

Raehal, K. M., J. K. Walker, and L. M. Bohn. 2005. 'Morphine side effects in beta-arrestin 2 knockout mice', *J Pharmacol Exp Ther*, 314: 1195-201.

Raffa, R. B., R. P. Martinez, and C. D. Connelly. 1994. 'G-protein antisense oligodeoxyribonucleotides and mu-opioid supraspinal antinociception', *Eur J Pharmacol*, 258: R5-7.

Reddy, B. V., and D. K. Sarkar. 1993. 'Effect of alcohol, acetaldehyde, and salsolinol on beta-endorphin secretion from the hypothalamic neurons in primary cultures', *Alcohol Clin Exp Res*, 17: 1261-7.

Rehm, J., P. Anderson, J. Barry, P. Dimitrov, Z. Elekes, F. Feijao, U. Frick, A. Gual, G. Gmel, Jr., L. Kraus, S. Marmet, J. Raninen, M. X. Rehm, E. Scafato, K. D. Shield, M. Trapencieris, and G. Gmel.

2015. 'Prevalence of and potential influencing factors for alcohol dependence in Europe', *Eur Addict Res*, 21: 6-18.

Rehm, J., R. Room, K. Graham, M. Monteiro, G. Gmel, and C. T. Sempos. 2003. 'The relationship of average volume of alcohol consumption and patterns of drinking to burden of disease: an overview', *Addiction*, 98: 1209-28.

Rodd-Henricks, Z. A., D. L. McKinzie, R. S. Crile, J. M. Murphy, and W. J. McBride. 2000. 'Regional heterogeneity for the intracranial self-administration of ethanol within the ventral tegmental area of female Wistar rats', *Psychopharmacology (Berl)*, 149: 217-24.

Rodd-Henricks, Z. A., D. L. McKinzie, V. E. Edmundson, C. L. Dagon, J. M. Murphy, W. J. McBride, L. Lumeng, and T. K. Li. 2000. 'Effects of 5-HT(3) receptor antagonists on daily alcohol intake under acquisition, maintenance, and relapse conditions in alcohol-preferring (P) rats', *Alcohol*, 21: 73-85.

Rodd, Z. A., R. L. Bell, Y. Zhang, A. Goldstein, A. Zaffaroni, W. J. McBride, and T. K. Li. 2003. 'Salsolinol produces reinforcing effects in the nucleus accumbens shell of alcohol-preferring (P) rats', *Alcohol Clin Exp Res*, 27: 440-9.

Rodd, Z. A., R. L. Bell, Y. Zhang, J. M. Murphy, A. Goldstein, A. Zaffaroni, T. K. Li, and W. J. McBride. 2005. 'Regional heterogeneity for the intracranial self-administration of ethanol and acetaldehyde within the ventral tegmental area of alcohol-preferring (P) rats: involvement of dopamine and serotonin', *Neuropsychopharmacology*, 30: 330-8.

Rodd, Z. A., S. M. Oster, Z. M. Ding, J. E. Toalston, G. Deehan, R. L. Bell, T. K. Li, and W. J. McBride. 2008. 'The reinforcing properties of salsolinol in the ventral tegmental area: evidence for regional heterogeneity and the involvement of serotonin and dopamine', *Alcohol Clin Exp Res*, 32: 230-9.

Rojkovicova, T., Y. Mechref, J. A. Starkey, G. Wu, R. L. Bell, W. J. McBride, and M. V. Novotny. 2008. 'Quantitative chiral analysis of salsolinol in different brain regions of rats genetically predisposed to alcoholism', *J Chromatogr B Analyt Technol Biomed Life Sci*, 863: 206-14.

Santis, R., M. L. Garmendia, G. Acuna, M. E. Alvarado, and O. Arteaga. 2009. 'The Alcohol Use Disorders Identification Test (AUDIT) as a screening instrument for adolescents', *Drug Alcohol Depend*, 103: 155-8.

Shenoy, S. K., and R. J. Lefkowitz. 2011. 'beta-Arrestin-mediated receptor trafficking and signal transduction', *Trends Pharmacol Sci*, 32: 521-33.

Shim, J., A. Coop, and A. D. MacKerell, Jr. 2013. 'Molecular details of the activation of the mu opioid receptor', *J Phys Chem B*, 117: 7907-17.

Singla, N., H. S. Minkowitz, D. G. Soergel, D. A. Burt, R. A. Subach, M. Y. Salamea, M. J. Fossler, and F. Skobieranda. 2017. 'A randomized, Phase IIb study investigating oliceridine (TRV130), a novel micro-receptor G-protein pathway selective (mu-GPS) modulator, for the management of moderate to severe acute pain following abdominoplasty', *J Pain Res*, 10: 2413-24.

Sjoquist, B., S. Liljequist, and J. Engel. 1982. 'Increased salsolinol levels in rat striatum and limbic forebrain following chronic ethanol treatment', *J Neurochem*, 39: 259-62.

Smyth, A., K. K. Teo, S. Rangarajan, M. O'Donnell, X. Zhang, P. Rana, D. P. Leong, G. Dagenais, P. Seron, A. Rosengren, A. E. Schutte, P. Lopez-Jaramillo, A. Oguz, J. Chifamba, R. Diaz, S. Lear, A. Avezum, R. Kumar, V. Mohan, A. Szuba, L. Wei, W. Yang, B. Jian, M. McKee, and S. Yusuf. 2015. 'Alcohol consumption and cardiovascular disease, cancer, injury, admission to hospital, and mortality: a prospective cohort study', *Lancet*, 386: 1945-54.

Soderpalm, B., H. H. Lido, and M. Ericson. 2017. 'The Glycine Receptor-A Functionally Important Primary Brain Target of Ethanol', *Alcohol Clin Exp Res*, 41: 1816-30.

Starkey, J. A., Y. Mechref, J. Muzikar, W. J. McBride, and M. V. Novotny. 2006. 'Determination of salsolinol and related catecholamines through on-line preconcentration and liquid

chromatography/atmospheric pressure photoionization mass spectrometry', *Anal Chem*, 78: 3342-7.

Storch, A., S. Ott, Y. I. Hwang, R. Ortmann, A. Hein, S. Frenzel, K. Matsubara, S. Ohta, H. U. Wolf, and J. Schwarz. 2002. 'Selective dopaminergic neurotoxicity of isoquinoline derivatives related to Parkinson's disease: studies using heterologous expression systems of the dopamine transporter', *Biochem Pharmacol*, 63: 909-20.

Takahashi, T., Y. Deng, W. Maruyama, P. Dostert, M. Kawai, and M. Naoi. 1994. 'Uptake of a neurotoxin-candidate, (R)-1,2-dimethyl-6,7-dihydroxy-1,2,3,4-tetrahydroisoquinoline into human dopaminergic neuroblastoma SH-SY5Y cells by dopamine transport system', *J Neural Transm Gen Sect*, 98: 107-18.

Toth, B. E., K. Homicsko, B. Radnai, W. Maruyama, J. E. DeMaria, M. Vecsernyes, M. I. Fekete, F. Fulop, M. Naoi, M. E. Freeman, and G. M. Nagy. 2001. 'Salsolinol is a putative endogenous neuro-intermediate lobe prolactin-releasing factor', *J Neuroendocrinol*, 13: 1042-50.

Trott, Oleg, and Arthur J. Olson. 2010. 'AutoDock Vina: improving the speed and accuracy of docking with a new scoring function, efficient optimization, and multithreading', *Journal of computational chemistry*, 31: 455-61.

Vanommeslaeghe, K., E. Hatcher, C. Acharya, S. Kundu, S. Zhong, J. Shim, E. Darian, O. Guvench, P. Lopes, I. Vorobyov, and A. D. Mackerell, Jr. 2010. 'CHARMM general force field: A force field for drug-like molecules compatible with the CHARMM all-atom additive biological force fields', *J Comput Chem*, 31: 671-90.

Vengeliene, V., D. Bachteler, W. Danysz, and R. Spanagel. 2005. 'The role of the NMDA receptor in alcohol relapse: a pharmacological mapping study using the alcohol deprivation effect', *Neuropharmacology*, 48: 822-9.

Vengeliene, V., F. Leonardi-Essmann, W. H. Sommer, H. M. Marston, and R. Spanagel. 2010. 'Glycine transporter-1 blockade leads to persistently reduced relapse-like alcohol drinking in rats', *Biol Psychiatry*, 68: 704-11.

Vetreno, R. P., and F. T. Crews. 2014. 'Current hypotheses on the mechanisms of alcoholism', *Handb Clin Neurol*, 125: 477-97.

Wallner, M, HJ Hanchar, and RW Olsen. 2014. 'Alcohol selectivity of β3-containing GABAA receptors: evidence for a unique extracellular alcohol/imidazobenzodiazepine Ro15-4513 binding site at the α+ β-subunit interface in αβ3δ GABAA receptors', *Neurochemical research*, 39: 1118-26.

Wang, H. L., J. Qi, S. Zhang, H. Wang, and M. Morales. 2015. 'Rewarding Effects of Optical Stimulation of Ventral Tegmental Area Glutamatergic Neurons', *J Neurosci*, 35: 15948-54.

Wang, W., K. Ameno, M. Jamal, M. Kumihashi, I. Uekita, S. Ameno, and I. Ijiri. 2007. 'Effect of direct infusion of acetaldehyde on dopamine and dopamine-derived salsolinol in the striatum of free-moving rats using a reverse microdialysis technique', *Arch Toxicol*, 81: 121-6.

Whistler, J. L., and M. von Zastrow. 1998. 'Morphine-activated opioid receptors elude desensitization by beta-arrestin', *Proc Natl Acad Sci U S A*, 95: 9914-9.

Xie, G., L. Hipolito, W. Zuo, A. Polache, L. Granero, K. Krnjevic, and J. H. Ye. 2012. 'Salsolinol stimulates dopamine neurons in slices of posterior ventral tegmental area indirectly by activating mu-opioid receptors', *J Pharmacol Exp Ther*, 341: 43-50.

Yamanaka, Y., M. J. Walsh, and V. E. Davis. 1970. 'Salsolinol, an alkaloid derivative of dopamine formed in vitro during alcohol metabolism', *Nature*, 227: 1143-4.

Yevenes, G. E., R. W. Peoples, J. C. Tapia, J. Parodi, X. Soto, J. Olate, and L. G. Aguayo. 2003. 'Modulation of glycine-activated ion channel function by G-protein betagamma subunits', *Nat Neurosci*, 6: 819-24.

Zimatkin, S. M., S. P. Pronko, V. Vasiliou, F. J. Gonzalez, and R. A. Deitrich. 2006. 'Enzymatic mechanisms of ethanol oxidation in the brain', *Alcohol Clin Exp Res*, 30: 1500-5.

## 12. ADDENDUM

Effect of Aldh1b1 knockout on brain gene expression of mice under ethanol treatment

In the brain, ethanol is metabolized to acetaldehyde mainly by the catalase and cytochrome P450 2E1 (CYP2E1) [1] (**Fig. 6**). Acetaldehyde is metabolized to acetate by an aldehyde dehydrogenase enzyme (Aldh). The ALDH enzymes vary in their specificity and potency towards different aldehyde substrates. For acetaldehyde metabolism in humans, the most important enzyme is Aldh2, with a $K_m$ of 0.2 µM [2], while the second of importance is Aldh1b1, with a $K_m$ of 55 µM [3]. Aldh1b1 shares 71% amino acid identity with Aldh2 and is an interesting target for the study of alcoholism because polymorphisms of its gene have been correlated with higher alcohol-induced hypersensitivity symptoms in Caucasian populations [4], similarly to what Aldh2 deficiency generates on Asian populations. Moreover, Aldh1b1 knockout mice had reduced acetaldehyde elimination after a high dose of ethanol (4g/kg intraperitoneal) [5]. There is no evidence, however, supporting the relevance of Aldh1b1 for acetaldehyde metabolism in the brain, or for the normal brain response to ethanol consumption. We sought to determine what was the effect of the lack of Aldh1b1 for the brain response to a chronic ethanol treatment, using Aldh1b1 knockout mice on a C57BL/6 background. The hypothesis was that Aldh1b1 is necessary to maintain a normal brain response after a chronic ethanol exposure in mice. The brain response was determined by gene expression, comparing the brain levels of mRNA of proteins relevant to the action of ethanol and acetaldehyde in wild-type and Aldh1b1 knockout animals.

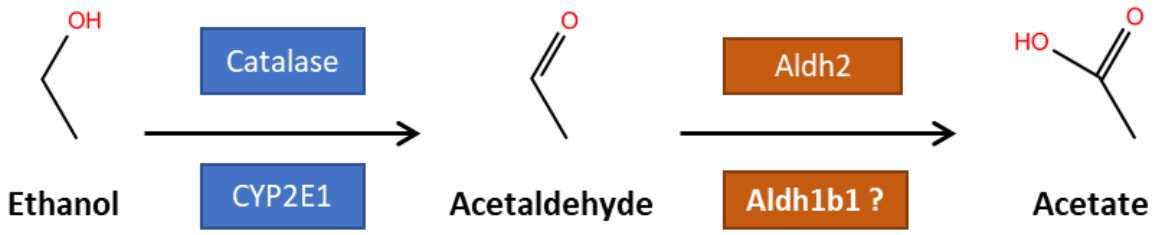


**Figure 6.** Route of ethanol metabolism in the brain. In the brain, ethanol is oxidized to acetaldehyde by catalase and the cytochrome P450 2E1. Acetaldehyde is oxidized to acetate by Aldh2. The possible impact of Aldh1b1 in acetaldehyde metabolism is unknown.

*Methods*

C57BL/6 wild-type or Aldh1B1 knockout mice, described by Singh [5], underwent a Lieber-De Carli ethanol liquid diet treatment for five weeks, following the protocol of Chaudhry [6] (**Table 3**). This diet fulfilled the nutritional requirements of the mice and water was available *ad libitum*. To add ethanol to the diet, the mixture contained less maltose to maintain the same calorie intake. Diet intake volume was recorded daily. The body weight was determined three times a week for the first two weeks and daily afterwards. Animals were sacrificed after the first neurological symptoms were observed. The liver and blood from the left ventricle were collected for ethanol and acetaldehyde determination by headspace GCMS. The brain was rapidly extracted and dissected, obtaining the midbrain, hippocampus, striatum, cortex and a region containing the hypothalamus for RNA extraction. The expression levels were determined on the dissected brain areas by RT-qPCR for the mRNA of (i) Aldh enzymes (Aldh1a1, Aldh1b1, and two variants of Aldh2 [Aldh2v1: NM_009656.4; Aldh2v2: NM_001308450.1); (ii) enzymes related to the acetaldehyde synthesis in the brain (catalase and CYP2E1); (iii) proteins related to the

effect of ethanol and salsolinol on the reward system (μ-opioid receptor and dopamine transporter); (iii) proteins related to GABA activity (GABA transporter and $GABA_A$ receptor subunits α1, α2, α4, β2, β3, γ2); and (iv) proteins related to glutamate activity (Glutamate transporter GLT-1 and NMDA receptor subunits NR1 and NR2A). Primers were designed using NCBI's Primers-BLAST tool, requiring that the primer must span within an exon-exon junction for mRNA specificity. Statistical significance between the same brain area in wild-types and knockouts animals were determined using the -ddCt method. Student's T-test was used for comparison of ethanol and acetaldehyde levels in the blood and the liver; two-way ANOVA was used for the analysis of the diet consumption, mouse body weight, and mRNA levels, using GraphPad Prism.

**Table 3**. Daily ethanol concentration in the Lieber-De Carli diet given to the wild-type and Aldh1b1 knockout mice.

| **Day** | **1-2** | **3-4** | **5-6** | **7-13** | **14-20** | **21-34** |
|---|---|---|---|---|---|---|
| **Ethanol diet** | 0% EtOH | 1% EtOH | 2% EtOH | 4% EtOH | 5% EtOH | 6% EtOH |

*Results*

Both wild-type (4 animals) and Aldh1b1 knockout (6 animals) mice were exposed to ethanol in their liquid diet *ad libitum*. The ethanol intake of both groups was similar and no significant differences were observed (**Fig. 7**). The consumption diminished over time as the ethanol percentage increased reaching ~10 mL of 6% ethanol, or 19 g/kg/day of ethanol for a 25-g mouse. One mouse of the Aldh1b1 knockout group died before the end of the third week because of liver damage (no other symptom was observed), this normally happens to some animals undergoing ethanol liquid diet, so the animal wasn't considered for the rest for analysis. The weight of the mice decreased dramatically towards the end of the fourth week (**Fig. 8**). Before the end of the fourth week another Aldh1b1 knockout mouse died, this time after a severe seizure, showing a trembling phenotype a few hours before. After this animal was lost, the rest of the mice were sacrificed for analysis (n=4). The fatal seizures were also observed in a Aldh1b1 knockout group used for a preliminary experiment (not shown).

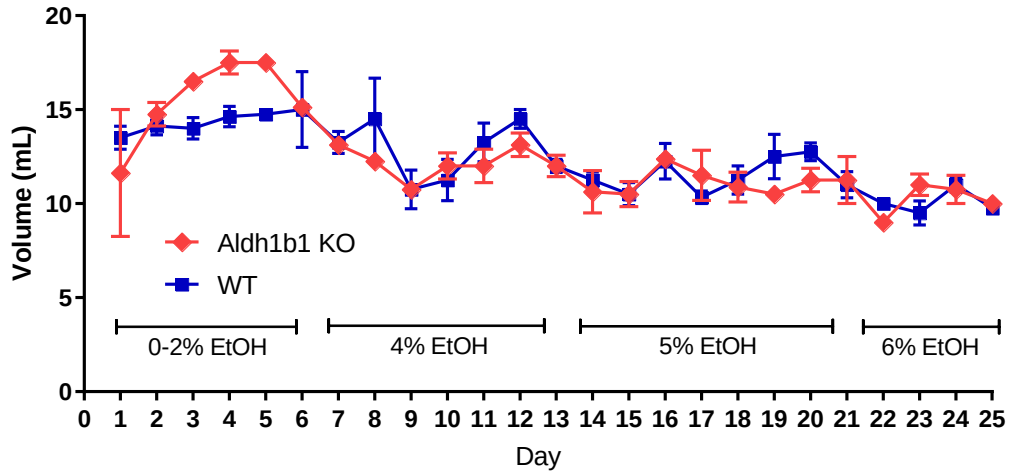


**Figure 7**. Daily liquid diet volume consumption. The Lieber-DeCarli liquid diet was mixed with ethanol to reach desired ethanol percentage. Only the animals that reached every step of the experiment were considered, discarding the mice that died early (n = 4, for each group).

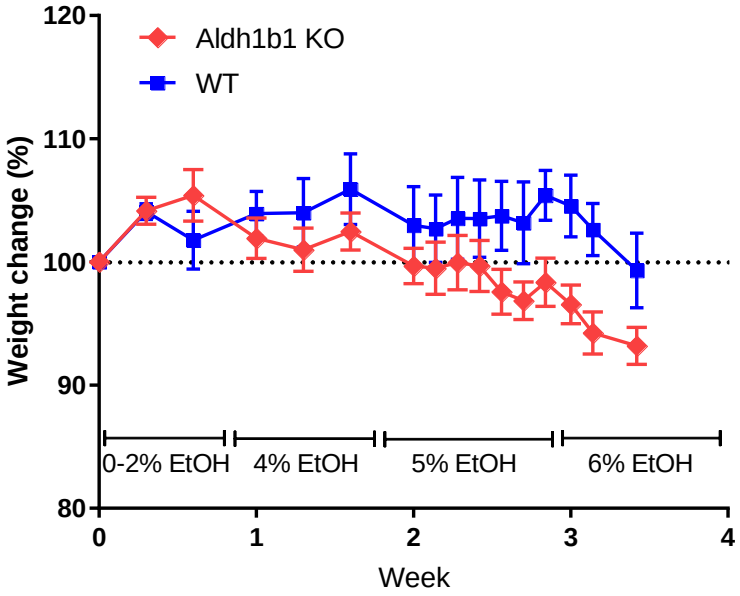


**Figure 8**. Mouse body weight change over the four weeks of treatment. The initial weight was considered as 100%. There was not a significant difference between the two animal groups at any point.

Although not significant, the Aldh1b1 knockout group showed higher of ethanol and acetaldehyde levels, both in the liver and blood in the moment of euthanasia (**Fig. 9A-D**). This is possibly related to a different hourly consumption pattern, because total daily intake was unchanged (**Fig. 7**) (more about this issue in the discussion section).

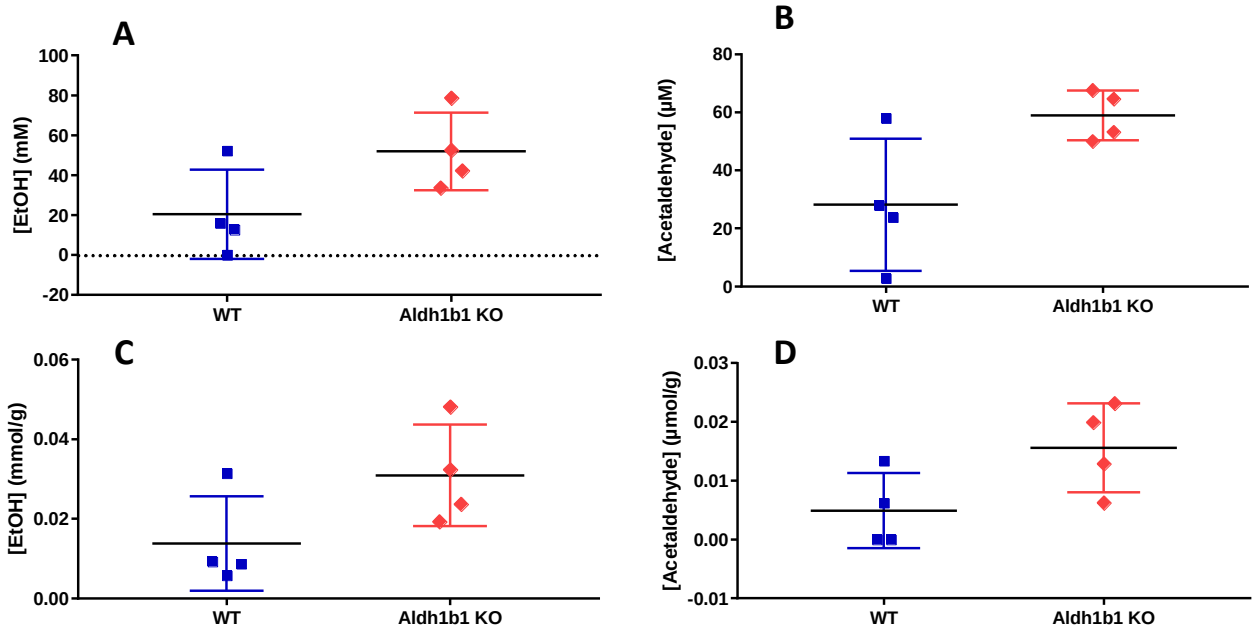


**Figure 9**. Ethanol and acetaldehyde levels in the blood (A, B) and liver (C, D). The points in the graph represent individual animals from each group. No significant differences were observed.

The analysis of Aldh1b1 mRNA levels showed that it was expressed in the wild-type brain with no significant difference among the studied areas. As expected, no expression of Aldh1b1 was observed in the knockout animals (**Fig. 10A**). No differences were observed for the other analyzed aldehyde dehydrogenase enzymes, Aldh1a1 and two mRNA variants of Aldh2 (**Fig. 10B-D**). Likewise, no statistical differences were observed in the mRNA levels of the acetaldehyde generating enzymes, catalase and CYP2E1. Interestingly, the highest catalase mRNA levels were observed in the thalamus/hypothalamus and midbrain, in agreement with previous reports studying the same brain areas (**Fig. 11**) [7].

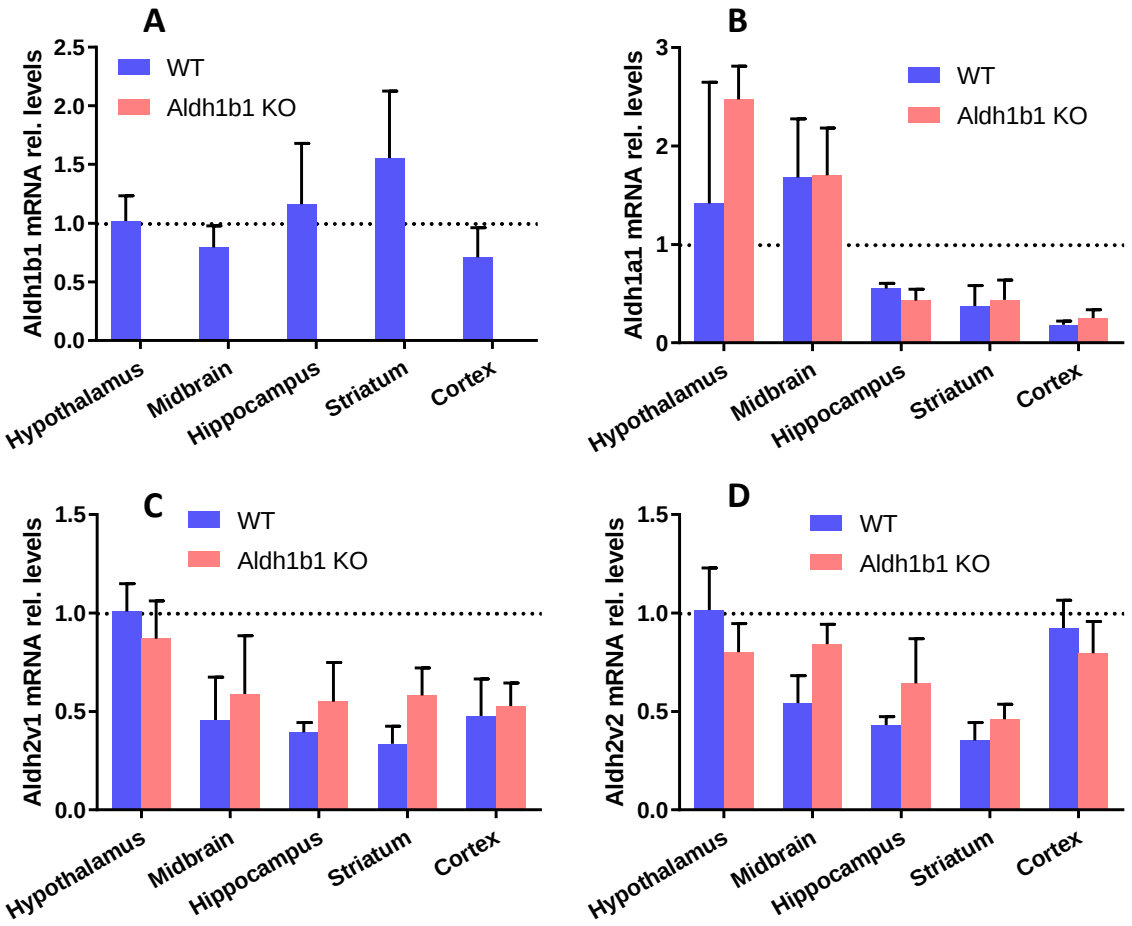


**Figure 10**. Relative mRNA levels of aldehyde dehydrogenase enzymes. The mRNA levels of Aldh1b1 (**A**), Aldh1a1 (**B**), Aldh2v1 (**C**) and Aldh2v2 (**D**) were measured by RT-qPCR and analyzed by the -ddCT method, from dissected tissue of different brain areas. No significant differences between groups were observed (n = 4 for each group, n= 3 for midbrain tissue).

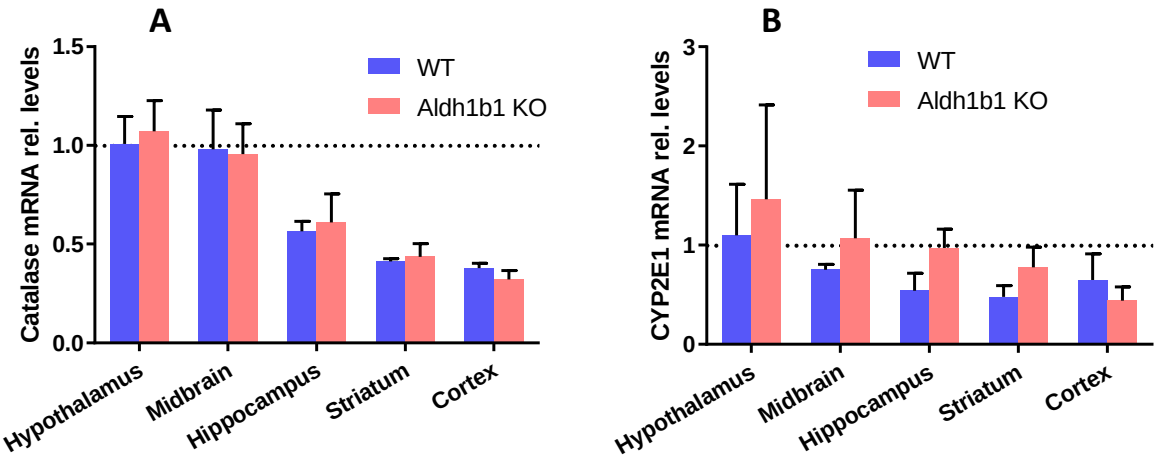


**Figure 11**. Relative mRNA levels of ethanol metabolizing enzymes. The mRNA of catalase (**A**) and cytochrome P450 2E1 (**B**) were determined by RT-qPCR and analyzed by the -ddCT method, from dissected tissue of different brain areas. No significant differences between groups were observed (n = 4 for each group, n= 3 for midbrain tissue).

Because the possible decreased acetaldehyde-metabolizing activity, Aldh1b1 knockout mice could generate more salsolinol after ethanol consumption, so protein targets related to salsolinol activity may have been affected as well. However, no significant difference in the mRNA levels of the μ-opioid receptor and the dopamine transporter (DAT) was observed between the two genotypes (**Fig. 12**).

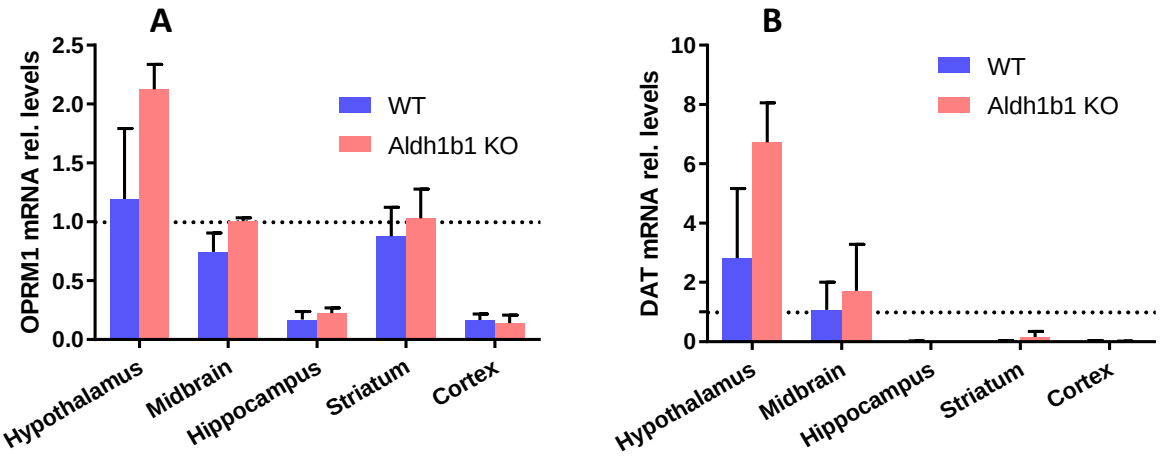


**Figure 12**. Relative mRNA levels of enzymes related to the activity of salsolinol. The mRNA of the μ-opioid receptor (**A**) and dopamine transporter (**B**) were determined by RT-qPCR and analyzed by the -ddCT method, from dissected tissue of different brain areas. No significant differences between groups were observed (n = 4 for each group, n= 3 for midbrain tissue).

The overt phenotype observed as trembling and fatal seizures could be the result of a disbalance of excitatory and inhibitory synapses in the brain. The gene expression of proteins related to the activity of excitatory and inhibitory neurotransmitters, GABA and glutamate, were analyzed. No significant differences were observed for the glutamate transporter Glt-1 and the NMDA receptor subunits NR1

and NR2B (**Fig. 13**). There were no changes in mRNA levels of the GABA transporter and the $GABA_A$ receptor subunits α1, α4, β2, β3, and γ2 between wild-type and Aldh1b1 knockout animals (**Fig. 14A, C-F**). However, significantly lower mRNA levels of $GABA_A$ receptor subunit α2 were found in the knockout mice compared to wild-types, in every studied brain area (**Fig. 14B**). This is interesting because it suggests that Aldh1b1 knockout mice expressed lower levels of this receptor protein, which would mean a diminished inhibitory effect of GABAergic synapses, which explain the high excitatory activity causing the seizures.

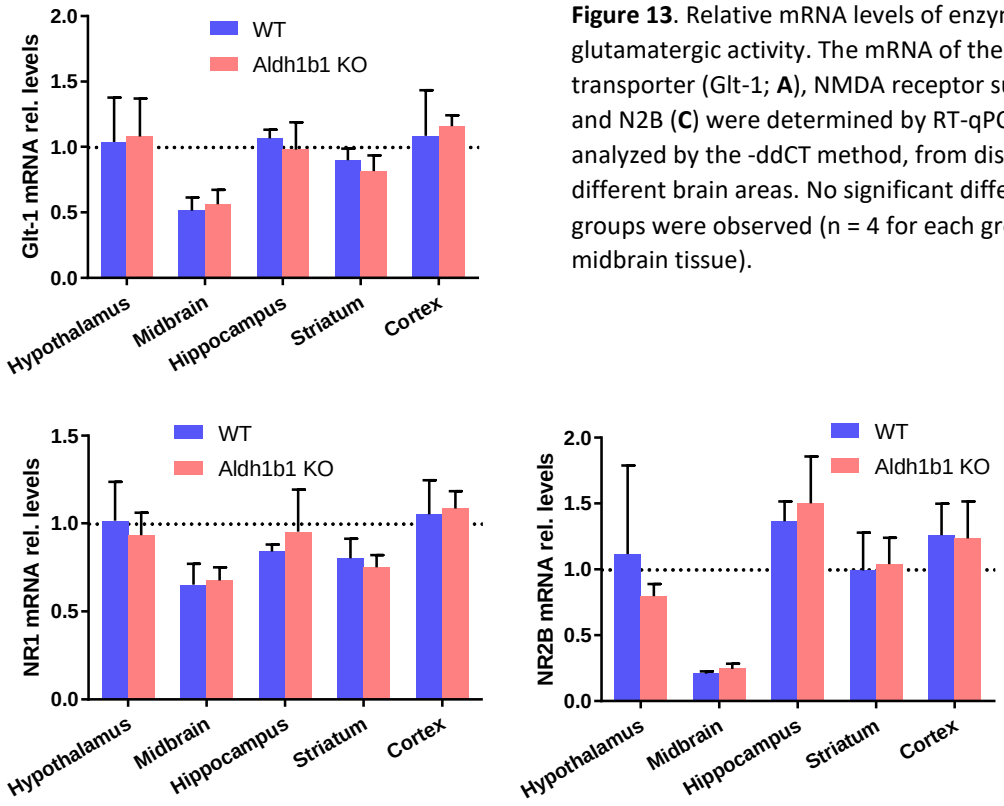


**Figure 13**. Relative mRNA levels of enzymes related to glutamatergic activity. The mRNA of the glutamate transporter (Glt-1; **A**), NMDA receptor subunits N1 (**B**), and N2B (**C**) were determined by RT-qPCR qPCR and analyzed by the -ddCT method, from dissected tissue of different brain areas. No significant differences between groups were observed (n = 4 for each group, n= 3 for midbrain tissue).

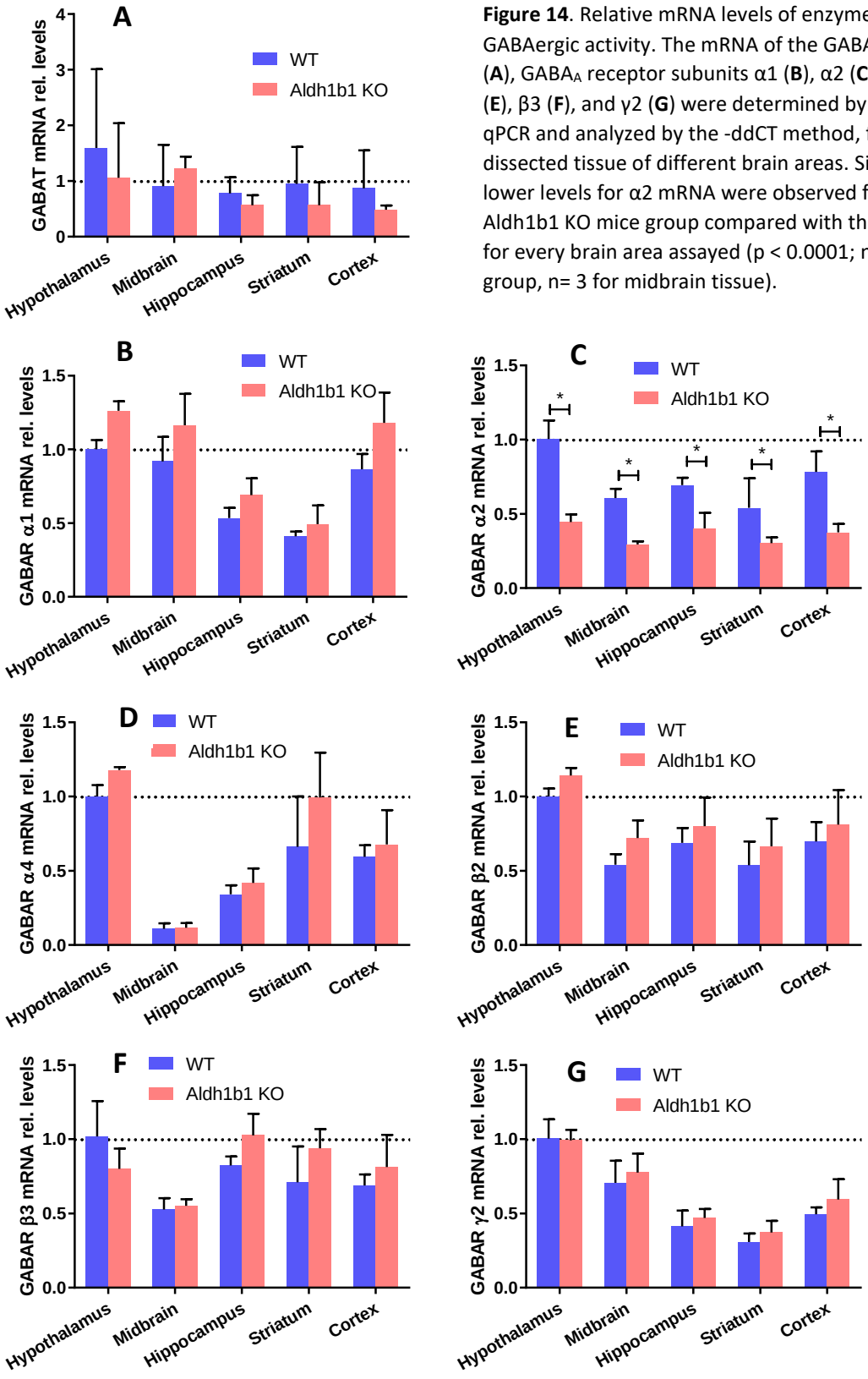


**Figure 14**. Relative mRNA levels of enzymes related to GABAergic activity. The mRNA of the GABA transporter (**A**), $GABA_A$ receptor subunits α1 (**B**), α2 (**C**), α4 (**D**), β2 (**E**), β3 (**F**), and γ2 (**G**) were determined by RT-qPCR qPCR and analyzed by the -ddCT method, from dissected tissue of different brain areas. Significantly lower levels for α2 mRNA were observed for the Aldh1b1 KO mice group compared with the wild-types for every brain area assayed ($p < 0.0001$; n = 4 for each group, n= 3 for midbrain tissue).

*Discussion*

The lack of Aldh1b1 in the knockout mice produced a major effect after less than four weeks of ethanol intake. A knockout mouse showed tremor and fatal seizures elicited by the ethanol exposure, which is reported for the first time. This fatal outcome also happened in an identical experiment that preceded the one discussed. Indeed, five Aldh1b1 knockout animals from a preliminary group died after trembling and seizures before tissue sampling (not included in the present report). In the present experiment, therefore, the animals were immediately sacrificed after the loss of the first mouse to determine acetaldehyde and ethanol blood and liver levels, and mRNA expression of related proteins in different brain areas. Although the mechanism causing the symptoms is unknown, trembling and seizures can be related to a severe ethanol withdrawal [8]. In this case, despite the mice having ethanol available *ad libitum*, the symptoms may need minutes instead of hours to appear in the Aldh1b1 knockout mice. Ethanol is an inhibitor of glutamate NMDA receptors [9] and a potentiator of $GABA_A$ receptor activity [10]. The brain responds to this inhibitory effect by down-regulating the glutamate transporter Glt-1 [11], resulting in increased extracellular glutamate levels and increased excitatory glutamatergic responses [12]. The excitatory response is intensified after the ethanol elimination, which triggers withdrawal symptoms. In the case of Aldh1b1 knockout mice, the animals appeared to have a decreased GABAergic inhibitory tonus, showing a decrease in GABA receptor α2 subunit mRNA levels (**Fig. 14C**). The normal excitatory response to chronic ethanol exposure seems badly counterbalanced by a decreased GABAergic activity. Thus, it is possible that the ethanol does not need to be completely eliminated for the occurrence of withdrawal symptoms. On the other hand, if the trembling and seizures are diminished by ethanol intake it would produce a negative reinforcing effect, making that the animals drink ethanol to decrease the probability of unpleasant symptoms. This could explain the higher, though not significant, ethanol and acetaldehyde levels shown by Aldh1b1 KO mice (**Fig. 9**).

No significant differences were found in mRNA of proteins associated to salsolinol activity. However, high levels of DAT mRNA were observed in hypothalamus containing samples, particularly in Aldh1b1 knockout mice (**Fig. 12**), compared with the modest DAT mRNA levels found in the hypothalamus of wild animals, where the most abundant levels are reported in the midbrain [13]. To a lesser extent, high, but non-significant μ-opioid receptor mRNA levels were observed in hypothalamus containing samples of Aldh1b1 knockout mice. This possibly indicates a hypothalamic response to the chronic ethanol consumption by the Aldh1b1 knockout mice. The null levels of DAT mRNA in striatum can be explained by the lack of dopaminergic cell bodies [14] (**Fig. 12**).

The study of the effect of ethanol consumption on Aldh1b1 knockout mice is in progress. It will be interesting to determine if an ethanol injection, NMDA blockage, or benzodiazepine administration (to increase GABAergic activity, used for ethanol withdrawal in humans) can relieve the trembling or seizures and whether the levels of glutamate or GABA are altered in the brain of these mice. These objectives will be explored after this thesis at Dr. Vasilis Vasiliou's laboratory at Yale University.

*References*


1. Zimatkin, S.M., et al., *Enzymatic mechanisms of ethanol oxidation in the brain.* Alcohol Clin Exp Res, 2006. **30**(9): p. 1500-5.
2. Klyosov, A.A., et al., *Possible role of liver cytosolic and mitochondrial aldehyde dehydrogenases in acetaldehyde metabolism.* Biochemistry, 1996. **35**(14): p. 4445-56.

3. Stagos, D., et al., *Aldehyde dehydrogenase 1B1: molecular cloning and characterization of a novel mitochondrial acetaldehyde-metabolizing enzyme.* Drug Metab Dispos, 2010. **38**(10): p. 1679-87.
4. Linneberg, A., et al., *Genetic determinants of both ethanol and acetaldehyde metabolism influence alcohol hypersensitivity and drinking behaviour among Scandinavians.* Clin Exp Allergy, 2010. **40**(1): p. 123-30.
5. Singh, S., et al., *ALDH1B1 links alcohol consumption and diabetes.* Biochem Biophys Res Commun, 2015. **463**(4): p. 768-73.
6. Chaudhry, K.K., et al., *Glutamine supplementation attenuates ethanol-induced disruption of apical junctional complexes in colonic epithelium and ameliorates gut barrier dysfunction and fatty liver in mice.* J Nutr Biochem, 2016. **27**: p. 16-26.
7. Brannan, T.S., H.S. Maker, and I.P. Raes, *Regional distribution of catalase in the adult rat brain.* J Neurochem, 1981. **36**(1): p. 307-9.
8. Romach, M.K. and E.M. Sellers, *Management of the alcohol withdrawal syndrome.* Annu Rev Med, 1991. **42**: p. 323-40.
9. Gonzales, R.A. and J.J. Woodward, *Ethanol inhibits N-methyl-D-aspartate-stimulated [3H]norepinephrine release from rat cortical slices.* J Pharmacol Exp Ther, 1990. **253**(3): p. 1138-44.
10. Mehta, A.K. and M.K. Ticku, *Ethanol potentiation of GABAergic transmission in cultured spinal cord neurons involves gamma-aminobutyric acidA-gated chloride channels.* J Pharmacol Exp Ther, 1988. **246**(2): p. 558-64.
11. Das, S.C., et al., *Binge ethanol withdrawal: Effects on post-withdrawal ethanol intake, glutamate-glutamine cycle and monoamine tissue content in P rat model.* Behav Brain Res, 2016. **303**: p. 120-5.
12. Rossetti, Z.L. and S. Carboni, *Ethanol withdrawal is associated with increased extracellular glutamate in the rat striatum.* Eur J Pharmacol, 1995. **283**(1-3): p. 177-83.
13. Cerruti, C., et al., *Dopamine transporter mRNA expression is intense in rat midbrain neurons and modest outside midbrain.* Brain Res Mol Brain Res, 1993. **18**(1-2): p. 181-6.
14. Letchworth, S.R., et al., *Effects of chronic cocaine administration on dopamine transporter mRNA and protein in the rat.* Brain Res, 1997. **750**(1-2): p. 214-22.